Copyright Warning & Restrictions

The copyright law of the United States (Title 17, United States Code) governs the making of photocopies or other reproductions of copyrighted material.

Under certain conditions specified in the law, libraries and archives are authorized to furnish a photocopy or other reproduction. One of these specified conditions is that the photocopy or reproduction is not to be "used for any purpose other than private study, scholarship, or research." If a, user makes a request for, or later uses, a photocopy or reproduction for purposes in excess of "fair use" that user may be liable for copyright infringement,

This institution reserves the right to refuse to accept a copying order if, in its judgment, fulfillment of the order would involve violation of copyright law.

Please Note: The author retains the copyright while the New Jersey Institute of Technology reserves the right to distribute this thesis or dissertation

Printing note: If you do not wish to print this page, then select "Pages from: first page # to: last page #" on the print dialog screen

ABSTRACT

ANGIOGENIC SUPPORTS FOR MICROVASCULAR ENGINEERING

by
Zain Siddiqui

Ischemic tissue disease is caused by a lack of circulation / blood supply to tissue. This can be treated by introducing a number of angiogenic (pro-blood vessel forming) factors into the tissue. This work presents strategies for ischemic tissue treatment utilizing a novel pro-angiogenic self-assembling peptide hydrogel platform. To demonstrate the utility of this platform, its use alone as an angiogenic therapeutic (both alone as a self-assembling hydrogel and with two-component systems), and its ability to vascularize implants is explored. Due to these angiogenic scaffolds demonstrating efficacy to regenerate microvasculature, this work evaluates diseases that can be treated by the regeneration of microvasculature – such as the soft tissue in the dental pulp and ocular microvessel healing.

ANGIOGENIC SUPPORTS FOR MICROVASCULAR ENGINEERING

by
Zain Siddiqui

A Dissertation
Submitted to the Faculty of
New Jersey Institute of Technology
and Rutgers University Biomedical and Health Sciences - Newark
in Partial Fulfillment of the Requirements for the Degree of
Doctor of Philosophy in Biomedical Engineering

Department of Biomedical Engineering

December 2022

APPROVAL PAGE

ANGIOGENIC SUPPORTS FOR MICROVASCULAR ENGINEERING

Zain Siddiqui

Dr. Vivek A. Kumar, Dissertation Advisor — Date
Associate Professor of Biomedical Engineering, NJIT

Dr. Eun Jung Lee, Committee Member — Date
Associate Professor of Biomedical Engineering, NJIT

Dr. Jonathan Grasman, Committee Member — Date
Assistant Professor of Biomedical Engineering, NJIT

Dr. Emi Shimizu, Committee Member — Date
Assistant Professor of Oral Biology, Rutgers School of Dental Medicine

---

Dr. Dominic Del Re, Committee Member — Date
Assistant Professor of Cell Biology and Molecular Medicine,
Rutgers University New Jersey Medical School, Newark, NJ

BIOGRAPHICAL SKETCH

Author: Zain Siddiqui

Degree: Doctor of Philosophy

Date: December 2022

Undergraduate and Graduate Education:

- Doctor of Philosophy in Biomedical Engineering,
  New Jersey Institute of Technology, Newark, NJ, 2022
  Rutgers University Biomedical and Health Sciences, Newark, NJ, 2022

- Master of Science in Biomedical Engineering,
  New Jersey Institute of Technology, Newark, NJ, 2019

- Bachelor of Science in Biomedical Engineering,
  New Jersey Institute of Technology, Newark, NJ, 2017

Major: Biomedical Engineering

Publications:

K. Kim, **Z. Siddiqui**, A. Acevedo-Jake, A. Roy, M. Choudhury, J. Grasman, V. Kumar. Angiogenic hydrogels to accelerate early wound healing. Macromolecular Bioscience 22 (2022) 2200067.

G. Park, S. Tarafder, S. Eyen, S. Park, R. Kim, **Z. Siddiqui**, V. Kumar, C. Lee. Oxo-M and 4-PPBP delivery via multi-domain peptide hydrogel toward tendon regeneration. Frontiers in Bioengineering and Biotechnology 10 (2022) 773004.

Y. Kobayashi, J. Nouet, E. Balinnyam, **Z. Siddiqui**, D. Fine, D. Fraidenraich, V. Kumar, E. Shimizu. iPSC-derived cranial neural crest-like cells can replicate dental pulp tissue with the aid of angiogenic hydrogel. Bioactive Materials 14 (2022) 290-301.

Z. Siddiqui, A. Acevedo-Jake, A. Griffith, N. Kadincesme, K. Dabek, D. Hindi, K. Kim, Y. Kobayashi, E. Shimizu, V. Kumar. Cells and material-based strategies for regenerative endodontics. Bioactive Materials 14 (2022) 234-249.

A. Acevedo-Jake, S. Shi, **Z. Siddiqui**, S. Sanyal, R. Schur, S. Kaja, A. Yuan, V. Kumar. Preclinical efficacy of pro- and anti-angiogenic peptide hydrogels to treat age-related macular degeneration. Bioengineering 8 (2021) 190.

Z. Siddiqui, B. Sarkar, K. Kim, A. Kumar, R. Paul, A. Mahajan, J. Grasman, J. Yang, V. Kumar. Self-assembling peptide hydrogels facilitate vascularization in two-component scaffolds. Chemical Engineering Journal 422 (2021) 130145.

Z. Siddiqui, B. Sarkar, K. Kim, N. Kadincesme, R. Paul, A. Kumar, Y. Kobayashi, A. Roy, M. Choudhury, J. Yang, E. Shimizu, V. Kumar. Angiogenic hydrogels for dental pulp regeneration. Acta Biomaterialia 126 (2021) 109-118.

B. Sarkar, X. Ma, A. Agas, **Z. Siddiqui**, P. Iglesias-Montoro, P. Nguyen, K. Kim, J. Haorah, V. Kumar. In vivo neuroprotective effect of a self-assembled peptide hydrogel. Chemical Engineering Journal 408 (2021) 127295.

S. Azizighannad, Z. Wang, **Z. Siddiqui**, V. Kumar, S. Mitra. Nano carbon doped polyacrylamide gel electrolytes for high performance supercapacitors. Molecules 26(9) (2021) 2631.

C. Moore, **Z. Siddiqui**, G. Carney, Y. Naaldijk, K. Guiro, A. Ferrer, L. Sherman, M. Guvendiren, V. Kumar, P. Rameshwar. A 3D bioprinted material that recapitulates the perivascular bone marrow structure for sustained hematopoietic and cancer models. Polymers 13(4) (2021) 480.

V. Harbour. C Casillas, **Z. Siddiqui**, B. Sarkar, S. Sanyal. P. Nguyen, K. Kim, A. Roy, P. Iglesias-Montoro, S. Patel, F. Podlaski, P. Tolias, W. Windsor, V. Kumar. Regulation of lipoprotein homeostasis by self-assembling peptides. American Chemical Society Applied Bio Materials 3(12) (2020) 8978-8988.

K. Crowe, **Z. Siddiqui**, V. Harbour, K. Kim, S. Syed, R. Paul, A. Roy, R. Naik, K. Mitchell, A. Mahajan, B. Sarkar, V. Kumar. Evaluation of injectable naloxone-releasing hydrogel. American Chemical Society Applied Bio Materials 3(11) (2020) 7858-7864.

B. Sarkar, **Z. Siddiqui**, K. Kim, P. Nguyen, X. Reyes, T. McGill, V. Kumar. Implantable anti-angiogenic scaffolds for treatment of neovascular ocular pathologies. Drug Delivery and Translational Research 10(5) (2020) 1191-1202.

X. Ma, A. Agas, **Z. Siddiqui**, K. Kim, P. Iglesias-Montoro, J. Kalluru, V. Kumar, J. Haorah. Angiogenic peptide hydrogels for treatment of traumatic brain injury. Bioactive Materials 5(1) (2020) 124-132.

K. Kim, **Z. Siddiqui**, M. Patel, B. Sarkar, V. Kumar. A self-assembled peptide hydrogel for cytokine sequestration. Journal of Materials Chemistry B 8(5) (2020) 945-950.

B. Sarkar, **Z. Siddiqui**, P. Nguyen, N. Dube, W. Fu, S. Park, S. Jaisinghani, R. Paul, S. Kozuch, D. Deng, P. Iglesias-Montoro, M. Li, D. Sabatino, D. Perlin, W. Zhang, J. Mondal, V. Kumar. Membrane-disrupting nanofibrous peptide hydrogels. American Chemical Society Biomaterials Science & Engineering 5(9) (2019) 4657-4670.

K. Petrak, R. Vissapragada, S. Shi, **Z. Siddiqui**, K. Kim, B. Sarkar, V. Kumar. Challenges in translating from bench to bed-side: Pro-angiogenic peptides for ischemia treatment. Molecules 24(7) (2019) 1219.

P. Nguyen, W. Gao, S. Patel, **Z. Siddiqui**, S. Weiner, E. Shimizu, B. Sarkar, V. Kumar. Self-assembly of a dentinogenic peptide hydrogel. American Chemical Society Omega. 3(6) (2018) 5980–5987.

B. Sarkar, P. Nguyen, W. Gao, A. Dondapati, **Z. Siddiqui**, V. Kumar. Angiogenic self-assembling peptide scaffolds for functional tissue regeneration. Biomacromolecules 19(9) (2018) 3597–3611.

P. Nguyen, B. Sarkar, **Z. Siddiqui**, M. McGowan, P. Iglesias-Montoro, S. Rachapudi, S. Kim, W. Gao, E. Lee, V. Kumar. Self-assembly of an anti-angiogenic nanofibrous peptide hydrogel. American Chemical Society Applied Bio Materials 1(3) (2018) 865-870.

Presentations:

Z. Siddiqui, K. Kim, A. Roy, M. Choudhury, A. Acevedo-Jake, J. Grasman, V. Kumar. Angiogenic self-assembly peptide hydrogels to accelerate wound healing. Poster. Northeast Bioengineering Conference (2022).

A. Roy, **Z. Siddiqui**, J. Dodd-o, P. Elguera, A. Azizogli, V. Kumar. Induced angiogenesis and myogenesis through an IGF mimicking self-assembling peptide hydrogel. Poster. Northeast Bioengineering Conference (2022).

Z. Siddiqui, K. Kim, A. Roy, A. Kumar, B. Sarkar, E. Shimizu, V. Kumar. Angiogenic peptide hydrogel for dental pulp revascularization in small and large animal models. Poster. Biomedical Engineering Society (2021).

A. Roy, S. Sanyal, **Z. Siddiqui**, S. Syed, S. Ramasamy, J. Dodd-o, A. Acevedo-Jake, S. Subbian, V. Kumar. Opsonization of SARS-CoV-2 through self-assembling peptides. Poster. American Chemical Society (2021).

S. Sanyal, A. Acevedo-Jake, S. Shi, **Z. Siddiqui**, V. Kumar. Age-related macular degeneration treatment efficacy via pro- and anti-angiogenic peptide hydrogels. Poster. American Chemical Society (2021).

S. Ramasamy, **Z. Siddiqui**, A. Roy, R. Kumar, A. Kolloli, T. Chang, V. Kumar, S. Subbian. SARS-CoV-2 spike binding peptides: A potential therapeutic approach for COVID-19. Poster. Virtual Immunology (2021).

S. Ramasamy, R. Kumar, **Z. Siddiqui**, A. Roy, S. Sanyal, A. Kolloli, T. Chang, V. Kumar, S. Subbian. Design and evaluation of novel SARS-CoV-2 spike binding peptides: A potential therapeutic approach for COVID-19. Poster. Theobald Smith Winter Symposium (2021).

A. Acevedo-Jake, S. Sanyal, S. Shi, **Z. Siddiqui**, V. Kumar. Efficacy of pro- and anti-angiogenic peptide hydrogels to treat age-related macular degeneration. Poster. Northeast Bioengineering Conference (2021).

S. Sanyal, V. Harbour, **Z. Siddiqui**, B. Sarkar, K. Kim, V. Kumar. Self-assembling peptides to mitigate familial hypercholesterolemia. Poster. American Chemical Society Virtual Meeting (2020).

G. Park, S. Tarafder, A. Alex, E. Lee, **Z. Siddiqui**, V. Kumar, C. Lee. Controlled delivery of Oxo-M and 4-PPBP via multidomain peptides for in situ tendon regeneration. Poster. Orthopedic Research Society (2020).

B. Sarkar, X. Ma, P. Iglesias-Montoro, **Z. Siddiqui**, A. Agas, K. Kim, J. Haorah, V. Kumar. Enhanced in vivo neuronal survival after traumatic brain injury facilitated by an injectable self-assembled peptide hydrogel. Poster. American Institute of Chemical Engineers (2019).

P. Nguyen, B. Sarkar, **Z. Siddiqui**, K. Kim, A. Mathew, V. Kumar. Novel drug delivery system using anti-angiogenic peptides for glioblastoma multiforme. Poster. Northeast Bioengineering Conference (2019).

X. Ma, B. Sarkar, P. Iglesias-Montoro, **Z. Siddiqui**, V. Kumar, J. Haorah. Vascular pathology mediated traumatic brain injury and the regenerative treatment using peptide hydrogel. Podium. Society for Neuroscience (2019).

CA Moore, **Z. Siddiqui**, GJ Carney, V. Kumar, P. Rameshwar. Development of novel hydrogel for 3D bioprinting applications that recapitulates the native bone marrow microenvironment. Poster. New Jersey Commission on Cancer Research 3rd Annual Symposium (2019).

CA Moore, **Z. Siddiqui**, CJ Carney, V. Kumar, P. Rameshwar. Development of novel hydrogel for 3D bioprinting applications that recapitulates the native bone marrow microenvironment. Poster. 26th Annual Rutgers Graduate Student Association Symposium (2019).

Z. Siddiqui, K. Kim, R. Naik, K. Mitchell, B. Sarkar, V. Kumar. Sustained release of naloxone through self-assembling peptide hydrogels for long-term management of opioid addiction. Poster. Biomedical Engineering Society (2019).

K. Kim, **Z. Siddiqui**, M. Patel, B. Sarkar, P. Nguyen, V. Kumar. Self-assembling peptides scaffolds for inflammatory response modulation. Poster. Biomedical Engineering Society (2019).

X. Ma, B. Sarkar, A. Agas, P. Iglesias-Montoro, **Z. Siddiqui**, K. Kim, J. Haorah, V. Kumar. Injectable self-assembled hydrogel for neuroprotection in vivo after traumatic brain injury. Poster. Biomedical Engineering Society (2019).

X. Ma, B. Sarkar, P. Iglesias-Montoro, **Z. Siddiqui**, V. Kumar, J. Haorah. Injectable self-assembling peptide hydrogel for angiogenesis after traumatic brain injury. Poster. Biomedical Engineering Society (2019).

B. Sarkar, **Z. Siddiqui**, K. Kim, R. Paul, A. Kumar, S. Weiner, E. Shimizu, V. Kumar. Regeneration of pulpal vasculature in a canine model guided by an injectable self-assembled hydrogel. Poster. Biomedical Engineering Society (2019).

E. Davidoff, **Z. Siddiqui**, V. Kumar, J. Sy. Self-healing hydrogels for improving brain implant biocompatibility. Poster. Biomedical Engineering Society (2019).

B. Sarkar, **Z. Siddiqui**, K. Kim, V. Kumar. Targeting regeneration of injured neuronal microenvironment by injectable self-assembled hydrogels. Poster. Biomedical Engineering Society (2019).

M. Pepper, B. Sarkar, **Z. Siddiqui**, K. Kim, J. Yang, V. Kumar. Functional hydrogels for modification of porous scaffolds. Poster. Biomedical Engineering Society (2019).

B. Sarkar, X. Ma, P. Iglesias-Montoro, **Z. Siddiqui**, K. Kim, A. Agas, P. Nguyen, J. Haorah, V. Kumar. Injectable neuroprotective peptide hydrogels. Podium & Press Conference. American Chemical Society (2019).

Z. Siddiqui, B. Sarkar, K. Kim, R. Paul, A. Kumar, J. Yang, V. Kumar. Nanofibrous peptide hydrogels for modulating angiogenic responses of implanted polymeric scaffolds. Podium. American Chemical Society (2019).

Z. Siddiqui, R. Naik, K. Mitchell, V. Kumar. Release of naloxone for long-term management of opioid addiction. Podium. Northeast Bioengineering Conference (2019).

P. Nguyen, W. Gao, B. Sarkar, **Z. Siddiqui**, S. Patel, E. Shimizu, S. Weiner, V. Kumar. Dentinogenic peptide hydrogels for pulpal regeneration. Podium. Materials Research Society (2018).

B. Sarkar, S. Park, P. Nguyen, D. Deng, W. Fu, **Z. Siddiqui**, S. Jaisinghani, R. Paul, W. Zhang, M. Li, DS Perlin, V. Kumar. Rational design of antimicrobial peptide nanofibers. Poster. Materials Research Society (2018).

Z. Siddiqui, P. Nguyen, B. Sarkar, D. Sabatino, V. Kumar. Photo-responsive peptide hydrogels for tailored drug delivery. Podium. Materials Research Society (2018).

Z. Siddiqui, M. McGowan, P. Nguyen, P. Iglesias-Montoro, B. Sarkar, V. Kumar. Programmable modulation of cellular viability using self-assembled peptide nanofibers. Podium. Biomedical Engineering Society (2018).

B. Sarkar, P. Nguyen, S. Jaisinghani, R. Paul, **Z. Siddiqui**, M. McGowan, P. Iglesias-Montoro, V. Kumar. Self-assembled antibacterial peptide nanofibers inspired by LL-37. Poster. Biomedical Engineering Society (2018).

To curiosity for experiment's sake

ACKNOWLEDGMENT

I would like to acknowledge my dissertation advisor Dr. Vivek A. Kumar for his endless support and guidance throughout my research journey. After completing my undergraduate studies, I approached Dr. Kumar asking to volunteer in his lab as a post-baccalaureate research assistant. Without hesitation, he helped me grasp and appreciate the complex world of research by showing me how to perform cell culture, synthesize and prepare hydrogels along with other polymeric biomaterials, go through ELISAs and other *in vitro* assays step by step, and performing *in vivo* studies all within that first year. With his mentorship, I was able to go from following protocols to answering my own curiosity driven research questions and for that I am forever grateful. I remember during my first podium presentation at Biomedical Engineering Society (BMES) in 2018, he helped me prepare the slides and practice presenting for 3–4 hours just before my talk. What may be the most indicative of his mentorship style though was that during the talk, he sat at the back of the room and with hand signals gave me pointers on how to answer questions from the audience. These past five years in Dr. Kumar's lab have been at times challenging but ultimately incredibly rewarding, both in terms of the academic research success – due in large part to his guidance, as well as having the opportunity to mentor over two dozen students and trying to instill that curiosity driven research approach to them too.

I would also like to thank my committee members, Dr. Eun Jung Lee, Dr. Jonathan Grasman, Dr. Dominic Del Re and Dr. Emi Shimizu for their support, encouragement and valuable input and suggestions. I took the Cell & Biomaterial Engineering Lab course with Dr. Lee during my undergraduate studies, back when I had no clue what we were learning were the basics of research. I would have never thought back then that I would have the

opportunity to one day teach that same course. I thank Dr. Lee for her instructing me on how to perform cell culture during my undergrad and especially for her valuable mentorship along my PhD journey. I thank Dr. Grasman for answering my somewhat never-ending questions, every time we have a research related discussion I inevitably learn something new and to approach research questions with a different perspective. I appreciate your help and input in publishing the work presented in this dissertation. I thank Dr. Del Re, I remember once in 2018 how he explained to Kakyung and me how to properly use an optical microscope at the medical school. I sincerely thank you for your patience on that day, as well your guidance throughout my research journey. I thank Dr. Shimizu, without her help and mentorship the work presented in this dissertation would not have been possible. You are the kindest researcher I have had the pleasure to meet and learn from, thank you for teaching us the importance and impact that research, especially *in vivo* studies, can have.

Additionally, I thank Dr. Jeong Seop Shim, Dr. Xueyan Zhang and Dr. Lingfen Rao for their training and guidance in using the core facilities at NJIT integral to my research.

I sincerely thank my lab mates and colleagues for for their constant support, getting through graduate school together, and helping make the day-to-day as memorable as possible. I thank our postdocs Dr. Peter Nguyen, Dr. Biplab Sarkar, Dr. Amanda Acevedo-Jake and Dr. Jatin Kashyap for their invaluable guidance. I thank Peter and Biplab for mentoring me as I joined the lab. I learned how to write and run my own protocols, analyze raw data to create publication quality figures, prepare manuscripts and tactfully respond to reviewer #1, 2, 3, ∞ comments. I thank Amanda for teaching me its ok to question PIs, just as long as you have solid rationale behind it. I thank Jatin for explaining a different facet to our research, namely in computational modeling. I would also like to thank my fellow

friends and colleagues that underwent and are currently traversing their own PhD journey in the lab, Dr. Kakyung Kim, Abhishek Roy, Joseph Dodd-o and Alexandra Griffith. I thank Kakyung for keeping me sane during the early parts of my graduate studies, and for always being there when we had experiments that ran till the early morning. Research can get tedious and difficult; I truly appreciate your continuing friendship and support to get through those times. Thank you, Abhishek, for your friendship and for reminding me that even though research can seem to be an all-consuming endeavor, it's ok to take time off or breaks in between to relax a bit before jumping back into the grind. Thank you to Joe and Alex for your friendship and for emphasizing that regardless of your "expertise" on a topic you can always discover a more optimal way to perform research. To the future students, research doesn't have to be a solo journey. Rely on each other to make that trek a tad less dull and a lot more memorable.

I thank the students that mentored me: Patricia, Will, Karen and Saloni. Thank you for your patience during my first year, I really appreciated it. Further, I would also like to thank the students I had the privilege to mentor: Victoria, Kaytlyn, Sreya, Arjun, Waleed, Reshma, Natalie, Ruhi, Kayla, Shareef, Anna, Manali, Jeena, Kamiya, Dana, Disha, Nurten, Paolo, Arslan, Francis, Abdul, Maria, Aman, and Bose. Each of you have taught me to become a better researcher in some fashion, whether it be questioning my own techniques and thus improving them to the importance of simplicity, clarity of thought and expression. I'd like to acknowledge the watchful protectors of the office, the mom and baby sloths, as well.

Finally, I would like to thank my parents, Ashfaq and Samina, and brother, Usman, for their endless support to help me run this marathon and cross the finish line.

TABLE OF CONTENTS

TABLE OF CONTENTS
(Continued)

TABLE OF CONTENTS
(Continued)

TABLE OF CONTENTS
(Continued)

LIST OF TABLES

LIST OF FIGURES

CHAPTER 1

INTRODUCTION

1.1 A Note on the Text

Majority of the work presented in this dissertation has already been published or is under review for publication. Each chapter (except for Chapter 5) is derived from a journal article and, therefore, a self-contained study, with its own Introduction, Methods and Materials, Results, Discussion, and Conclusion sections (wherever applicable). I acknowledge the co-authors that have assisted me in completing the work described. It is with their help, guidance, and mentorship that I was able to accomplish such a large and varied body of work and I look for every opportunity to thank them. Also, I note the journal, year, and volume number in which the work was published.

1.2 An Introduction to Ischemic Tissue Disease

Ischemic tissue disease is caused by a lack of circulation/blood supply to tissue [1]. Angiogenesis is a crucial component to allow supply of oxygen, nutrient exchange, and prevent tissue necrosis [2]. There are various avenues utilized to induce angiogenesis in tissue engineering strategies, including promoting a pro-angiogenic M2 immune environment, delivery of growth factors such as fibroblast growth factor (FGF), platelet-derived growth factor (PDGF) and vascular endothelial growth factor (VEGF), and stem cell solutions such as mesenchymal stem cells (MSCs) secreting VEGF [3-9]. Further, there are various biomaterials strategies that have been used for promoting angiogenesis and revascularization which include electrospinning grafts, three-dimensional (3D) printing/bioprinting approaches, and cell sheets derived from MSCs to forms tissue

engineered blood vessels [10-14]. However, these strategies have inherent limitations and disadvantages. Tsang et al. outlined various 3D tissue fabrication techniques including utilizing traditional polymer techniques including adhesives or molding, fabrication by cellular assembly, and other techniques however each present unique disadvantages such as limited resolution or fabrication conditions [15]. Recently, Peterson et al. fabricated a collagen-fibrin construct loaded with microbeads that demonstrated angiogenic potential *in vitro*, however their fabrication process is time and resource intensive [16]. Bezgin et al. tested revascularization of platelet-rich fibrin, or PRP, however concluded that it didn't provide any markedly differences compared to traditional scaffolds [17]. Nguyen et al. have shown the development of dentinogenic nanofibrous hydrogels that promote dental pulp stem cell (DPSC) proliferation *in vitro* but did not show efficacy *in vivo* for pulp revascularization [18]. Many promising vascularization strategies require cumbersome cell sourcing or may result in rapid diffusion of bioactive factors from the delivery site with ectopic side effects. There remains a significant need for an off-the-shelf material-based alternative that is injectable, biodegradable, and capable of promoting *in situ* vascularization [19].

Development of an acellular biomaterial that promotes tissue revascularization *in vivo* without added growth factors is an ideal angiogenic solution to revascularization. Hydrogels offer the ability to design an economical 3D scaffold that can aid in particular biological functions, such as cell adhesion and proliferation, and can be delivered to an injury site effectively due to being syringe injected and aspirated. These self-assembling peptide hydrogels (SAPH) have the unique characteristic of these 3D gels that form antiparallel β-sheets, which can be observed by various analytical tests such as circular

dichroism (CD) and Fourier transform infrared spectroscopy (FTIR). These peptide hydrogels consist of a sequence of amino acids, and they can be divided into two portions; the self-assembling domain or "backbone" which self-assembles into these nanofibrous structures and the "mimic", which attaches covalently to the backbone. This work presents strategies for ischemic tissue treatment utilizing a novel proangiogenic self-assembling peptide hydrogel (SAPH) platform, termed SLan. We have shown that this self-assembling peptide (SAP) platform demonstrates injectability, tunable biodegradation, cytocompatibility with HepG2 cells and biocompatibility *in vivo* (subcutaneous implantation in Wistar rats to assess normal-physiological responses). At the molecular scale, SAPH self-assembles into β-sheets in aqueous solution interweaving into nanofibers that mimic the extracellular matrix. Further, owing to non-covalent supramolecular interactions guiding self-assembly, peptides rapidly self-assemble (aggregate into fibers and hydrogels), and exhibit thixotropic behavior. This is exploited to inject rapidly *in situ* gelling scaffolds for therapeutic revascularization.

The objectives of this dissertation are: i) demonstrate angiogenesis of SLan alone or loaded into biodegradable scaffolds and to ii) determine the pre-clinical efficacy of SLan for use in regenerative endodontics and wet aged-related macular degeneration (wet-AMD). Our central hypothesis is that SLan hydrogels represent an acellular approach for therapeutic (micro)revascularization for ischemic tissue. To test this hypothesis, we have the following three aims:

Aim 1: Design, synthesize and characterize SLan. Preliminary work from our lab has shown that angiogenic self-assembling peptides can assemble into long range fibers, while presenting angiogenic domains on the edges of fibers. We have optimized these

scaffolds and present herein the results of this analysis. Our goal is to successfully generate: i) VEGF mimicking peptides, ii) self-assembling peptides that can aggregate into a gel, iii) demonstrate that this gel is injectable and promotes angiogenesis *in vivo*. This will lay the foundation for the *in vivo* efficacy studies in pathogenic disease models in subsequent aims.

Aim 2: Evaluate safety and angiogenic potential of SLan in a canine pulpectomy model. Preliminary data has shown the ability of SLan to promote robust *in vivo* angiogenesis, with excellent cytocompatibility. To ensure the utility of SLan in a disease model, we evaluated the regenerative capacity of SLan in a tissue space which is predominantly perfused with microvasculature – the tooth pulp – in a large animal model – potentially mimicking regeneration in non-human primates/humans. Our goal is to successfully generate scaffolds that provide a niche for the ingrowth of vital pulp from the peri-apical tissue. Native, uninfected pulp, will be extirpated, and then the root canal cleaned and filled with SLan to evaluate the regenerative potential in a normophyiosologic injury model. Pulp regeneration will be evaluated compared to other SAP and carrier control – for regenerated vascularized pulp-like architectures using H&E, Masson's Trichrome and immunostaining.

Aim 3: Characterize SLan in a laser induced CNV model for wet-AMD. Preliminary data have revealed that SLan promotes robust and mature microvessel formation – 15-50 μm diameter, microvessels that are lined with CD31+ endothelial cells and α-SMA+ smooth muscle cells. This suggests that potential angiogenic hydrogels may offer a mechanism to heal the aberrant and immature vasculature growing on the retina in diabetic retinopathy/ wet-Age-related Macular Degeneration (wet-AMD). Scaffolds will be injected into the eyes of laser induced choroid injury models to note the leakiness and

proliferation of vessels. Our goal is to successfully generate: i) scaffolds that do not cause inflammation in the eye, ii) that are well tolerated in the ocular space, iii) reduce leakiness and proliferation of immature vessels.

Altogether, these studies will underscore key translational criteria for angiogenic SAP.

1.3 Cells and Material-based Strategies for Regenerative Endodontics[1]

1.3.1 Tooth Structure

Humans have two sets of teeth: 20 primary/deciduous teeth and 32 permanent teeth [20], each composed of organized, mineralized tissue layers of dentin [21], cementum and enamel [20]. In native tooth architecture, an enamel encased crown surrounds the live internal pulp chamber and roots [20].

Enamel is derived from oral epithelium tissue, while dentin, pulp and periodontium derive from the neural crest (Figure 1.1) [20, 21]. In healthy tooth anatomy, the dentin-pulp complex lies below a continuous layer of ordered enamel, protecting the vessel- and nerve-rich pulp [20]. In the dentin layer, odontoblasts create and regulate tissue matrix components [21, 22]. Epithelial-mesenchymal interactions are essential for the transition of mesenchymal embryonic pulp cells to the pre-odontoblastic stage [22]. Signaling molecules from the inner enamel epithelium encourage differentiation of peripheral dental papilla cells, odontoblast precursors, which eventually become secondary odontoblasts [22].

Human dental pulp stem cells (DPSCs) originate from migrating neural crest

[1]Reproduced from **Z. Siddiqui**, A. M. Acevedo-Jake. A. Griffith, N. Kadincesme, K. Dabek, D. Hindi, K. Kim, Y. Kobayashi, E. Shimizu, V. Kumar. Cells and Materials-based Strategies for Regenerative Endodontics. **Bioactive Materials**. 14 (2022) 234-249.

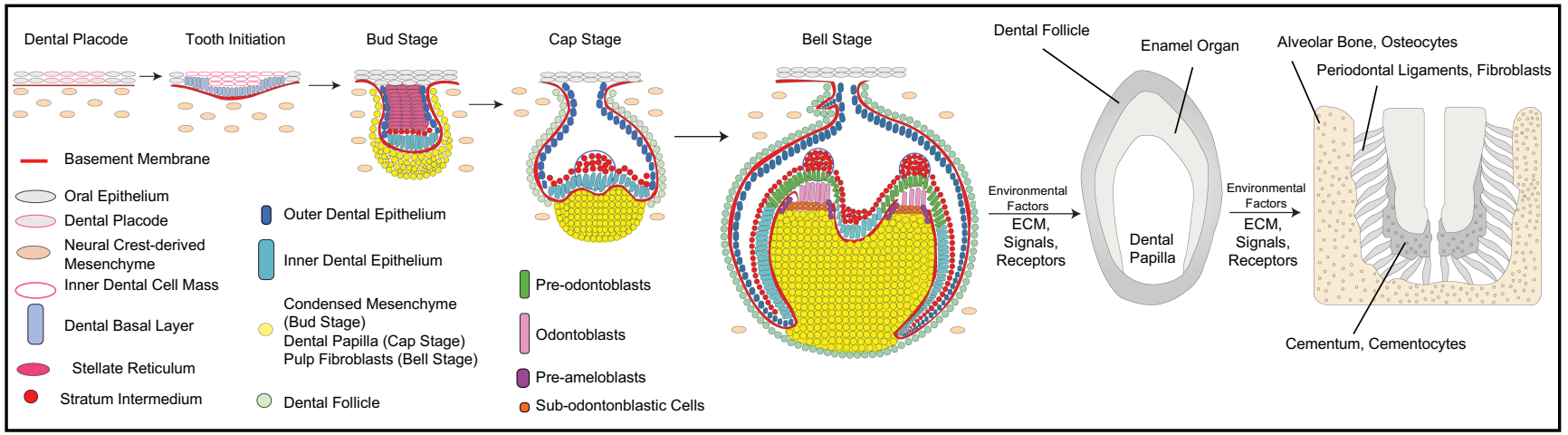

Figure 1.1 Formation of a tooth. Tooth development begins in utero and follows 5 stages: dental placode formation, tooth initiation, the bud stage, the cap stage and finally the bell stage. Environmental factors stimulate tooth maturation further, encasing the dental papilla beneath the enamel organ and dental follicle. Finally, osteocytes foster alveolar bone formation, fibroblasts generate periodontal ligaments and cementocytes deposit cementum.

cells, are derived from the embryonic ectoderm layer and possess mesenchymal stem cell properties [23]. This feature confers them vast differentiation potential, in addition to their ability to secrete trophic factors and their immunoregulatory properties [24]. DPSCs can differentiate into odontoblasts, osteocytes/osteoblasts, adipocytes, chondrocytes, or neural cells [24]. DPSCs can also regenerate dental tissue composed of vascular, connective, and neural tissues [24]. During tooth development, primitive ectomesenchyme becomes enclosed within the prospective teeth to form the dental pulp [25], a rich source of stem cells. Odontogenesis (the process of tooth development) involves the matrix of cell types and specific cellular processes which result in the differentiation, growth, maturation and eruption of developing teeth in the mouth [20].

1.3.2 Tooth Pathology

When the tooth structure is compromised by pathologies such as caries, odontoblasts attempt to seal off dentinal tubules to protect the pulp [20]. The carious process gives rise to the formation of porous lesions which expose and damage organic material which lies below the enamel [21]. At the plaque-enamel border, for example, acids secreted by bacteria demineralize enamel [26] and creates pores of increasing size on the tooth surface; breached enamel leads to pulp involvement via tubular fluid and odontoblastic processes, and requires endodontic intervention [26]. Deep caries with pulp or near pulp involvement are often treated with medical paste or pulp capping to prevent further inflammation and prevent bacterial invasion [27].

The most common cause of traumatic dental injuries is sport-related activity as participation in such sporting activities has increased over the last decade, so has the frequency of such injuries [22], making this type of injury a recognized public health

problem worldwide. In the United States specifically, almost every third child with primary teeth and every fourth adult has evidence of traumatic dental injuries [22]. Traumatic dental injuries are often detrimental for odontoblasts in close proximity to the lesion site, and their cell death triggers activation of dental pulp stem/progenitor cells [28]. Although the exact stored location of these mesenchymal cells is not yet known, this type of damaging event causes these cells to proliferate, migrate and differentiate [28].

Other pathologies that require endodontic intervention include but are not limited to: pulpitis, pulp necrosis, and apical periodontitis including acute and chronic apical abscesses [29]. Apical periodontitis is inflammation caused by a diverse category of microbiota outside necrotic root canals (primary), or improperly treated root canals with persistent infection (secondary) [25]. Both primary apical periodontitis and secondary apical periodontitis-causing bacteria exacerbate other systemic diseases in patients. Although approximately 200–300 bacterial species can be cultured from samples collected in the oral cavity, only few of these species have been isolated from necrotic root canals [23]. This area is populated by strictly anaerobic bacteria. The identification of bacterial taxa differentially abundant in primary and secondary infections may provide a basis for targeted therapeutic approaches aimed at reducing the incidence of apical periodontitis [24]. If bacteria from the oral microbiome gain systemic access, this leads to systemic ailments such as bacteremia, endocarditis and atherosclerosis [30].

1.3.3 Treatment Options

Currently root canal treatment and apexification are two standard treatment options available in the clinic [31]. Choice of procedure depends on the stage tooth development. Apexification is appropriate for immature permanent teeth with open apexes, whereas root

canal procedure is more suitable for mature teeth with closed apexes [32]. Application of these techniques, however, results in the loss of tooth vitality [33]. Conversely, if the pulp is partially vital with no inflammation present, then irreversible pulpitis, pulpotomy and pulp capping procedures can be considered to treat exposed pulp [33, 34].

1.3.3.1 Conventional Root Canal Treatment. Conventional root canal procedures (Figure 1.2) [31] remove inflamed pulp and repair root canal structure, rather than focusing on tissue regeneration [35], have been standard treatment options and have been well described elsewhere [36-39].

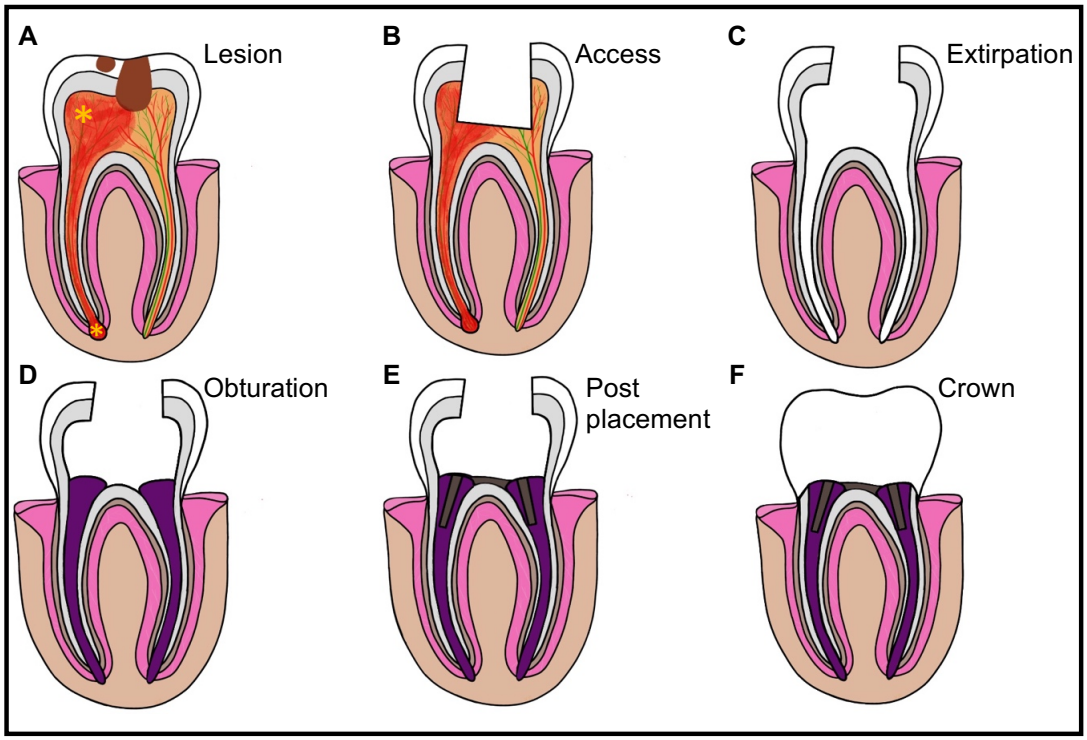

Figure 1.2 Endodontic treatment of an apical tooth abscess with concurrent caries. (A) A diseased tooth with caries results in soft tissue inflammation and damage to tooth enamel, exposing the pulp. Initially (B) access to the pulp is obtained to (C) extirpate inflamed and necrotic tissue and disinfect the tooth cavity. (D) Obturation fills the emptied tooth, typically employing inert materials such as gutta-percha. Treatment is completed with (E) post and core installation and finally (F) placement of an artificial crown to form a protective barrier.

Table 1.1 A Comparison of Current Disinfectants used in Endodontic Procedures

Material	Advantages	Disadvantages	Ref.
Sodium Hypochlorite (NaOCl)	Bactericidal Tissue dissolution	Not biocompatibile Inactivates dentin-matrix components Altered tissue mechanical properties	[31, 47, 48]
Saline	95% bacterial reduction when used with instrumentation	Insufficient sanitization	[49]
EDTA / Citric Acid	Growth factor solubilization Dentin formation Antimicrobial	Dentin erosion	[47, 49]
Chlorhexidine (CHX)	Highly effective against yeast, gram-positive and gram-negative bacteria	Lack of tissue dissolving properties	[49]
MTAD and Tetraclean	Easy removal of smear and organic layer in infected canals	Does not treat infection	[49]
Calcium Hydroxide	Strongly antimicrobial	Cytotoxic upon long exposure	[49]
Triple Antibiotic Paste (TAP)	Strongly antimicrobial	High concentration lowers cell survival and proliferation	[49, 50]

Table 1.2 Commonly used Materials Categorized by their Procedure Type

Procedure	Material	Advantages	Disadvantages	Ref.
Obturation	Gutta-percha	Stable Biocompatible Low toxicity	Low adhesion Microleakage	[51-53]
	Resin	Good seal formation tooth strengthening	Limitations in physical and mechanical properties	[51]
Apexification	Calcium Hydroxide	Strengthens immature roots	Long application process Lowers mechanical strength of tooth	[48]
	Mineral Trioxide Aggregate (MTA)	Biocompatible Sterile One-step Superior sealing ability Stimulates high quality/quantity dentin	Expensive Best suited for revascularization	[48, 51, 54]
Pulp Capping	Calcium Hydroxide	Bactericidal Promotes odontoblast differentiation High pH	Poor bonding to dentin can cause secondary inflammation	[55-57]
	Mineral Trioxide Aggregate (MTA)	Bactericidal Low solubility Good sealing properties Thick and fast dentin-bridge formation, Biocompatible	Expensive Long setting time Tooth discoloration Poor mechanical properties	[55, 56]
	Biodentine	Dentin-like mechanical properties organized odontoblast layers stimulates dentin-bridge formation	Not significantly different from MTA	[58, 68]

Materials and techniques used in the disinfection, filling or sealing processes affect the overall success of the procedure [40, 41], and today many different disinfectants (Table 1.1), core materials and sealers (Table 1.2) are available to clinicians when performing traditional root canals [42].

While roots canals show a high success rate in treating apical periodontitis, teeth that undergo root canals lose vitality and important functions like dentin formation, and root thickening, lengthening and maturation [31, 43], giving rise to teeth which are non-vital, brittle, prone to reinfection, and susceptible to fracture [33]. A retrospective study showed treatment success is highly dependent on the correct canal filling length and the position of the treated tooth, with posterior teeth showing greater healing rates than anterior teeth [44]. When this endodontic procedure fails, other treatment options include revision, apicoectomy or finally, extraction. This is generally not preferred because of negative effects on oral health and quality of life [45, 46]. Improper or incomplete extraction of the tooth also results in physical, financial, and emotional burden to the patient [47].

1.3.3.2 Apexification. Apexification offers another strategy to treat immature dental pulp with open apexes (without apical closure) [34, 48, 49]. In this technique, a mineralized barrier, such as CH or MTA, is placed near the apex of the root for the closure [48-50]. MTA is preferable to materials such as CH for this step as it has few negative effects on dentin anatomy and performance, does not require multiple follow-up clinical visits and has a significantly higher success rate [34, 51]. MTA plugs, however, are markedly more expensive, and overall apexification as a treatment option does not show great potential for root maturation or immunity, both required for tooth vitality and development [34, 48-50].

Because of this, vital pulp therapies offer an attractive alternative to preserve tooth functionality while preventing the tooth loss.

1.3.3.3 Vital Pulp Therapy and Apexogenesis. Vital pulp therapy (VPT) treats teeth with partially vital pulp or reversible pulpitis [52] and maintains pulp tissue vitality and root maturation [53], making it more desirable than traditional root canal therapy. Apexogenesis is a similar technique to apexification (applied on necrotic pulp) and can only be applied to the immature permanent teeth with open apexes (without apical closure) and with some remaining vital pulp [34]. In apexogenesis, the inflamed pulp tissue is removed, and an apical barrier agent (typically CH or MTA) is applied along healthy portion of the pulp [32, 34]. Final outcomes include root, and dentin-bridge formation, and continued physiological tooth development, although these results may take up to 2 years to fully realize [32].

1.3.3.4 Pulpotomy and Pulp Capping. Direct pulpotomy and pulp capping treat exposed vital pulp while avoiding necrosis [33]. A pulpotomy removes infected, inflamed pulp, prevents the spread of infection and ensures the health and function of unaffected pulp [54]. If tooth inflammation is not severe, pulp capping is used to establish a protective barrier, protecting the tooth interior, maintaining pulp vitality, fostering healthy regeneration and dentin bridge formation [55]. Pulp capping is either direct or indirect; in indirect pulp capping, pulp tissue is not exposed, and a biomaterial is applied to the thin dentin layer already present [54]. In direct pulp capping, the biomaterial is applied directly as an interface against the remaining exposed vital pulp tissue, creating a seal to prevent further exposure to the oral environment. Similar to indirect pulp capping, direct pulp capping helps maintain pulp integrity and vitality, and facilitates tertiary dentin formation [54-56].

Pulp capping is well-suited for immature permanent teeth, as it helps stimulate root maturation, an outcome not observed in apexification [56]. Ultimate treatment success, however, is highly dependent on the capping material [43]. The final deciding factor between pulpotomy and pulp capping is related to infection severity, with more severely infected teeth undergoing the former [55]. Despite their potential, insufficiencies still exist in current treatments, including a lack of data on long-term efficacy [57], reliably preventing bacterial contamination, minimizing scar tissue formation [43], and the formation of new dentin structures which are imperfect or irregular [33]. Many of these shortcomings are being addressed by newly emerging biomaterial strategies, discussed later.

1.3.4 Dental Tissue Regeneration

Dental pulp regeneration is a new and developing technique for dental procedures aimed at revitalizing infected, necrotic or lost dental pulp to restore natural functions such as mineralization, pulp immunity and sensitivity [58]. This technique incorporates and balances three main components: cells (mostly stem cells), bioactive molecules (generally growth factors), and scaffolds.

Regenerative signals can originate from growth factors, the scaffold, plasma or cells such as dentin/odontoblasts, pulp fibroblasts or endothelial cells [59]. The release of dentin-originated bioactive molecules is stimulated by bacterial acids produced during caries-restoring procedures, or the placement of MTA or calcium hydroxide agents during pulp capping [59, 60]. The secretion of bioactive molecules and growth factors by odontoblasts and their incorporation within the dentin extracellular matrix (dECM) leads to dentin production (dentinogenesis). Some growth factors utilized in dECM by calcium

hydroxide, white MTA, and grey MTA include VEGF, FGF-2, PDGF, transforming growth factor-beta 1 (TGFβ-1), and insulin like growth factors (IGF-1, IGF-2) [59, 60]. Pulp fibroblasts and endothelial cells are other sources of growth factor release for specific tasks such as cell migration, proliferation, differentiation, and angiogenesis.

Newly regenerated dentin-pulp tissue must be similar to the original tissue, which consists of well-organized connective dentin tissue and live vascularized, innervated pulp. Currently, most studies focus on revascularization and dentin deposition of new tissue [61]. Revascularization procedures show promising results for immature teeth and are easier to apply in the clinic. Tissues formed in the root canal with this procedure, however, are not consistently representative of native true dentin-pulp complex [35, 62]. Studies still struggle to regenerate a new pulp which is morphologically and functionally similar to natural pulp [48]. In addition to vascularization and proper soft tissue regeneration, success criteria for the regeneration includes observing remineralization cell-matrix interactions, innervation, growth factor incorporation, controlled bio-degradation, and pathogen control and mitigation in the regenerated tissue [43]. Observation of tooth changes such as apical closure, root lengthening, radiographic criteria, and dentin wall thickening suggest improved root maturation, dentinogenesis (formation of dentin), and wound healing [48, 50, 63]. Additionally, the direct availability of the cell constructs is important, especially for older patients who may not have enough autologous cells to recruit [18, 35, 48, 50, 62, 64].

One approach to achieve dentin-pulp regeneration is cell-based therapy, or cell transplantation [61]. Via this method, many different cells (mostly stem cells) are isolated and cultured *in vitro*, and then placed in an appropriate scaffold to be inserted into the root

canal [61]. Similarly, a second cell-guided route to generate dentin-pulp complex is through endogenous regeneration, or cell homing. In this method a specialized niche is created at the injury site for host cell mobilization and homing. This site is also amenable to native cell proliferation and differentiation for repair [65]. Kang et al. at the University of California are conducting a clinical trial in which mesenchymal stem cells are implanted within the dental cavity to assess its angiogenic potential in dental pulp revascularization; one of many ongoing clinical trials for dental regeneration (Table 1.3).

Table 1.3 Clinical Trials and their Strategies to Treat Dental Pathologies

Strategy	Trial Size	Clinical Trial	Ref.
Tissue transplantation	50 participants (7 – 50 y.o.)	N/A	UCLA School of Dentistry, Unites States of America
Apexification/revascularization	30 participants (7 – 25 y.o.)	Phase 4	University of Liverpool, United Kingdom
Pulp necrosis with biodentine and MTA	26 participants (8 – 15 y.o.)	N/A	Cairo University, Egypt
Pulp necrosis	80 participants (7 – 12 y.o.)	N/A	Fourth Military Medical University, China
Pulp necrosis with MTA, double antibiotic paste & triple antibiotic paste	10 participants (7 – 60 y.o.)	Phase 1	The University of Texas Health Science Center at San Antonio, United States of America
Revascularization with antibiotic paste and MTA	30 participants (7 – 25 y.o.)	Phase 4	University of Liverpool, United Kingdom
Revascularization with triple antibiotic paste, ciprofloxacin/propolis, ciprofloxacin/metronidazole and propolis/metronidazole	40 participants (8 – 18 y.o.)	Phase 4	Ain Shams University, Egypt

To avoid the complications of harvesting and maintaining one or multiple cell types, some methods employ growth factors to promote the migration, proliferation, and differentiation of local stem cells. Much recent research in the field of hard and soft tissue dental regeneration has focused on the use of materials, such as traditional and bioceramics, naturally derived biomaterials and scaffolds, and synthetically prepared materials, all matrices which themselves can be used or tuned to serve as origins of

regenerative signals. Exciting new research in synthetic biomimetic materials recapitulates aspects of each of these materials, giving rise to simply formulated sophisticated materials to guide hard or soft tissue regeneration. Below we discuss each of these approaches in detail, and for each category highlight recent work regarding tissue regeneration in the dental niche.

1.3.4.1 Stem Cell-based Therapies. Many cell types have been used successfully in cell-based pulp cell-matrix interactions, innervation, growth factor incorporation, regeneration studies (Figure 1.1) [58, 66-75]. Adult mesenchymal stem cells (MSCs) are common as they can differentiate into many specialized tissues and cell types which are crucial for maintaining tooth homeostasis, including odontoblasts (cells that produce dentin), chondrocytes, myocytes, and adipocytes [31, 55]. Most (though not all) stem cell populations in the tooth share properties of bone marrow-derived mesenchymal stem cells, also called dental mesenchymal stem cells [76]. Five dental stem cells involved in tooth formation are: DPSCs, stem cells from human exfoliated deciduous teeth (SHED), stem cells from the apical part of the dental papilla (SCAP), periodontal ligament stem cells (PDLSC), and stem cells from the dental follicle (DFSC) [55], all named according to their tissue of origin. DPSCs, SHED and SCAP are especially crucial in pulp regeneration studies since they are derived from native pulp or precursor tissue [55]. In addition, when dental epithelial stem cells (DESCs) are combined with dental mesenchymal stem cells, the mixed population together can regenerate a dentin-enamel-like complex structure [31].

When using DPSCs for dentin pulp tissue regeneration, the effect of appropriate growth factors must also be investigated and understood. Growth factors are released from multiple sources, including stem cells themselves, dentin, other cells, or scaffold materials,

all of which work together to regulate the behavior of immature undifferentiated DPSCs [30]. Growth factors induce cell proliferation, angiogenesis, and neovascularization, all essential steps in the tissue regeneration process [30-32]. Signaling molecules work in together with chemotactic agents and other signaling factors to attract stem cells to the defect site in need of repair and stimulate local regeneration [31, 32]. These polypeptide growth factors mediate a wide range of functions, such as enhancing DPSC migration through three-dimensional (3D) collagen gels (stromal cell-derived factor-1, SDF-1, and basic fibroblastic growth factor, bFGF) and odonto/osteogenic differentiation (bone morphogenic protein BMP7) [32].

Pulp regeneration is specifically associated with vascular endothelial growth factor (VEGF), bFGF, platelet-derived growth factor (PDGF), nerve growth factor (NGF), and BMP7 [31, 32]. VEGF plays a critical role in angiogenesis and revascularization as it binds to heparin and increases endothelial cell proliferation and neovessel formation [31, 32]. bFGF has angiogenic potential and recruits DPSCs to migrate and proliferate without differentiating [32]. Platelets release PDGF which is important in cell proliferation and angiogenesis [31]. PDGF can significantly enhance DPSC proliferation and odontoblastic differentiation [33]. NGF expression is high during tooth development and at areas of tooth defects, when it aids in the survival and proliferation of sensory and sympathetic neuronal cells [33]. Finally, BMP7 induces dentin formation (dentinogenesis) [31].

Gronthos et al. utilized MSC-like stem cells from dental pulp tissue obtained from human third molars, termed dental pulp stem cells [77]. Distinct advantages of SHED over DPSCs include a higher proliferation rate and enhanced differentiation potential. Sonoyama et al. confirmed that SCAP arise from the soft tissue at the tooth apex [78].

Besides dental stem cell-based approaches, non-dental stem cells are also used in tooth and periodontal tissue regeneration, including bone marrow-derived mesenchymal stem cells (BMMSCs), adipose-derived stem cells (ADSCs), embryonic stem cells (ESCs), neonatal stem cells from the umbilical cord, and induced pluripotent stem cells (iPSCs). iPSCs' ability to differentiate into mesenchymal stem cells and osteoprogenitor cells makes them an attractive choice for dental tissue regeneration [31, 55]. Additionally, as they are produced by adult somatic cells (which cannot further differentiate back to a pluripotent condition), iPSCs are a good alternative for older patients who no longer have sufficient pulp tissue for regeneration [48].

For *in vivo* observation of pulp-dentin regeneration, many different animal models are used to test cell-based therapies [79]. Initial studies were conducted on small animals such as mice and rats due to their accessibility [64]. Larger animal studies, however, such as those that employ dog and swine models, provide an environment more similar to human oral tissue [64]. Scaffolds based on various natural, synthetic or hybrid materials have been used carriers in these studies [80]. The scaffold creates a supportive environment for stem cell delivery to the pulp and can provide or mimic growth factors to enhance and guide differentiation [80, 81]. Cordeiro et al. observed the successful differentiation of SHEDS into odontoblast-like and endothelial-like cells *in vivo* by transplanting the cells into immunocompromised mice within a biodegradable scaffold [82]. Zhang et al. used a composite of hydroxyapatite (HA), silk fibroin (SF) and ultra-small super paramagnetic iron oxide (USPIO) as a scaffold for the delivery of DPSCs [83]. HA and SF were biocompatible, biodegradable, had desirable mechanical properties and fostered DPSCs proliferation and osteoinduction *in vivo* to regenerate dental pulp tissue [83]. Additionally,

because of their paramagnetic properties, USPIO could be used for noninvasive imaging[83]. Gronthos et al. demonstrated successful dentin/pulp-like tissue regeneration *ex vivo* using DPSCs embedded in a hydroxyapatite/tricalcium phosphate (HA/TCP) scaffold; transplantation of their material into 10 week old immunocompromised mice gave comparable results to controls employing bone marrow stromal cells (BMSCs)[77]. Xuan et al. inserted DPSC aggregates into the root canals of human teeth and implanted the root subcutaneously into female immunocompromised mice for 8 weeks; notably this study observed the *in vivo* differentiation of DPSCs into sensory neurons [84]. In another study, a copolymer of a poly-D,L-lactide and glycolide (PLG) scaffold included SCAPs and DPSCs, and was subcutaneously implanted to female severe combined immunodeficient mice (6–8 week old) for 3–4 months. After explanting, a continuous layer of dentin-like tissue was observed on the canal dentinal wall. At the study conclusion, well-vascularized pulp-like tissue regenerated in the root canal space [85]. Large animal models such as swine have also been used to develop pulp and dentin regeneration strategies. In one study, dentin regeneration was achieved through mixing porcine deciduous pulp stem/progenitor cells (pDPSCs) with a β-tricalcium phosphate (b-TCP) scaffold [86]. Xuan et al. isolated and implanted DPSCs into the empty root canals of female minipigs *in vivo* and saw vascular, innervated tissue regeneration within the odontoblast layer (Figure 1.3) [84].

Similarly, Xuan et al. conducted a study on young patients (aged 7–12) with injured teeth using a cell-based method and electrical pulp tests to assess the pulp vitality [84]. The periapical tissue was probed to induce bleeding and induce subsequent clot formation in the apical foramen. Successful regeneration of ordered 3D pulp tissue with new blood

vessels and sensory nerves was observed, and promisingly, in follow-up studies, closure of apical foramen and elongation of roots were noted [84].

In a different study, autologous pulp stem/progenitor (CD105+) cells and stromal derived factor-1 (SDF-1) were combined in a collagen scaffold and transplanted into canine root canals [87]. After 14 days, the CD105+ cells expressed angiogenic and neurogenic

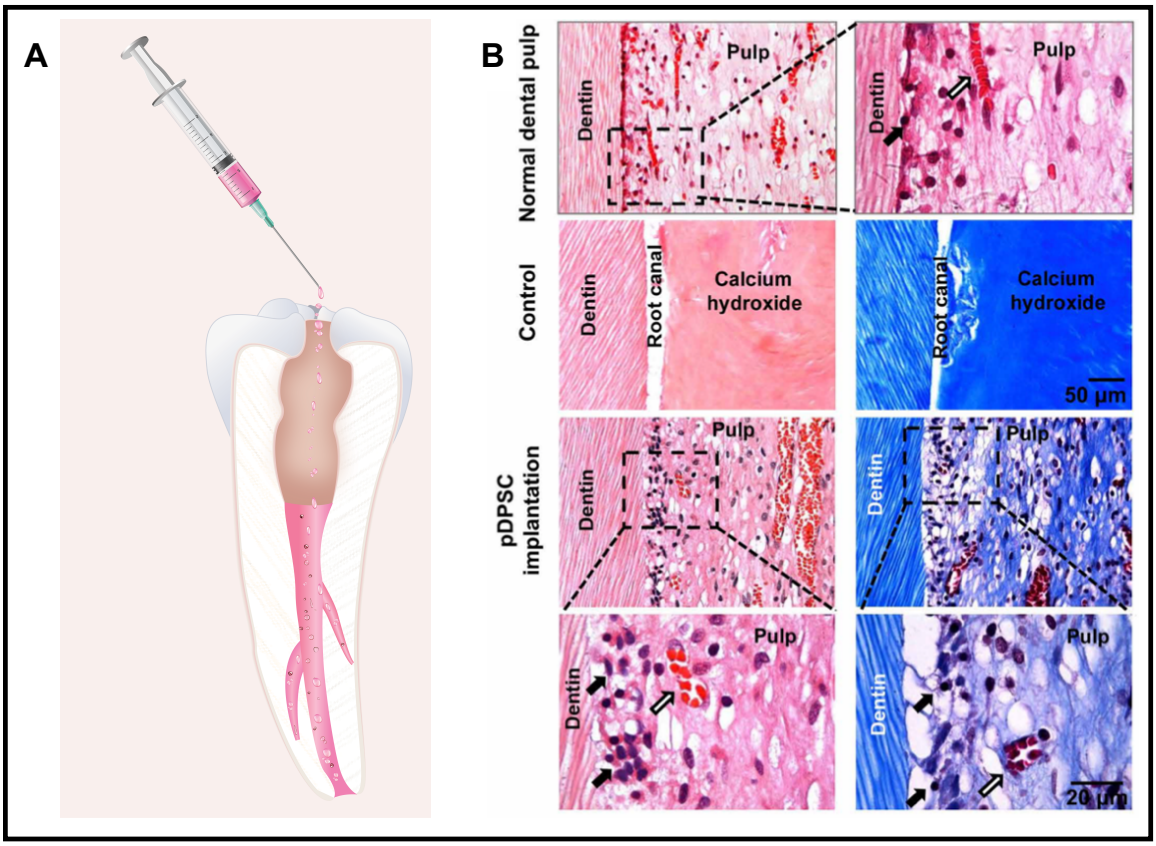

Figure 1.3 Procedure and histological analysis of pig DPSCs implanted into minipigs. A) Pig DPSCs (pDPSCs) were implanted into permanent incisors of minipigs after pulpectomy (n=3). B) H&E staining (left) and Masson staining (right) demonstrate pulp tissue regeneration 3 months after pDPSC implantation. As a control, CH instead of pDPSCs was inserted into young permanent incisors in minipigs (n=3). After 3 months, no pulp tissue was regenerated and only calcium hydroxide was observed. Normal pulp tissue of minipigs was stained for comparison (top). Scale bar, 50 μm. Enlarged images show odontoblasts (black arrow) and blood vessels (open arrow) in select regions of regenerated pulp tissue. Scale bar, 50 μm.

Source: K. Xuan, B. Li, H. Guo, W. Sun, X. Kou, X. He, Y. Zhang, J. Sun, A. Liu, L. Liao, S. Liu, W. Liu, C. Hu, S. Shi, Y. Jin, Deciduous autologous tooth stem cells regenerate dental pulp after implantation into injured teeth, Science Translational Medicine 10(455), 2018.

factors, and regeneration of pulp tissue was seen [88]. Similarly, Itoh et al. prepared DPSC constructs by shaping sheet-like aggregates of DPSCs with a thermosresponsive hydrogel and showed stem cells within the constructs remained viable after prolonged culture [66]. Pulp-like tissues rich with blood vessels formed within the human tooth 6 week post subcutaneous implantation in immunodeficient mice [66]. The authors also noted DPSCs in contact with dentin differentiated into odontoblast-like cells [66].

For patients who do not possess enough native tissue for endogenous MSCs, recent methodologies have developed induced MSCs (iMSCs) which led to the acquisition of stem characteristics and an epithelial-mesenchymal transition [58]. These cells generate normal human epidermal keratinocytes (NHEKs) through the epithelial-mesenchymal transition [48]. Although these studies have promising results, this procedure is challenging to apply under clinical conditions [66, 89]. Some current challenges still facing cell-based therapies include the high expense of current good manufacturing practice (cGMP) facilities, a lack of information in the scientific community regarding the outcome of allogenic dental MSC for pulp/dentin regeneration, a lack of a centralized dental stem cell banking system, and a lack of recognition and practice of cell-based pulp/dentin regeneration therapies by the medical field [90]. In addition, these complicated procedures remain more difficult to obtain procedural approval [89].

Stem cell sheets have been explored as an alternate strategy to promote dental pulp regeneration. Hu et al. cultured and fabricated three stem cell sheets from cell types located within and around the vital pulp:DPSCs, periodontal ligament stem cells (PDLSCs) and SCAPs [91]. Several *in vitro* assays were performed to determine biocompatibility and the stemness of these sheets including RT-PCR to evaluate OCT4, SOX2 and TERT

expression. Further, the authors stained for various marker genes such as collagen type-1 and fibronectin. All 3 sheets retained the expression of these markers and there was no distinguishable difference between the scaffolds in signaling. The 3 stem cell sheets were then implanted subcutaneously in 10 week old immunocompromised binge mice for 8 weeks, explanted and processed for histology. The SCAP stem cell sheet displayed significantly greater mineralization and fibronectin expression compared to the DPSC and PDLSC sheets [91]. This strategy, while time consuming, provides encouraging alternative solutions for mineral tissue regeneration.

In a cell-homing technique, instead of an exogenous scaffold, a blood clot is created within the pulp canal to itself act a scaffold [90, 92, 93] and recruit endogenous cells via native growth factors (GFs) [61, 90]. Fibroblasts and fibrocytes are the greatest contributors to the regenerative response and GF expression. Duncan et al. observed that the revitalization of pulp-like tissue is possible with the release of selected exogenous GFs with transplanted stem cell scaffolds [94]. Kim et al. used bFGF, VEGF, PDGF, NGF and BMP-7 to promote angiogenesis and mineralization after 3 weeks. In their study, teeth which had already undergone endodontic treatment were implanted subcutaneously filled with either a cytokine-loaded or cytokine-free collagen gel into 5–7 week old male mice [92].

Blood clot formation for revascularization is the most common of the cell-homing strategies applied clinically for dentin-pulp regeneration [51, 84]. In 2011, the American Dental Association (ADA) approved the use of apical revascularization (AR) as a new treatment modality [95]. The regeneration of pulp is stimulated by localizing blood into the entire root canal. This procedure is applied either by over instrumentation or using platelet-

rich plasma (PRP), platelet rich fibrin (PRF) or autologous fibrin matrix [96]. Over-instrumentation is a strategy in which a blood clot is induced to form a fibrin-based scaffold, and has the highest effectiveness in the adult population [72]. Although this technique is generally used to treat pulp necrosis, it can only be used for immature teeth with open apices and is only acceptable for teeth with completely developed roots [95].

Periapical radiography with paralleling can help monitor root development [97]. Although some clinical studies showed positive results using sensibility test after regenerative endodontic treatment (RET), there is limited histological tooth data [55, 97]. Without any histological analysis, regeneration cannot be observed or confirmed radiographically. Shimizu et al. conducted the first study to determine the histological results of regeneration/revascularization in the root canal of necrotic immature permanent human teeth with irreversible pulpitis (Figure 1.4A) [98]. The approach proved successful and at 3.5 weeks after the revascularization procedure, loose connective tissue and collagen fibers were observed in the canal (Figure 1.4A). Spindle-shaped fibroblasts or mesenchymal stem cells were observed at the periapical area, as well as blood vessels and cellular components inside the canal (Figure 4.1B). Also, odontoblast-like cells were observed along the pre-dentin and root apex surrounded by epithelial-like cells. No nerve fibers were observed however (Figure 4.1B) [98].

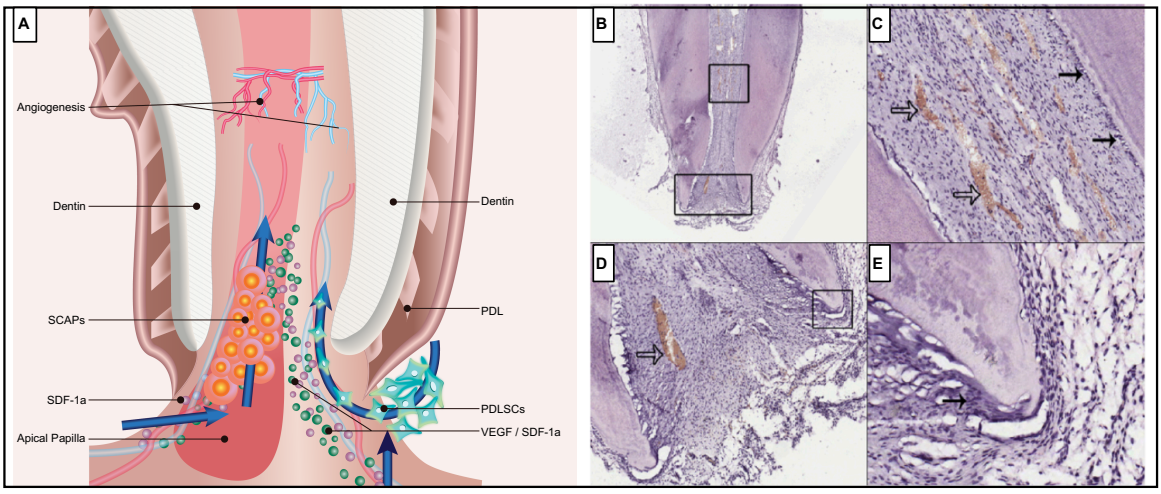

Figure 1.4 Schematic representation and histologic observation of a human immature permanent tooth with irreversible pulpitis after revascularization/regeneration procedure. (A) Migration of cells (PDLSCs, SCAPs) and growth factors (VEGF, SDF-1a) into the tooth interior promotes angiogenesis in the tooth cavity. (B) Histology of an extracted revascularized tooth, from which the MTA plug was removed prior to histological tissue processing. Connective tissue and collagen fibers fill the canal space. (C) A higher magnification image of the square in B showing the apical root canal. Solid arrows indicate flattened odontoblast-like cells lining the predentin, and open arrows reveal the presence of many blood vessels filled with red blood cells. (D) A higher magnification image of the rectangle in B showing the apical foramen. The presence of blood vessels is indicated by arrows. (E) A higher magnification image of the square in D showing part of the root apex. Arrows indicate layers of epithelial-like HERS surrounding the root apex.
Source: E. Shimizu, G. Jong, N. Partridge, P.A. Rosenberg, L.M. Lin, Histologic observation of a human immature permanent tooth with irreversible pulpitis after revascularization/regeneration procedure, Journal of Endodontics 38(9), 2012.

By bleeding induction, MSCs can be delivered into the root canal space and irrigators such as EDTA can promote growth factor release from dentin [48]. In a pilot clinical study, mobilized dental pulp stem cells (MDPSCs) were transplanted into 5 patients; 3 showed successful dentin formation, though further extended studies are still required to allow dentin to fully cover pulp tissue and prevent microleakage [99]. Clinical study shows that when revascularization is supplemented with a PRP scaffold carried on a collagen sponge, a better healing process is observed than in the induced revascularization group (Figure 1.5) [63]. This might be due in part to specific advantages that the PRP

provides, including growth factors, anti-inflammatory agents, cell differentiation signals and the ability to modulate the inflammatory response [54].

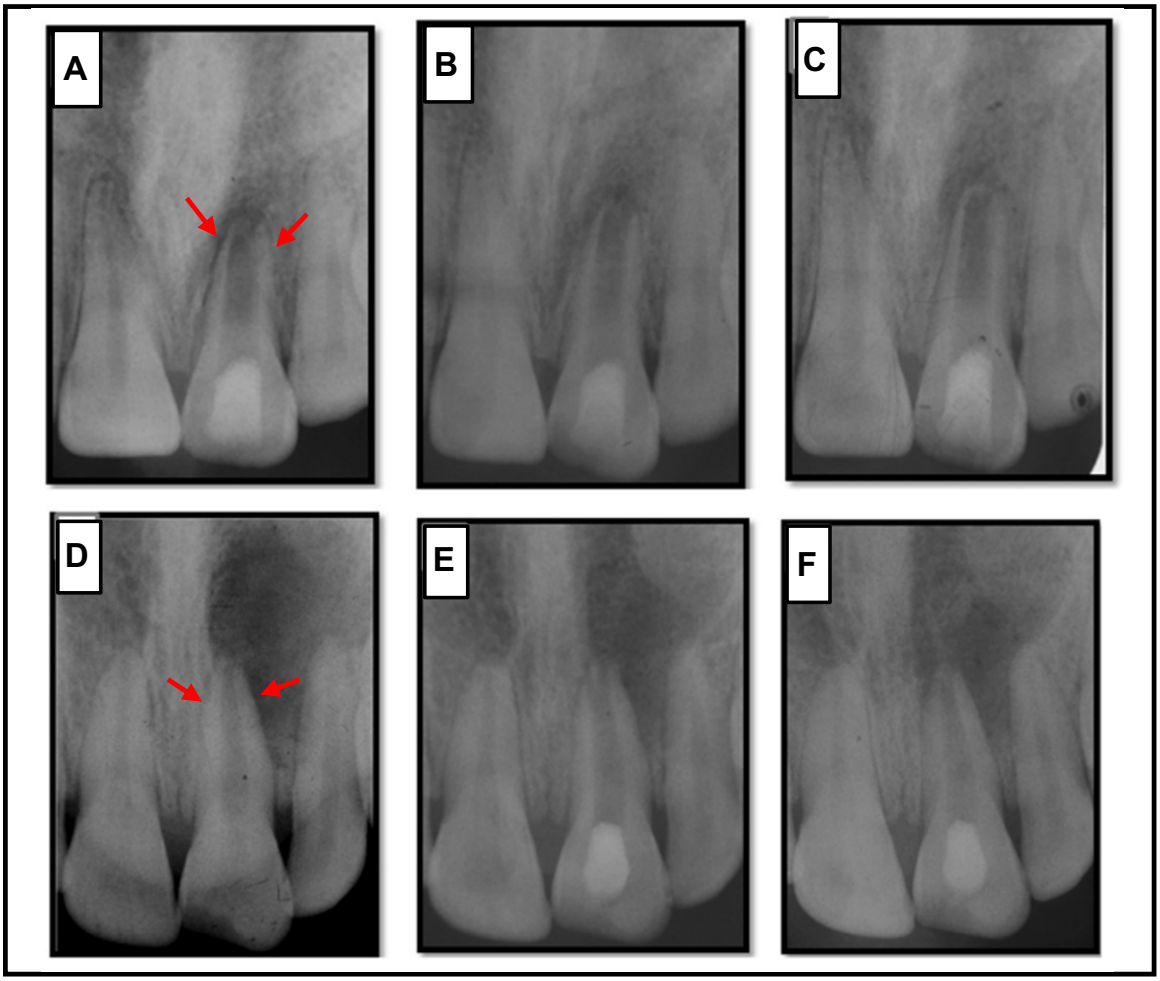

Figure 1.5 X-ray of teeth with revascularization. (A–C) Show teeth with revascularization. (A) The dentinal walls (red arrows) for this patient, a 9 year old girl, are thin with a larger opening at the apex. (B) After 6 months, there is calcification present at the apex. (C) After 1 year, revascularization of the tooth is achieved, primarily through the bridge composed of calcium at the apical section and root lengthening. (D–F) Show teeth with revascularization and PRP. (D) Similar to above, the dentinal walls (red arrows) are thin with a larger opening at the apex for this patient, a 15 year old boy. This patient underwent a treatment an identical procedure however supplemented with PRP. (E) At 6 months, the calcium barrier was reduced at the apex compared to the 9 year old girl and the patient reported to be symptom free. (F) After 1 year, revascularization of the tooth is successful and is comparable to a normal apical tooth.
Source: G. Jadhav, N. Shah, A. Logani, Revascularization with and without platelet-rich plasma in nonvital, immature, anterior teeth: a pilot clinical study, Journal of Endodontics 38(12), 2012.

While revascularization is easier to perform in a clinical environment compared to a stem-cell based therapy, it still has some inherent limitations [89, 90]. The successful release of growth factors depends on many different elements, including disinfection or rinsing after endodontic access and the total migration of stem cells [94, 100-103]. In addition to growth factor release, to protect the thin root canal walls and stem cell vitality at the apical tissue for eventual root maturation, lower concentrations of disinfectants (mostly NaOCl and EDTA) and intracanal medicaments (TAP or CH) are preferred for regenerative applications [48]. Some studies show, however, that this causes incomplete disinfection [48]. Having too few cells recruited may also affect or impede the root development, and cause insufficient bleeding [48]. Besides these complications, to date, the observation of revascularization is associated with regeneration of the entire dentin-pulp complex. Despite these promising lead results, further studies need to be conducted to develop robust methods to properly deliver signaling molecules and regenerate an organized 3D pulp structure [55].

1.3.5 Cell and Materials-based Strategies

1.3.5.1 Endodontic Treatment using Traditional Ceramics. While cell and growth factor-based strategies show good promise for regenerative endodontics, materials-based strategies have traditionally pervaded clinical applications, with the majority of these to date based on ceramics and geared toward apexification, apexogenesis and pulp capping [104]. Generally, these materials have a high pH to help neutralize the low pH environment of the oral cavity [54]. CH and tricalcium-silicate materials, especially MTA, are the two most often used in the clinic [105]. CH is desirable because of its reliability, bactericidal properties and ability to promote odontoblast differentiation. It has known drawbacks,

however, including poor bonding, long-term failure, tunnel defects, and incomplete sealing resulting in microleakage [54]. Pulp capping studies with MTA have also been successful [56] because of MTA's high biocompatibility and antibacterial properties. This material sets in the tooth with a significant hardness and then presents with a low solubility [54], giving it better long-term outcomes in clinical studies compared to CH [105]. Additionally, Tomson et al. studied the effects of pulp capping agents on bioactive molecule release and observed MTA releases more bioactive molecules than CH, helping partially explain better patient outcomes with MTA treatment [60]. In pulp capping, MTA is also associated with the formation of a thicker layer of odontoblasts in the dentin bridge [54]. Known disadvantages of MTA include its high cost, tendency for discoloration of the tooth, and weak mechanical properties, features which are being addressed and improved upon by current materials research [54, 105]. A recent alternative to MTA in pulp capping, Biodentine is a bioactive tricalcium silicate [106] with dentin-like properties. When in direct contact with vital pulp tissue, it facilitates the generation of dentine. A comparative study between Biodentine and CH showed Biodentine was more effective in creating an extended, thick and homogenous dentine-bridge, resulting in a better barrier to completely seal tissue pulp [107]. Biodentine shows a promisingly high success rate (82.6%) as a pulp capping agent, though patient age does affect the observed outcome [106].

While there have been significant advances improving the cytocompatibility of glass and ceramic biomaterials for regenerative endodontics, there is still a need for pulp capping agents which can facilitate new tissue growth. Tailored amorphous multiporous TAMP scaffolds, composites of calcium oxide and silicates, are a promising new class of material which has demonstrated robust regeneration and preservation of bone and soft

tissues [87, 108-110], and more recently shown good biocompatibility as a pulp capping agent with human and swine DPSCs *in vitro* and with pulp *in vivo* [111]. After 4.5 month testing in mini-swine, the presence of remaining TAMP and new mineralized dentin bridge tissue has formed in all cases, and is the first instance of this type of material being tested for dental applications to be followed up by further large animal *in vivo* studies [111].

1.3.5.2 Naturally Derived Biomaterials and Scaffolds. A notable disadvantage of both the new and traditional approaches outlined above is the lack of extracellular matrix (ECM) or ECM-mimetic scaffolds to support cell proliferation and differentiation, crucial to long-term tooth vitality and tissue homeostasis. Materials-based strategies that combine the previous approaches, or which confer inherent bioactivity to guide regeneration, will prove most efficacious long-term, and below we highlight timely examples which harness naturally derived scaffold materials.

In these applications, naturally derived materials are often synthetically modified or prepared as material composites to improve and tune their physical and biological properties. In one recent example, xenograft equine bone hydroxyapatite modified with a poly(E-caprolactone) was generated to recapitulate the morphological and biochemical features of native bone, and notably did not induce infection or immune response [112]. The authors report that an increase in the bioceramic content improved calcium deposition, cell viability and osteogenesis [112]. Electrospinning of these solutions generated aligned mats of nanofibers which were better able to promote osteogenic differentiation in DPSCs than controls [112], in line with previous reports that show aligned structures significantly improve cell adhesion and proliferation [113-116]. In a similar report, naturally derived equine bone was coated with polyethylenimine (PEI) [117]. The composite bone-PEI

particles were well distributed with sizes below 500 nm, displayed a higher charge density and calcium ion concentration, and had better cytocompatibility than naked PEI. Excitingly, the bone-PEI nanoparticles could be used for successful BMP-2 plasmid delivery to promote osteogenic differentiation in DPSCs, almost twice as effectively as free PEI [117]. While many reports detail the success of synthetically prepared hydroxyapatite materials for non-viral gene delivery [95, 118-120], this *in vitro* study is the first to employ naturally derived hydroxyapatite and paves the way for new and innovative *in vivo* designed oligonucleotide delivery agents for regenerative endodontics. As proteomics analysis has expanded, more information has become available corroborating commonalities between human and animal dentin matrix molecules, which in both stimulate cell migration, proliferation, differentiation and mineralization [121], validating these low-cost materials which are readily available.

While the rise of standardized, general treatments using materials from animal-derived sources, such as the above, will greatly improve clinical outcomes and advance the bioengineering field, many disparate fields of biomedicine and tissue regeneration are now moving instead towards patient-specific personalized treatments, an approach known to significantly improve individual patient diagnosis, treatment and outcome [122-136]. Though personalized medicine is still a burgeoning aspect of regenerative endodontics [137], some groups have recently reported encouraging examples of personalized bone engineering [138, 139].

In one specific example, human demineralized dentin matrix-based materials were used as bio-ink for the fabrication of patient-specific dental tissue [139]. A composite ink of demineralized dentin and a fibrinogen-gelatin mixture was developed, and the authors

demonstrated an increase in relative amount of demineralized dentin improved the mechanical and handling properties of the new material, eventually generating a 3D printable construct with a minimum line with of 252 μm. Excellent cytocompatibility (>95% cell viability) and robust osteogenic differentiation of DPSCs was reported. This ink, when co-printed with DPSCs and polycaprolactone, enabled the generation of 3D tooth-shaped cellular construct (2 cm height); after a 15 day culture in medium, robust mineralization was observed as a result of odontogenic differentiation inside the construct [139]. The development of materials such as this which have excellent performance in tissue regeneration and good printability (highly resolved line widths, good stacking behavior, shear thinning), vastly increase their practicality and therapeutic range.

More traditional materials such as collagen and decellularized ECM are common for pulp regeneration therapy. In particular collagen scaffolds supplemented with dental pulp stem cells are widely studied for dental pulp regeneration. Coyac et al. developed a dense collagen hydrogel containing suspended SHED cells through plastic compression, and investigated their biocompatibility, viability, SHED metabolic activity and mineralization over 24 days *in vitro* [140]. Live/Dead staining confirmed viability and proliferation over a 16 day period. Mineralization proteins such as the alkaline phosphatase protein and the osteopontin protein were evaluated via Western blot, and the group noted increased expression from day 0 up to day 24 for these markers. SEM imaging after 16 days of *in vitro* culture of the collagen gels with SHED cells revealed mineralized tissue formation throughout the core of the scaffold, indicating the potential of this hybrid approach in bone formation [140].

Decellularized ECM has also been explored as a natural scaffold to regenerate vital pulp. Alqahtani et al. developed a protocol to decellularize porcine dental pulp while still maintaining integral ECM proteins including collagen type 1, dental matrix protein 1 and dentin sialoprotein (DSP) [141]. The group implanted the decellularized ECM construct in beagles with collagen sponge controls and determined the collagen sponge resulted in disorganized tissue formation. The ECM scaffold, however, exhibited strong immunostaining for DSP throughout the bulk of the implant as well as increased cell proliferation [141].

Biopolymers such as chitosan and hyaluronic acid, which are naturally derived, low-cost, commercially available and readily modified or prepared as composites, similar to the above examples, are at the forefront of many current research efforts. Recently, these types of biopolymers have shown increased sophistication in addition their established success as scaffolds for endodontic regeneration.

In one report, Ducret et al. developed a chitosan hydrogel fibrin, and performed *in vitro* testing to evaluate human dental pulp regeneration. The authors prepared the composite fibrin-chitosan hydrogel and altered the relative amount chitosan (0.2–1.0% w/w) as well as chemically modifying the material through acetylation (40% acetylation determined as optimal) to find preferable mechanical handling properties to support cell proliferation and differentiation [142]. Hydrogel prepared at 10 mg/mL showed optimal mechanical properties and was chosen to be seeded with DP-MSCs (cultured over a 7 days). The nanofibrous ultrastructure was evaluated in addition to Live/Dead and collagen production assays. The authors demonstrated the fibrin-chitosan composite hydrogel showed a significant improvement in antimicrobial efficacy against *Enterococcus faecalis*,

supported ECM deposition, dental pulp tissue neoformation and encouraged native fibroblast-like morphology of dental pulp-mesenchymal stem/stromal cells [142].

More recently reported by Osmond and Krebs, composites of carboxymethyl-chitosan hydrogels embedded with calcium phosphate nanoparticles were prepared and tested as pulp capping agents [143]. Their material supported DPSC proliferation for up to 3 weeks, had a high storage modulus (>1 MPa), and encouraged odontogenesis [143]. To model the release of growth factors, drugs or proteins, BSA levels were monitored and showed sustained release for 1 month, suggesting their future use as depots for long-term delivery [143].

In a similar report, a composite scaffold of chitosan and gelatin (crosslinked with either 0.1% or 1.0% glutaraldehyde) was prepared and evaluated for its potential to support DPSCs, which had or had not been pre-exposed to recombinant human BMP-2 [144]. Both constructs supported cell viability and proliferation through the final 14 day time point and each revealed significant amounts of native-like biomineralization [144]. The scaffold with a lower percentage of glutaraldehyde was more efficacious at odontogenesis (evidenced through more significant expression of Osterix, IBSP and DSPP), and *in vivo* the authors report a time-dependent mineralization which was more pronounced in recombinant human BMP-2 pre-treated cell populations [144]; overall reports such as this are encouraging, and offering viable sophisticated treatment options or orofacial bone tissue engineering. Aside from these specific examples, chitosan, modified chitosan and chitosan containing composites have well-established success rates, and many of these materials are being translated towards the clinic [145].

Hyaluronic acid-based materials and composites are well-understood and have become increasingly relevant in regenerative endodontics [146-148]. Many of these have advanced to the clinical trial stage, where they are reported to restore diminished interdental papilla and reduce inflammation in patients with peri-implantitis [149, 150]. Commercially available hyaluronic acid-based hydrogels such as Restylane offer practical advantages over other established materials such as Matrigel because of increased SCAP cell viability and proliferation, and enhanced differentiation and mineralization (evaluated through ALP, dentin matrix acidicphosphoprotein-1, dentin sialophosphoprotein and matrix extracellular phosphoglycoprotein) markers by qRT-PCR [151].

The molecular weight and size of assembled hyaluronic acid-based gels impacts its biological response, although most applications employ higher molecular weight species [146-148, 151-158]. In the dental niche, low (the result of enzymatic cleavage) and high molecular weight hyaluronic acid can differentially affect adjacent cells and tissue [159]. DPSCs treated with either low, medium or high (800, 1600 or 15,000 Da) molecular weight hyaluronic acid show significant differences in proliferation, cell morphology and size, and surface marker expression [159]. DPSCs treated with low molecular weight hyaluronic acid maintain many of their characteristic phenotypic markers (CD29, MSC and DPSC markers; CD44, T cell receptor signaling; CD73, MSC and DPSC stromal associated marker; CD90, MSC and DPSC markers), as well as additional markers not observed in the control groups (CD29, MSC and DPSC markers; CD34, transmembrane phosphoglycoprotein; CD90, MSC and DPSC markers; CD106, endothelial cell adhesion molecule; CD117-, transmembrane receptor tyrosine kinase involved in the Akt pathway and cell proliferation; CD146, melanoma cell adhesion molecule; CD166, stromal

associated adhesion molecule) [159]. While the majority of reports focus only on high molecular weight hyaluronic acid-based materials, the results of this study suggest the importance in understanding the effect and timing of biomaterial degradation kinetics [159]. Further evidence supporting this idea comes from reports evaluating the impact of low and high (18 and 270 kDa) molecular weight 2-aminoethyl methacrylate-modified hyaluronic acid hydrogels *in vitro* with DPSCs [153]. The degradation, mechanical properties and swelling behavior was readily tuned by molecular weight, and these gels were readily prepared by UV crosslinking, showed no cytotoxicity and helped maintain proper DPSC cell morphology and stemness (evidenced through increased expression of NANOG and SOX2 markers) [153].

Similar to the use of other scaffolds to sequester and modulate the release payloads, hyaluronic acid-based hydrogels/matrices offer excellent potential for controlled and tunable release of charged species [160-162]. In a recent publication from the Gomes group, injectable hyaluronic acid gels were fabricated *in situ* and evaluated for their potential to encourage rapid vascularization of soft endodontic tissues [154]. Incorporation of cellulose nanocrystals improved the hydrolytic and enzymatic stability of the material, and platelet lysate to support cell proliferation and viability [154]. Hydrogels were prepared through the use of a double barrel syringe fitted with a static mixer, with barrel A containing a mixture of aldehyde modified hyaluronic acid and aldehyde modified cellulose nanocrystals while barrel B contained a mixture of platelet lysate and hydrazide-modified hyaluronic acid; simultaneous co-injection of both materials into molds generated stable crosslinked hydrogels which could then be tested for their physical properties and their *in vitro* and *ex vivo* performance for soft tissue regeneration [154]. This fabrication

method readily facilitated incorporation of additional growth factors, PDGF and VEGF, to encourage local revascularization; furthermore these growth factors showed improved and sustained release profiles relative to the amount of included cellulose nanocrystals, hypothesized by the authors to arise partially from the high density of charged sulfate groups which might aid in adsorption and immobilization of growth factors [154]. An *ex vivo* chick chorioallantoic membrane (CAM) assay was used to evaluate performance of these composite materials, which generally showed promising angiogenesis, and no inflammatory response [154]. In addition, the authors noted that the addition of platelet lysate increased the elasticity of the material, showed a strong chemotactic effect, and could potentially be used to control the formation of new convergent blood vessels [154]. Finally, platelet lysate doped materials showed improved stability compared toother gels; this and cellulose nanocrystals both improved the swelling properties of the resultant gels, likely improving the local substance exchange [154].

Gels are unique treatment options as their composition can be readily altered to include active pharmaceutical agents such as antiseptics, disinfectants or bioactive substances, to improve patient outcomes [130, 163-167]. In a promising recent report, a hyaluronic acid hydrogel was modified through click chemistry to promote encapsulation of a bone morphogenetic protein-2 mimetic peptide to guide osteogenic differentiation *in vitro* and *in vivo* [168]. Crosslinking and inclusion of the BMP-2 mimetic peptide did not disrupt hydrogel formation or injectability, and the modified material served as an excellent scaffold for hDPSCs [168]. Prepared through simple mixing of a tetrazine-modified hyaluronic acid and cyclooctene-modified hyaluronic acid, this crosslinked scaffold

evaded enzymatic degradation and persisted longer both *in vitro* and *in vivo*, allowing for sustained localized osteogenic differentiation for over one month [168].

1.3.5.3 Growth Factor Guided Revascularization. Growth factor guided treatments have gained much recent attention and can similarly regenerate both soft and hard tissues which recapitulate native morphology, especially when combined with cell-based therapies. Growth factors can be used to stimulate or recover cell populations, as evidenced by a recent publication by Luo et al [169]. The authors used extracted human CD146+ DPSCs which had been cryopreserved for 3 months, and then recovered and treated the cells with basic fibroblast growth factor bFGF in order to improve their long-term performance post-thawing [169]. Treatment with 20 ng/mL bFGF significantly improved proliferation, activated the ERK pathway, upregulated transient receptor potential canonical 1 (TRPC1) and decreased apoptosis, all while maintaining robust stemness and pluripotency of the affected DPSCs compared to controls [169]. Long-term maintenance and viability are crucial for encouraging DPSCs and related stem cells, as a delicate balance of cytokine type and timing of application can play large role in local cell behavior and final observable outcome, demonstrated by Jaukovic et al. using IL-17 and bFGF [170]. With 7 day treatment, both growth factors could be used to modulate the behavior of SHEDs and DPSCs cell populations [170]. Treatment with either growth factor was seen to affect the relative stemness of both DPSCs and SHEDs, as demonstrated by key pluripotency markers such as OCT4, NANOG and SOX2 at both the gene and protein level [170]. The combination of IL-17 and bFGF together increased CD73 expression and decreased CD90 expression, while each factor separately induced expression of IL-6 [170]. Both SHED and DPSCs show improved proliferation and clonogenicity after bFGF treatment, similar to

previous results [171, 172], while IL-17 treatment stimulated SHED proliferation and clonogenicity only [170]. Their results offer new evidence suggesting bFGF and IL-17 mediate stem cell properties during different stages of growth, which could be harnessed in future therapeutic systems in which treatment timing differentially impacts patient outcome.

Recent data suggests concentrated growth factor can be used to stimulate proliferation and mineralization of dental pulp cells [103], in addition to its known ability to modulate stemness and function in bone marrow stromal cells [173], periodontal ligament cells [174], DPSCs [175] and mesenchymal stem cells [173]. Concentrated growth factor, containing many important individual growth factors including PDGF, FDF, TGF-β, VEGF and IGF, is known to impact many cell processes important in regenerative endodontics including adhesion, proliferation, migration, differentiation and local remodeling and angiogenesis [173-177]. In their study, Tian et al. demonstrated concentrated growth factor could be used to improve the migration, proliferation and mineralization of dental pulp cells [103]. Odontogenic differentiation was evaluated via qPCR and Western blot, revealing concentrated growth factor mechanistically upregulates gene expression of DSPP, DMP-1, BSP and ALP while simultaneously increasing protein expression of ALP, BMP2, SMAD5, Runx2 and p-SMAD [103]. The effect of concentrated growth factor on direct pulp capping was tested by the authors *in vivo* in canines, and after 3 months experimental groups showed good re-calcification, pre-dentin formation and healthy odontoblasts with regular morphology in the dental pulp [103].

1.3.5.4 Synthetic Materials. An ideal scaffolding material for pulp regeneration supports attachment, proliferation, and differentiation of seeded stem cells, leading to eventual

vascularization and innervation of pulp tissue [178-182]. Synthetic materials and naturally derived synthetic scaffolds offer high control over material properties such as degradation rate, stiffness, reproducibility, structural tunability, epitope presentation and charge density, and have been widely applied in tissue engineering applications [180].

Synthetic polymers such as polylactic acid (PLA), poly lactic co-glycolic acid (PLGA) and self-assembling peptides can be engineered to biodegrade as new tissue forms, leaving no permanent foreign body. Functional groups in synthetic polymers can be incorporated to attract cells or bind small molecules like growth factors [183]. Sakai et al. demonstrated formation of vascularized soft connective, pulp-like tissue and new tubular dentin when SHED cells were seeded onto PLA scaffolds [183]. Additionally, Huang et al. showed the formation of pulp-like tissue formation and dentin deposition along the root canal wall using SCAP and DPSC seeded onto PLGA [183].

Biodegradable PLA supports undifferentiated dental pulp cell adhesion and shows ideal chemical composition for mature dental pulp proliferation, performing better than collagen or calcium phosphate scaffolds [183]. Numerous studies using dental pulp stem cells report poor pulp-like structure formation with irregular shapes and orientations [184]. Mooney et al., however, combined a soft tissue core with surrounding hard tissue and seeded DPSCs into a PGA scaffold, which supported native pulp-like tissue formation better than collagen gels and alginate [77].

Another materials-based approach is the tooth slice/scaffold model in which a commercially available synthetic hydrogel composed of a 16 amino acid sequence, Puramatrix, is cultured with SHED cells [185]. Promising data has shown regeneration of pulp-like tissue and new dentin formation [185]. Multilayered and 3D printed scaffolds

have shown efficacy in regenerating dental pulp [185]. Bottino et al. constructed a multilayered scaffold with 1 core layer (CL) and 2 surface layers located atop and underneath the CL [168]. This poly(DL-lactic-de-co-ε-caprolactone) (PLCL) scaffold was electrospun with the addition of hydroxyapatite nanoparticles (HAp) to help augment bone formation. Bottino et al. has shown periodontal regeneration *in vivo* with this hybrid scaffold design [185].

Orti et al. transplanted a 3D printed hydroxyapatite scaffolds containing peptide hydrogel combined with DPSCs in an immunocompromised mice model [81]. With these scaffolds, the authors showed blood vessel infiltration, pulp-like tissue formation and DPSC differentiation [55]. DPSCs have great potential in cell replacement strategies for dental tissue engineering due to their origin, and have been effectively used in numerous *in vivo* models, specifically for dental pulp regeneration [55]. Another strategy that has seen promise is 3D printing, as demonstrated by Orti et al., where it was used to successfully minimize scaffold variability. With their material, the authors noted consistent vascularized pulp formation and osteodentin generation *in vivo*. Further research is still required, however, to fully optimize the potential of hDPSCs, and in particular to assess and improve up the varying degrees of vascularization, innervation and hard tissue formation.

In addition to the materials discussed above, carbon-based graphene oxide materials have received much attention in biomedicine for tissue engineering and drug delivery [186, 187]. The Zhang and Gu labs prepared a graphene oxide-copper nanocomposite with good water solubility and tested its ability to encourage dentin-pulp complex regeneration; promoted DPSCs adhesion, proliferation, odontoblast

differentiation and secretion of VEGF and glia-derived neurotrophic factor (GDNF) [188]. When HUVECs were treated with their graphene oxide-copper nanocomposite, the authors noted robust migration, tube formation and good VEGF expression again [188]. Subcutaneous transplantation into nude mice for 8 weeks showed promising growth of new dentin-pulp complex-like features characterized by vasculature and collagen deposition surrounded by mineralized dentin-like tissue [188]. Immunofluorescence of the explanted tissue confirmed both DPSC odontogenic differentiation (visualized with dentin sialophosphoprotein), angiogenesis (CD31 and VEGF signaling via Akt-eNOS-VEGF and Erk1/2-HIF-1alpha-VEGF) and neurogenesis (GAP43), showing excellent promise for this and related materials in regenerative endodontics [188].

1.3.5.5 Synthetic Biomimetic Materials. Recent revascularization treatments like those outlined previously are used to promote angiogenesis and revolve around growth factor- and stem cell-based therapies. Currently, growth factors such as FGF and VEGF can be delivered *in vivo* to stimulate angiogenesis [189]. VEGF isoforms VEGF-A121 and VEGF-A165 are presently being used in clinical trials [189]. RNA-based techniques utilizing microRNA (miRNA) have developed efficacious drugs such as antagomir-92a, whose angiogenic effects significantly decreased toe necrosis in mice [189, 190]. Sophisticated mimicry of natural angiogenic scaffolds may prove to be the most successful, particularly with the use of self-assembling peptide hydrogels with high density epitopes mimicking VEGF [189].

Moon et al. developed an antibacterial and biomimetic nanomatrix gel which releases nitric oxide to improve upon current clinical regenerative endodontic procedures [191]. *In vitro* experiments verified antibacterial efficacy, including culture-examinations

of multispecies endodontic bacteria challenged with the loaded gel (to sequester antibiotics like ciprofloxacin and metronidazole in addition to nitric oxide). Based on promising results against the bacteria, the constructs were implanted into beagles and the group was able to show their self-assembling peptide amphiphiles promoted tooth revascularization and root canal maturation. The study demonstrated nitric oxide showed dose-dependent antimicrobial efficacy, which could be used in the future to improve outcomes in current regenerative endodontic procedures and clinical trials [135].

Muller et al. developed a synthetic clay-based hypoxia-mimetic hydrogel (0.15–5 w%) co-cultured with dental pulp derived stem cells to regenerate pulp, and determined that these constructs were both biocompatible and stimulated VEGF production within 1 hour of culture [192]. Hydrogels supplemented with DPSCs have shown great promise in many studies; similar to above, Luo et al. used DPSCs/heparin-poloxamer hydrogel combinations to promote viable tissue regeneration [193].

Peptide based strategies developed by the D'Souza, Hartgerink, and Kumar groups have exploited bioactive domains such as cell adhesion motifs, matrix metalloproteinase cleavable sites, heparin binding sequences and dentinogenic domains to regenerate pulp-like tissue [18, 194-210]. These strategies employ short peptides of 5–50 amino acid residues which self-assemble into thixotropic hydrogels that can be syringe-aspirated and injected with 18–20 gauge needles *in situ* [211].

In one example, the Kumar group demonstrated *in vitro* efficacy of a dentinogenic self-assembling peptide hydrogel (SAPH) termed SLd which contains a bioactive mimic of matrix extracellular phosphoglycoprotein (MEPE) previously shown to play a vital role in dental pulp stem cell (DPSC) proliferation [18]. The C-terminal bioactive domain is

adjacent to a designed self-assembling domain, and contains six repeats of alternating hydrophobic leucine and hydrophilic serine residues with flanking positively charged lysines. This unique design gives rise to spontaneously self-assembling nanofibrous β-sheets which form a stiff hydrogel at 40 mg/mL in aqueous solution. The resulting thixotropic gel SLd showed good cytocompatibility, supported proliferation and increased calcium phosphate deposition in a dose-dependent manner. While SLd displayed great efficacy *in vitro*, it did not demonstrate comparable results *in vivo* [18]. The Kumar group has further explored the use of this dentinogenic peptide hydrogel SLd and another angiogenic peptide hydrogel, SLan, in a 1 month canine pulpectomy model. Interestingly, the carrier control and SLd induced the formation of disorganized tissue within the root canal space, while SLan caused rapid infiltration of cells extending from the apex to the crown and regenerated organized vascularized pulp-like tissue.

1.4 Conclusion

The degradation of mineralized and organic tooth tissue due to poor oral hygiene or injury results in pain and eventual loss of permanent structures within the tooth, and often requires surgical procedures to replace the infected pulp with inert materials such as gutta-percha. Recently, several strategies, including stem cell-based and cell-homing methods, have been explored to circumvent these root canal procedures to opt instead for dental pulp regeneration. Some advantages of these strategies are sufficient biocompatibility and proliferation, however, the requisite time scale (typically months-long procedures) hampers their viability in clinical settings. As an alternative, traditional materials-based strategies have been expanded upon and explored for revascularize and regeneration of hard and soft dental tissues. Traditionally, these materials are inert or are prepared as

composite materials, the latter allowing for tunability though complicating validation and preparation. Synthetic materials and biomimetic materials are advantageous as revascularization of the dental pulp is achieved through growth factors or the innate ability of unique polymers to regenerate dental pulp, many of which can be harvested directly from low-cost sources, or derived directly from the patient to facilitate personalized treatment options. Materials such as peptide hydrogels confer many of the desirable physical and biological properties found in the more common regenerative endodontic materials, without the complications in validation and preparation that arise from composite materials. Recently developed angiogenic peptide hydrogels can be syringe injected and reassemble to fill the dental cavity, simplifying their practical use and formulation, and have shown efficacy in a 1 month canine pulpectomy model. While there are still significant challenges remaining in the field of regenerative endodontics, such as long-term efficacy, new biomimetic materials-based strategies have shown promise in regenerating dental pulp.

CHAPTER 2

ANGIOGENIC HYDROGELS FOR DENTAL PULP REVASCULARIZATION[2]

2.1 Introduction

In the human body, most cells are within 150 μm of a capillary – due to inherent diffusion limits to the supply of nutrients and oxygen [212]. Unsurprisingly, therapeutic angiogenesis is critical for tissue regeneration [1, 194, 213], especially after ischemic tissue damage [214]. Specific vascularization strategies could be clinically relevant for ischemic diseases such as coronary artery disease [215] and critical limb ischemia [216], improving islet transplant tolerability [217], and optimizing vascularization of osteo-conductive implants [218]. Where pre-vascularized/pre-cellularized tissue engineering strategies are not viable due to lack of oxygen/nutrient supply, *in vivo* vascularization may prove especially valuable [219, 220]. Many promising vascularization strategies require cumbersome cell sourcing or may result in rapid diffusion of bioactive factors from the delivery site with ectopic side effects [194, 221]. There remains a significant need for an off-the-shelf material-based alternative that is injectable, biodegradable, and capable of promoting *in situ* neovascularization and matrix deposition – for wider adoption, lower cost and clinical use.

Injectable hydrogels that can assemble to conform to tissue defects *in vivo* can augment and repair injured soft tissues [18]. Optimally, these gels would be injected by a needle or a catheter to form *in situ* depots that integrate with the host tissue, biodegrade over time, and help regenerate vascularized soft tissues [194, 214].

[2]Adapted from **Z. Siddiqui**, B. Sarkar, K. Kim, N. Kadincesme, R. Paul, A. Kumar, Y. Kobayashi, A. Roy, M. Choudhury, J. Yang, E. Shimizu, V. Kumar. Angiogenic hydrogels for dental pulp revascularization. **Acta Biomaterialia.** 126 (2021) 109-118.

Self-assembling peptides are a class of short (2–50 amino acid) amphiphilic peptides with the canonical sequence Z_a-$(XY)_b$-Z_c, where a, b, and c can be tweaked to optimize material properties, allowing self-assembly into β-sheets (X and Y are hydrophilic and hydrophobic residues, respectively) – with demonstrated utility in numerous *in vitro* and *in vivo* applications [195, 222, 223]. These peptides have demonstrated facile injectability as tissue depots, which can be used for wound healing, tissue regeneration, and *in situ* local drug delivery [223, 224]. Self-assembly of amphiphilic peptides can be directed to yield ECM-mimetic (ECM = extracellular matrix) nanofibrous hydrogels [223-225]. The hydrogels can be injected directly into the target tissue, where they re-gel after injection. The storage moduli of the materials (generally 100–1000 Pa) are especially suitable for facilitating soft tissue regeneration (e.g., dental pulp, bone marrow, or brain parenchyma) [226].

The therapeutic utility of self-assembling peptides can be extended via modification of the N- or C-terminus with bioactive domains [194, 214, 224, 227]. We have recently reported the development of proangiogenic constructs with the addition of a bioactive mimic from vascular endothelial growth factor (VEGF-165), termed QK, to a self-assembling domain [195, 214]. These preliminary injectable angiogenic supports established a proof-of-principle for injectable self-assembled growth factor mimics that remain localized for robust neovascularization [194, 214, 226].

Optimization of biophysical and biochemical properties of angiogenic peptide hydrogels now allow for a versatile range of applications to be explored [18, 211, 222, 224, 225, 227]. In the previous design of the construct, an MMP-2 cleavage domain in the midblock resulted in rapid degradation [214]. Herein, we have optimized the design of the

angiogenic self-assembling peptide sequence (Figure 2.1A) by removal of this domain. This angiogenic peptide (termed SLan, Table 2.1) forms stiff, robust hydrogels, which promotes vascularization in both small and large animal models.

Table 2.1 Angiogenic and Dentinogenic Peptide Sequences

Peptide	Sequence	Format	Conformation
SLan *(angiogenic)*	$K(SL)_6K$–G–KLTWQELYQLKYKGI	hydrogel	β-sheet
SLed *(dentinogenic)*	$E(SL)_6E$–G–TDLQERGDNDISPFSGDGQPFKD	hydrogel	β-sheet

Here, we demonstrate the angiogenic efficacy of SLan in a suitable preclinical translational model – pulp revascularization in adult canine teeth. Pulp revascularization requires defined microvascular regrowth within the tooth root chamber after extirpation of inflamed pulp. The technique is useful for treating juvenile patients after traumatic dental injury and some cases of soft tissue infection and inflammation. Over-instrumentation of the apex may lead to formation of vascularized pulp-like tissue, if residual apical papilla cells are viable (generally the case in juveniles). If those cells are not present (adults) or not viable (potentially due to apical periodontitis), a muted regenerative response is observed – leading to intracanal a vascular ossified tissue formation by periodontal ligament (PDL) or bone marrow cells [228]. Thus, in adults, gutta percha is still widely used as the standard-of-care elastomeric filler for root obturation [98].

Harvested stem cell transplants have shown tremendous clinical potential in recreating intracanal soft tissue niche in large animal models and humans [84]. In contrast, tissue-engineered materials have had more mixed results in recapitulating native microenvironment [229, 230]. Despite showing promise in rodent models, purely materials-based regeneration of sustainable vasculature in the root canal has not been

demonstrated in large animal models. We demonstrate that pulp revascularization can be stimulated by implantation of the self-assembling peptide hydrogel SLan in an adult canine teeth after pulpectomy – presenting an acellular materials-based approach to promote pulp-like soft tissue regeneration *in vivo*.

2.2 Methods and Materials

2.2.1 Solid Phase Peptide Synthesis

All chemicals were purchased from Sigma Aldrich (St. Louis, MO) unless otherwise specified. Peptides were synthesized with a CEM LibertyBlue solid phase peptide synthesizer using standard Fmoc chemistry. The sequences used are shown in Table 2.1. All peptides were C-terminal amidated and N-terminal acetylated. The crude peptides were cleaved with 2.5% each of H2O, Triisopropylsilane (TIS), and 3,6-dioxa-1,8-octanedithiol (DoDT) and 92.5% Trifluoroacetic acid (TFA) (10 mL total for 0.1 mM scale synthesis) for 30 minutes at 37°C. The cleaved peptides were crashed out in cold (-20°C) ether, centrifuged, ether decanted, and left to dry overnight. The resulting crude peptide pellets were dissolved in Milli-Q water at a concentration of ~1 mg/mL, pH adjusted to 7, and dialyzed with Spectra/Por S/P 7 RC dialysis tubing at a 2000 Da cutoff tubing against DI water for 3 days. The purified peptides were frozen and lyophilized for at least 3 days, which resulted in a white cotton-like powder. Peptide mass and purity were verified >85% by an Agilent 1100 series HPLC instrument with an Agilent (Santa Clara, CA) C3 reverse phase column. The molecular weights of the peptides were verified with an Orbitrap Q Exactive LC/MS (Thermo Scientific, Waltham, MA) instrument. To verify commercial manufacturing potential, the peptides were manufactured at gram scale with

similar purity (>90%) by AmbioPharm Inc (Beech Island, SC), a manufacturer of peptide APIs for the US market.

2.2.2 Fourier Transform Infrared Spectroscopy

1% w/v (10 mg/mL) hydrogel samples were prepared for SLan with sucrose and 1X HBSS and were diluted in MilliQ water at 0.1 mg/mL. Samples were pipetted onto the IR plate for spectra analysis between 400 and 4000 cm^{-1} with a background of Milli-Q water subtracted from each reading. The reported spectral region is 1500–1700 cm^{-1} to highlight the amide I and amide II regions.

2.2.3 Circular Dichroism

Circular dichroism (CD) experiments were performed using the Jasco J-810 spectropolarimeter (Oklahoma City, OK, USA). Experiments were conducted at room temperature using a 1 mm cuvette with SLan samples at a concentration of 0.2 mg/mL in HBSS (10 mM HEPES, 150 mM NaCl pH 7.4) buffer at the wavelength range 190–260 nm.

2.2.4 Preparation of Nanoporous Peptide Scaffolds (hydrogel)

SLan was initially dissolved in 298 mM sucrose to yield a viscous 2 w% solution. Self-assembling peptides exhibit enhanced self-assembly with the addition of multivalent counterions such as phosphate in PBS or HBSS (to form salt-bridges between the terminal lysines of peptides, Figure 2.1). Equivalent volumes of HBSS were added to SLan hydrogels to promote robust hydrogelation.

2.2.5 Scanning Electron Microscopy

200 µL aliquots of 1 w% SLan hydrogel were crosslinked overnight with 2% glutaraldehyde (Sigma). The crosslinked peptide hydrogels were washed three times with DI water and ethanol dehydrated (50%, 75%, 90%, 95%, 99%, and 100% ethanol/water ratio) for 15 minutes each. The samples were critical point dried in a Tousimis AutoSambri-795 critical point drying instrument (Rockville, Maryland). The chamber was filled with 100% ethanol ¾ of the way to the top. The samples, submerged in 100% ethanol, were added to the chamber and topped off with 100% ethanol up. The lid on the chamber was secured and evenly tightened. The instrument was switched on and cooled to about 4°C. Liquid ethanol was exchanged for liquid CO_2 under high pressure for 20 minutes with continuous purging. Samples were maintained in liquid CO_2 for 1 hour prior to another 20 minutes wash with continuous purging. Samples were then heated to 37°C and a pressure of ~1070 psi. At the critical point, the chamber was slowly vented (over 30 minutes) to prevent condensation of CO_2. The samples were then sputter coated with Au/Pd (8 nm thickness) using an EMS 150 TES sputter coater (Quorum, East Sussex, UK) and imaged with an JSM-7900 (Jeol, Peabody, MA) scanning electron microscope at 5.0 kV accelerating voltage and a working distance of 10 mm.

2.2.6 Atomic Force Microscopy

Atomic force microscopy was used to study nanostructure of the peptide. SLan hydrogels were diluted in DI water to 0.1%. Freshly cleaved mica disks were prepared and adhered by the underside using double-sided tape to a thin metal disk. The diluted peptide solution spin coated by drop-casting 10 µL increments three times and centrifuging to allow the peptide to evenly spread and dry on the Mica surface. ScanAsyst

mode on a Dimension Icon instrument (Bruker, AZ) with sharpened silicon (0.2–0.8 N/m, Al reflective coating) AFM tips (Bruker,AZ) was used to obtain images.

2.2.7 Rheometry

The viscoelastic properties of the peptide hydrogels were tested with a Kinexus oscillatory rheometer (Malvern Instruments, United Kingdom). Two tests were run: the strain sweep test which provides information regarding the injectability of the material, and shear recovery test which determines how viscoelastic the material is. In the strain sweep test, 40 μL of hydrogel was pipetted onto the bottom plate of the rheometer and pre-strained for 5 minutes at constant 1% strain and frequency of 1 Hz with a 4 mm geometry and 250 μm gap (n=4) for 5 minutes. Immediately after, a strain sweep was run for 5 minutes with increasing strain (0.1 – 100 % strain). The oscillatory shear recovery test alternates between periods of low strain (1%) and high strain (100%) under the same conditions. This indicates the shear thinning and shear recovery potential and kinetics of hydrogels.

2.2.8 *In vitro* Cytocompatibility

Cytocompatibility of SLan peptides was evaluated at 0.1, 0.01, and 0.001 w% with a mammalian (human) cell (line) that has been extensively used prior: HEPG2 cells (ATCC, Manassas, VA). SLed cytocompatibility *in vitro* has been published [18]. The HEPG2 cells were utilized after their first passage and seeded at a cell density of 10,000 cells/well in a 96 well plate (n=5) in complete HEPG2 media (90% DMEM, 10% FBM, 1% Pen-Strep, and 1% Glutamax) for 24 hours in an incubator maintained at 37°C and 5% CO_2. The complete HEPG2 media was aspirated and the peptide conditions prepared in serum-free media (DMEM) and control (serum-free media) were introduced. The peptide conditions

and controls were incubated for 6 hours. The samples were aspirated, the wells were washed with 200 μL of PBS, aspirated once more, 100 μL of PBS was added to each of the wells with 10 μL of CCK8 stain (Dojindo, Japan). After 1 hour incubation, the 96 well plate was read in a TECAN M200 Infinite plate reader at an absorbance of 450 nm against a reference wavelength of 650 nm. The results were analyzed and normalized to the serum-free media control.

2.2.9 Subcutaneous Implantation

All animals were treated in accordance with NJIT-Rutgers Newark Institutional Animal Care and Use Committee (IACUC) and AALAC guidelines. Female Wistar rats (250–275 g) were used for dorsal subcutaneous implantation. The rats were anesthetized using 2.5% isoflurane for induction and 1.5% for maintenance, followed by shaving of dorsal regions, isopropanol, and betadinesterile preparation of the surgical site. For subcutaneous (sub-Q) hydrogel implants, 200 μL boluses of SLan 1 w% hydrogels were injected in n=4 per timepoint – 7, 14, and 28 days. At 7 (acute), 14 and 28 days rats were sacrificed, and implant regions were excised. Harvested tissue sections were immediately fixed with 10% formalin. Samples were then processed by the histology core at the Rutgers Cancer Institute of New Jersey. The formalin embedded sections were ethanol series dehydrated, solvent exchanged for xylene, and then paraffin using a tissue processor. Samples were blocked in paraffin, sectioned to 6–8 μm sections, and stained using hematoxylin and eosin (H&E) or Masson's Trichrome (MT) (Sigma Aldrich, St. Louis, MO). Other sections were deparaffinized and immunostained (protocol and reagents detailed below).

2.2.10 Pulp Revascularization Model

All studies were approved by the Rutgers-NJIT IACUC committee and followed USDA guidelines. Adult male Beagles' incisors were used to evaluate pulp revascularization after a full pulpectomy. In two Adult Beagles' (22–26 months of age, male), 6 maxillary and 6 mandibular incisors were cleaned and exposed (n=12 implant sites for each canine). Using this model, we were able to see clear differences in the tissue regenerative response in each tooth, independent of adjacent teeth – minimizing the number of canines used. Animals were sedated with ketamine and diazepam, anesthetized with isoflurane and intubated. They were dosed peri-operatively and post-operatively with buprenorphine for pain management and convenia for potential infections.

The oral cavity (including teeth) was cleaned by Peridex (0.12% Chlorhexidine rinse). A round diamond bur attached to a high-speed handpiece was used to drill through to the pulp chamber. The pulp tissues were removed by H-files (#10). At same time, the working length was measured by an Apex locator. The canal spaces were expanded by K-files (#10-30). The canal space and apical area were widened by the Rotary Niti files with Endo motor handpiece. The canal space was irrigated by 5.25% sodium hypochlorite and then PBS. As is standard procedure, to induce growth factors from the dentin matrix, 17% EDTA was soaked in the canal space for 5 minutes. The canal space was then irrigated with phosphate buffered saline (PBS). To manage apical breeding, paper points were utilized. Uniform root canals were filled with 10–25 μL of hydrogels (SLan, SLed, SLan + SLed (50:50)), PBS). Composite resins were sealed at the top of canal spaces. At 28 days, animals were sedated and anesthetized as above, the 12 teeth were extracted, washed in PBS and immediately placed in formalin for 24 hours followed by decalcification using

10% EDTA for 21 days. Samples were processed by the histology core at the Rutgers Cancer Institute of New Jersey. The decalcified teeth samples were blocked in paraffin, sectioned to 5–8 μm sections and stained using H&E, MT, or immunostained, as above.

2.2.11 Immunohistochemical Staining

Sections were de-paraffinized in 5% xylene for 10 minutes, then 100%, 95%, 90%, 70%, 60%, 50% ethanol, and water and then immersed in PBS three times at 3 minutes each. The de-paraffinized samples were washed with PBS for 5 minutes. Then 2% bovine serum albumin was used to block non-specific absorption for 30 minutes. Samples were then immunostained with 3 different antibodies and counterstained with DAPI: i) Dental sialoprotein (DSP, Santa Cruz Sc33587) at 1/400 dilution in antibody buffer, 4°C overnight; secondary: Dk-anti-rb-FITC (Invitrogen 488 Alexa Fluor A21206), at 1/1000 dilution for 30 minutes. ii) S-100 (ab14849, Ms-anti-rb) at 1/400 dilution in antibody buffer, 4°C overnight; secondary: Dk anti-Ms-NL557 at 1/200 dilution for 30 minutes. iii) PECAM (bs-0468R, Rb anti-Rt) at 1/400 dilution in antibody buffer, 4°C overnight; secondary: Dk-anti-rb-FITC (Invitrogen 488 Alexa Fluor A21206), at 1/1000 dilution for 30 minutes. Then the samples were washed with PBS again 3 times for 5 minutes each. Mounting media with DAPI (Invitrogen SlowFade Diamond Antifade Mountant with DAPI) was used as a mountant in cover slipping. A Leica SP8 microscope (Leica, Switzerland) was used to image samples using conventional confocal and fluorescent microscopy techniques.

2.2.12 Implant Image Analysis

The cell density, infiltration, collagen deposition, blood vessel density and degree of regeneration for subcutaneous and pulp revascularization samples were calculated using the program QuPath [231]. The polygon tool was used to draw along the border of the entire implant. The cell detection tool was selected to adjust threshold and minimum area parameters to get the most accurate count of cells (threshold usually set between 10 and 15 and area set between 5 and 10). Cell detection was executed with the area of region and number of cells recorded. The area was converted from pixels to mm based on image scale bar size conversion factors. The cell density was determined by dividing the number of cells by outlined area in mm^2. The blood vessel density was calculated within each region and determined by dividing the number of blood vessels by outlined area in mm^2. Analyses were performed across all the regions within each slide (n=4 regions per slide), and then all slides (n=4 different implants per group) for 7 day, 14 day and 28 day samples.

2.2.13 Data Analysis and Statistical Evaluation

Data is represented as mean ± standard deviation. Differences between paired data were compared using Student's t-test. ANOVA with Tukey post hoc analysis was used for multiple comparisons of parametric data, and Kruskal Wallis ANOVA with Dunn's post hoc analysis was used for non-parametric data. Values of $p<0.05$ were considered statistically significant.

2.3 Results

2.3.1 Facile Synthesis of an Angiogenic Hydrogel

SLan (an acronym derived from the midblock (Serine-Leucine) repeats with an appended angiogenic domain) has a central self-assembling domain with a high β-sheet propensity. The peptide is easily synthesized and purified by standard solid-phase peptide synthesis to yield a lyophilized powder, confirmed for purity and identity with high performance liquid chromatography (HPLC) and electrospray ionization mass spectroscopy (ESI-MS), respectively (Figure 2.1). Lyophilized SLan self-assembles into nanofibers (Figure 2.2A) in aqueous solution, forming a hydrogel (Figure 2.2B). These peptides self-assemble through β-sheet formation, as shown via the FTIR peak at 1624 cm^{-1} (Figure 2.2C) and circular dichroism (CD) minima at 217 nm, at both room temperature (25°C) and at physiological temperature (37°C) (Figure 2.2D). The crosslinked nanofibrous mesh constituting the hydrogel was imaged by scanning electron microscopy (SEM) (Figure 2.2E), and the individual self-assembled nanofibers were observed by atomic force microscopy (AFM) (Figure 2.2F).

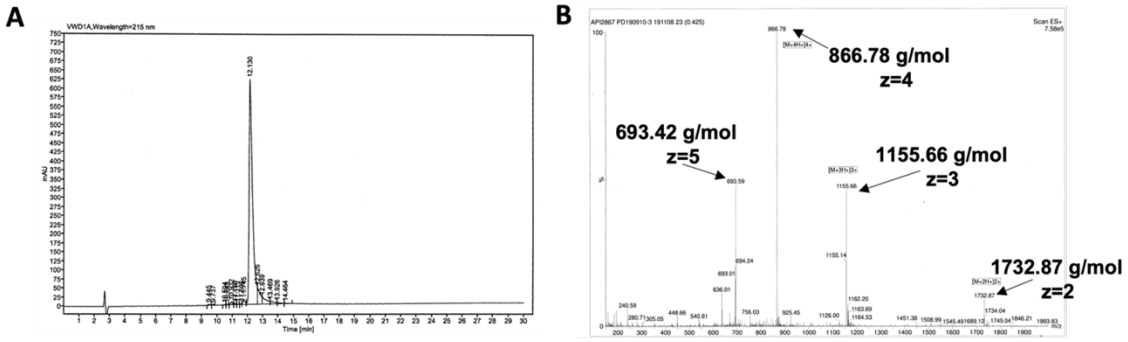

Figure 2.1 HPLC and ESI-MS of SLan. (A) HPLC confirms >85% purity of SLan, (B) ESI-MS confirms identity of SLan with corresponding mass-to-charge, or m/z, peaks.

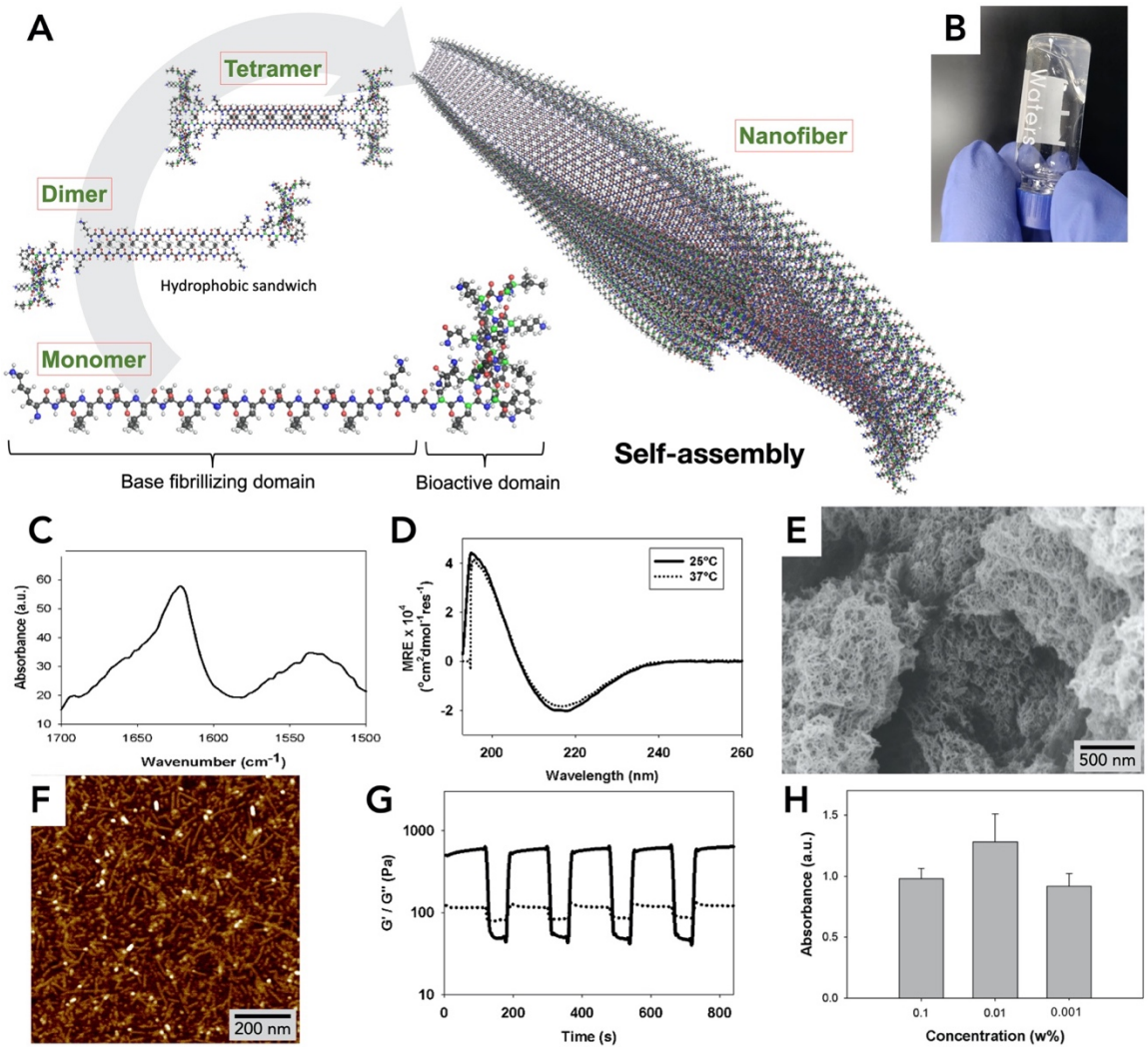

Figure 2.2 Biophysical properties of SLan hydrogel. (A) Self-assembly of SLan. In aqueous solution dimers and tetramers form assemble into a β-sheet based nanofibers. (B) 1% SLan hydrogel, (C) FTIR spectrum shows β-sheet secondary structure 1624 cm^{-1} peak) confirmed by (D) Circular dichroism spectra (~195 nm maxima and ~217 nm minima. (E) Scanning electron micrograph of critical-point-dried SLan hydrogel. (F) Individual SLan nanofibers observed in atomic force microscopy. (G) 1% SLan hydrogels are thixotropic. At low strain (1%), G'>G" (indicating solid-like elastic properties), at high strain (100%), G'<G" (signifying liquefaction of the hydrogel and showing dominance of viscous modulus). The switch in rheological properties is fast and reversible (representative plot shown). (H) *In vitro* cytocompatibility (n=4, $p<0.05$, CCK8 dye absorbance) of HEPG2 cells shows that SLan did not exhibit cytotoxicity.

The underlying nanofibrous architecture corresponds to a thixotropic hydrogel at the bulk scale. The hydrogel is reversibly shear-responsive (Figure 2.2G) [225]; thus can be easily injected *in vivo*, where it is reconstituted into a stiff bolus. SLan has similar

biophysical properties to other self-assembling peptides within this platform (Table 2.1) [18, 195, 211, 225, 227]. SLan has a proangiogenic "QK" domain derived from VEGF-165, presented at a constitutively high epitope density within self-assembled nanofibers (Figure 2.2A) [232]. Optimization of SLan over previous angiogenic SAP [214] by removal of an MMP-2 susceptible –LRG– midblock sequence promotes robust hydrogelation and prolongs *in vivo* persistence. *In vitro* cytocompatibility utilizing the CCK8 metabolic dye showed compatibility with mammalian HEPG2 cells (Figure 2.2H); SLan did not exhibit any cytotoxicity normalized to serum-free media control.

2.3.2 Biocompatibility

Biocompatibility of SLan was confirmed *in vivo* our benchmarked subcutaneous biocompatibility model [214]; 200 μL boluses were injected subcutaneously (sub-Q) under the backs of adult rats. Peptide hydrogels degraded over a 1 month period (Figure 2.3A–F). Cells rapidly infiltrated scaffolds (without any fibrous encapsulation) and promoted the development of vasculature and deposition of collagen within implants (Figure 2.3G–L). Cell density within implants decreased over time owing to the degradation of the hydrogel (Figure 2.3M). The number of blood vessels increased from 7–14 days but resorbed by 28 days (Figure 2.3N). The degree of infiltration consequently showed a marked decrease after scaffolds had degraded (Figure 2.3O). These results show that the bolus angiogenic peptide hydrogels stay localized after injection and degrade leaving native tissue over a 28 day period. Notably, no animals tested with these scaffolds (of the hundreds of rodents tested within the SAP platform) have shown incidence of systemic side effect, tumorigenicity or adverse side effect (up to 10 mg SC in a 200–250 g rat) [18, 214, 222, 224]. The use of the

rat sub-Q model allows for determination of preliminary safety to large doses (~10 mg/kg) compared to intratooth canine implants below (~0.05 mg/kg).

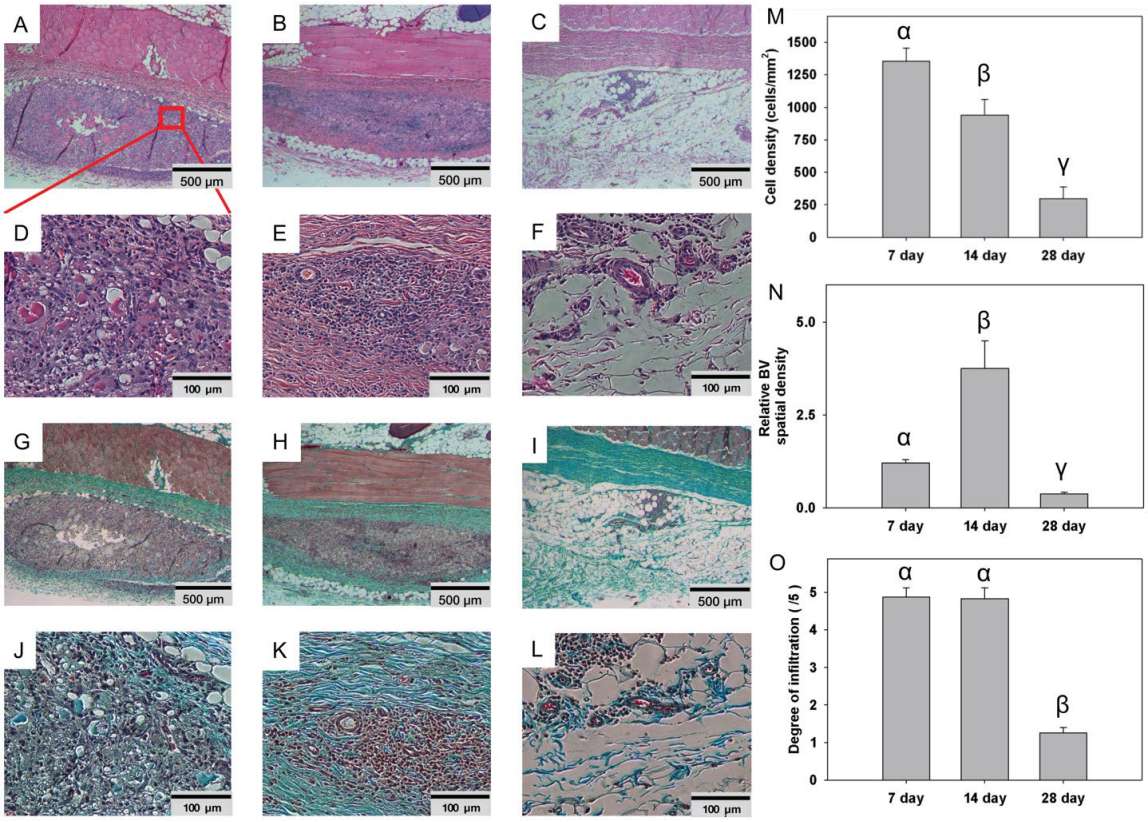

Figure 2.3 Dorsal subcutaneous implants of SLan in rats. Implants (n=4) showed rapid infiltration of cells – H&E images of 200 µL bolus implants in Wistar rats as early as day 7 (A: 500 µm, region magnified in D: 100 µm), completely into the center of implants by day 14 (B: 500 µm, E: 100 µm), and fully degraded by day 28 (C: 500 µm, F: 100 µm). Similarly, extracellular matrix (ECM) deposition (collagen, blue) was noted in Masson's Trichrome staining, with infiltration of blood vessels as early as 7 days (G: 500 µm, J: 100 µm), Day 14 (H: 500 µm, K: 100 µm), with complete resorption of superfluous collagen and vasculature by 28 days (I: 500 µm, L: 100 µm). (M) Cell density analysis of 7,14, and 28 day SLan rat subcutaneous samples. (N) Blood vessel density analysis of 7,14, and 28 day SLan rat subcutaneous samples. (O) Degree of infiltration analysis of 7, 14, and 28 day SLan rat subcutaneous samples.

2.3.3 Material-guided Dental Pulp Revascularization

After full pulpectomies, the pulp canals of the canines were irrigated. Bleeding was managed using paper points before filling the extirpated canals with 15–50 µL of SLan,

carrier, control peptide SLed, or 1:1 SLan + SLed (Figure 2.3). Terminal explants at 28 days showed poor disorganized tissue in growth in carrier and non-SLan SAP (SLed, Table 1) filled teeth (Figure 2.4D, G). SLan-filled teeth showed organized soft tissue in the canal (Figure 2.4E, F, H, I), with collagen deposition and large, clearly visible vessels carrying red blood cells (Figure 2.3H–I). Nerve bundles are visible (Figure 2.4I, L) with an odontoblast-like layer apposed to the intracanal dentin (Figure 2.4I–K), representing tissue regeneration within implants (Figure 2.4N). Importantly, in all 8 SLan treated teeth, at day 28, implants were free of any observable calcification or disorganized hard tissue, and all had significant cellular infiltration, matrix deposition, and DSP^{+} cells (with signs of protrusions into dentinal tubules, Figure 2.4J, K). These findings, along with robust revascularization (Figure 2.4O) fulfill key features of biomaterials needed for targeted *in situ* regeneration of the dental pulp [18, 64]. Overall, we show that SLan is capable of consistently regenerating vascularized tissue in the canine pulp space. Prior to the canine studies, we screened and eliminated a number of self-assembling peptides in rodent sub-Q studies, as they did not fulfill our target criteria. We have previously shown that a pro-dentinogenic SAP (SLed, Table 2.1) promotes *in vitro* dental pulp stem cell proliferation [18], but in our canine *in vivo* experiments, SLed failed to revascularize pulp, compared to the angiogenic peptide SLan, despite having similar material properties (Figure 2.4M–O).

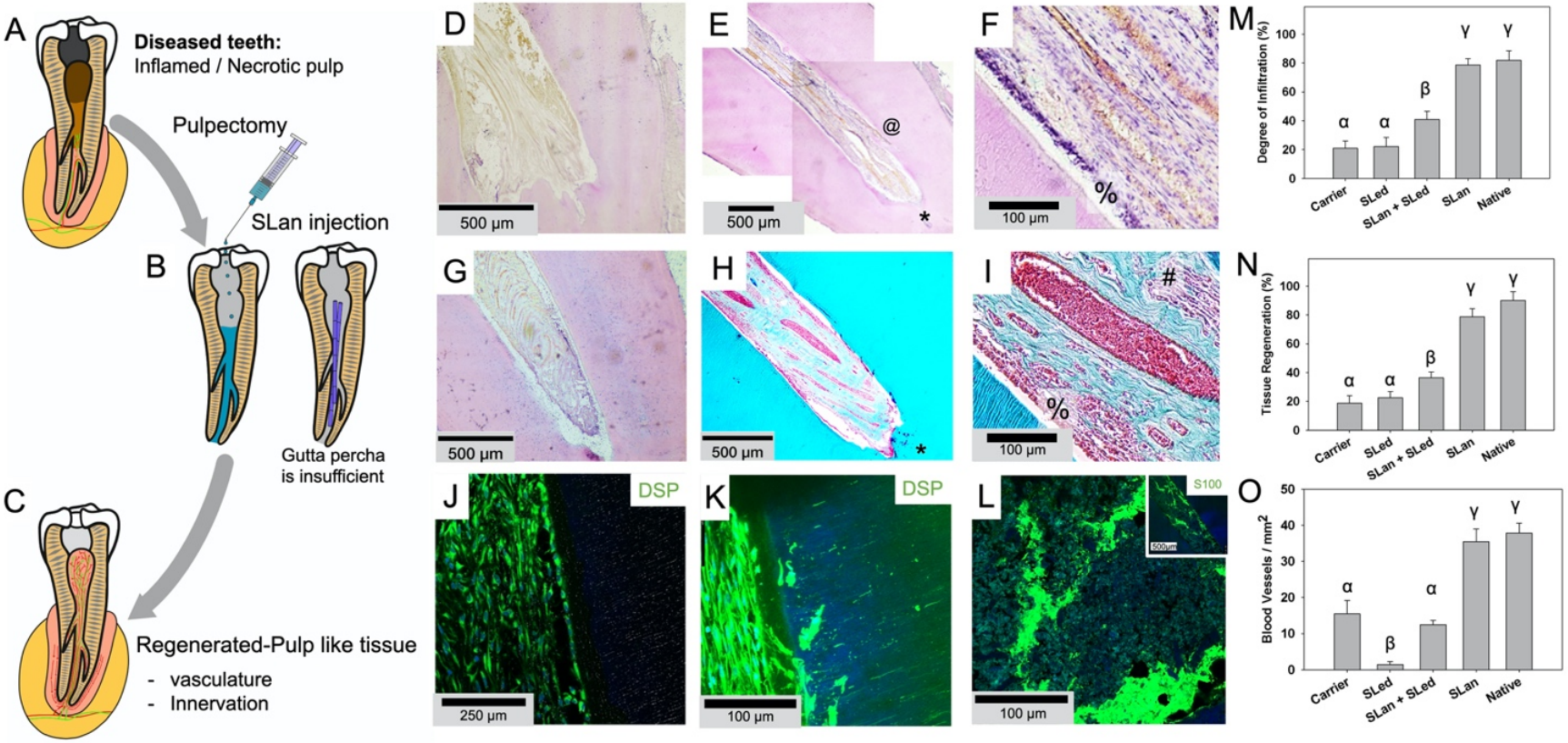

Figure 2.4 Regeneration of vascularized soft tissue in canine root canals. (A) Caries and trauma may lead to the inflammation and necrosis of the pulp. (B) After pulpectomy, implantation of injectable angiogenic SLan hydrogels help regenerate (C) vascularized pulp-like soft tissue in 28 days, unlike inert materials such as gutta percha. In a canine pulpectomy model, disorganized blood clots form for over-instrumentation carrier filled (sucrose-HBSS) control (D). H&E staining of tooth roots of SLan filled teeth showed rapid infiltration of cells and tissue (E), and within crevices in the canal space (@), along with an odontoblast-like layer in apposition to the

to the dentin wall (F-%). In contrast, control dentinogenic SLed hydrogels lead to disorganized tissue (G). Trichrome staining of SLan implants reveals blood vessels (H, I) with collagen deposition (blue); and an odontoblast-like layer (I-%) which stains with dental sialoprotein (DSP) (J) with cytoplasmic protrusions into dentinal tubules (K). $S100^{+}$ Nerve bundles (Trichrome I-#) were regenerated along the length of the canal (L and inset). (M) Degree of infiltration, (N) degree of tissue regeneration, and (O) densities of blood vessels were similar for SLan and native teeth but significantly greater than controls. (n=8 for SLan, n=4 for all other groups; values are reported as mean ± standard deviation; different Greek letters indicate statistical significance between groups $p<0.05$).

2.4 Discussion

2.4.1 Optimal Biophysical Properties

Self-assembly of SLan into a thixotropic hydrogel (Figure 2.2A, B) yields a cytocompatible material that not only has an ECM-mimetic ultrastructure (Figure 2.2E, F), but also contains a VEGF-mimicking bioactive domain in its primary sequence. Our work builds on a growing literature of acellular supramolecular biomaterials [233, 234], especially those with bioactive domains encoded directly in the scaffold [195, 214, 227, 235]. The β-sheet conformation of the supramolecular nanofiber leads to presentation of this active moiety at a high density to cell-surface receptors. Such functionalizability is the principal advantage of the therapeutic platform. However, the functionalization strategy rests on the high propensity of the core amphiphilic domain to form nanofibers in physiological pH and ionic strength [205, 223-225]. The nanofibrous architecture is key to mimicking native extracellular matrix at a subcellular scale, and the resultant hydrogels have viscoelastic properties similar to soft tissues.

2.4.2 Establishment of Angiogenic Niche *in vivo*

SLan presents a versatile platform to develop tailorable vascularized tissues *in vivo* that may have broad impact in vascularizing ischemic tissue, wound healing, and replacing

injured soft tissue. Alone, SLan results in robust angiogenesis and rapid vascularization of mature blood vessels within 7 days. In the subcutaneous niche, SLan induced formation of new vasculature and matrix deposition in 28 days. When supporting tissue ingrowth in tissue voids (tooth root canal), SLan promotes robust and sustained vascularization and soft tissue regeneration via scaffold-based signaling (Figure 2.3). It's interesting to note that the degradation of SLan hydrogels seem to be faster in the subcutaneous niche (Figure 2.3), compared to the intra-dental microenvironment (Figure 2.4). We ascribe the difference to the variance of access to peripheral circulation (and hence clearance by immune cells such as macrophages).

2.4.3 Challenges for Dental Pulp Tissue Engineering and Pulp-revascularization Therapy

Teeth are complex organs as a target for tissue regeneration. It hosts one of the softest tissues in our body (pulp) right next to the hardest tissues (enamel and dentin). It has been recognized as early as 1931 that dentinal injury adversely affects the dental pulp and the pulp-dentin complex [236], and recent investigations demonstrate the active role of dental pulp cells in repairing dentin after traumatic injury [237]. Both enamel and dentin are avascular and the apical foramen is the sole source of blood supply to the pulpal soft tissue [238]. If the dental pulp is replaced, the nutrient supply to the remodeled tissue may be disrupted, unless the tissue facilitates angiogenic sprouting into the niche. The peripheral circulation is also a potential source for infiltrating immune and progenitor cells into the pulpal cavity.

Pulp revascularization therapy is currently accepted by the American Dental Association and the American Association of Endodontics as a treatment modality to revitalize the tooth after pulp damage [239]. Over-instrumentation can be used over root

obturation (blocking/filling with gutta percha), especially in young patients, as the inert elastomeric material is an impediment to tissue remodeling in patients with open root apices [240]. Over-instrumented teeth result in blood clots (fibrin scaffolds) that resorb (~7 days) and allow tissue infiltration. Periapical tissues including survived apical papilla cells and periodontal ligament cells can proliferate in the pulp space afterwards. Infiltrating tissue leads to markedly differential responses depending on the age of the animals and procedural technique used. In adult humans, over-instrumentation has poor success rates, due to the absence of apical papilla cells and a lack of suitable matrix to support infiltrating cells and essential vasculature [98]. An off-the-shelf material-based strategy that consistently regenerates vascularized pulp like tissue is critically needed.

2.4.4 Features of the Regenerated Soft Tissue

We demonstrate that acellular SLan hydrogel scaffolds consistently regenerate vascularized organized soft tissue in the canal space post-pulpectomy in adult canines (Figure 2.4). As we combined over-instrumentation with material implantation, we were able to use an acellular formulation, as the matrix then has access to infiltrating cells. In SLan hydrogel implants, a column of DSP^+ odontoblast-like cells (DSP = dental sialoprotein) formed apposed to the dentinal tubules (Figure 2.4F, I, J). Such an odontoblast layer is present in native tissue and similar layers have been recapitulated by stem cell delivery in minipig models [84, 241]. The DSP^+ cells formed at the periphery of the SLan implant send cellular protrusions into dentinal tubules (Figure 2.3K), similar to odontoblast processes observed in native tissue [242]. The identity, source, and lineage of the DSP^+ cells need further investigation, to distinguish them from osteo-odontogenic cells. Longer

term studies may help define stability of the regenerated soft tissue and possible induction of osteogenesis/mineralization by infiltrating cells.

An unexpected but encouraging observation in our studies was that the regenerated soft tissue in the canal not only contained blood vessels, but also S100+ peripheral nerve fascicles (Figure 2.4I, L) [243]. In retrospect, this data conforms to previous reports of co-formation of nerve filaments and blood vessels in implanted self-assembling hydrogel scaffolds [224]. In addition, angiogenic factors also tend to be nerve-guiding factors, and axonal growth cones share structural similarities with endothelial tip cells crucial for angiogenesis [244]. Nerves in the dental pulp detect pain sensation [245] and the perineural niche has been identified as a source of stem cells this [246, 247] – thus innervation of the scaffold has functional implications. Based on prior studies, the odontoblast-like layer, blood vessels, and the nerve filaments may be potentially derived from stem cells recruited from the apical papilla, the periodontal ligament, or the bone marrow (via peripheral circulation) [93, 98, 248, 249].

2.4.5 Choice of the Animal Model

Ectopic subcutaneous implantation of tooth slices in immuno-compromised mice remains an important model for testing materials and stem cells for pulp and dentin regeneration [66, 229, 250-254], and for exploring mechanistic pathways to facilitate cellular reprogramming into regenerative phenotypes [249, 255]. However, for translational purposes they are inferior to orthotopic models [84, 249], such as the one employed in this study — since the latter exposes the pulpal chamber to naturally occurring signals present in its native environment. The immunocompromised mouse models often lack adaptive immune responses and thus cannot recapitulate a critical complexity of human pathology.

We selected a non-immunocompromised orthotopic canine model as our pre-clinical model since: (a) the anatomy and size of canine teeth closely mimic human teeth [191], (b) the healing process is similar, and (c) adult canines have tapered growth curves and maturation into adulthood like humans (vs. teeth of rodents that continue to grow until death) [18, 48, 50, 62, 64]. Our selection is congruent with the use of the canine models for preclinical studies [35, 48, 64, 88, 256-259], although we acknowledge the limitation that dogs have dental radicular anatomy distinct from humans (e.g., spider-webbed foramina instead of a single foramen), and alternative minipig models have been successfully used for other pre-clinical studies [84, 249]. Our animal model of choice is also superior to orthotopic rodent models [260, 261], as rodent teeth have permanent open apices and show dental pulp regeneration after over-instrumentation in mature animals, unlike adult dogs (and humans).

2.4.6 Comparison with Previous Tissue Engineering Strategies

Stem cell delivery, with or without added growth factors and scaffolds, have been the major thrust of dental pulp tissue engineering [66, 84, 88, 229, 230, 241, 250, 251, 253, 254, 256-259, 262]. Choice of stem cells, especially after full pulpectomy, is appealing as they can differentiate into both the parenchyma and the stroma of the dental pulp. Stem cell therapy has been tested for dental pulp regeneration in large animals [84, 88, 241, 256-259, 262] and in a preclinical human trial [84]. As our approach does not involve added stem cells, we attribute the success of our strategy to migration of endogenous cells into the implanted scaffold, thus the combination of material implantation with over-instrumentation can yield some of the same regenerative benefits as stem cell transplantation.

Implanted scaffolds may help support soft tissue remodeling. Some of the materials that have been used for pulp regeneration include peptide hydrogels [229, 230, 250], collagen [249, 250], silk fibroin [259], and various polymeric scaffolds [241, 252, 261, 263]. The functional self-assembling peptide hydrogel that we characterized builds on these advances by encoding bioactive signals directly in the sequence. Although VEGF-loaded scaffolds have shown limited promise in ectopic tooth slice models [229, 252, 263], we improve on these results by demonstrating success of scaffolds with VEGF-mimicking functionality in a large animal model. Similar VEGF-mimic scaffolds have demonstrated ability to facilitate formation of smooth muscle lined mature blood vessels in implants [195, 214].

Mao and colleagues have reported that recombinant Wnt3a delivered in a decellularized collagen gel can help regenerate vascularized pulp-like tissue post-pulpectomy (by recruiting endogenous cells) in an orthotopic pig model [249]. The study unequivocally demonstrates that it's possible to regenerate pulpal vasculature after complete removal of the pulp without cell transplantation, in a large animal model. Similar to our work, this acellular formulation enabled formation of $S100^{+}$ nerve filaments in the regenerated soft tissue [249].

Stem cells, recombinant factors, and decellularized matrices have batch-to-batch variabilities, sourcing issues, and problems with scaling up, all of which can be avoided by synthetic biomimetic matrices such as SLan. Scaffold-based signaling, as employed by SLan, obviates two elements of the cell-signal-scaffold triad [264] in cases where the scaffold has access to infiltrating endogenous cells [265], and thus has an operational elegance that may be useful for clinical applications and the economy of scale.

2.4.7 Limitation and Future Direction

While SLan addresses key features of pulp regenerative materials, further experiments are needed to evaluate radiographic root thickening, root lengthening, and pulp sensitivity. Bridging a critical barrier in the field, SLan-based angiogenesis presents a crucial step in developing intracanal materials, providing an option for patients who do not have the time to wait for the expansion of autologous stem cells, and who may have immune sensitivity to recombinantly expressed biologics, or who can't afford costly transplant treatments. The low cost of material synthesis indicates the potential for widespread translatability in clinical care [18, 48, 62, 64].

Critically, we demonstrate the versatility of injectable off-the-shelf SLan for vascularized tissue regeneration and material only efficacy in pulp revascularization in a large animal (adult canine) model. Overall, SLan may present a robust vascularizing hydrogel with demonstrated utility and efficacy in a variety of tissue regeneration strategies. The clinical potential of the acellular biomaterial approach may be extended to include antimicrobial activity [225] and neuroprotective functionality [227] in the scaffold and encapsulating complementary soluble factors [266].

2.5 Conclusion

We demonstrate that a soft biomimetic acellular peptide hydrogel can recapitulate the vascular niche in the dental root canal after pulpectomy. Presentation of a growth-factor mimic within the primary sequence of the constituent peptide enables retention of angiogenic functionality *in vivo* for up to a month. The material property of the hydrogel is similar to native dental pulp and in a canine pulpectomy model the material facilitates excellent biointegration and soft tissue regeneration. Supramolecular peptide hydrogels

promise to be a great addition to our tools for tissue engineering [194, 223, 234, 267, 268], as functional acellular biomaterials [233].

CHAPTER 3

SELF-ASSEMBLING PEPTIDE HYDROGELS FACILITATE VASCULARIZATION IN TWO-COMPONENT SCAFFOLDS[3]

3.1 Introduction

Acellular biomaterials [233] have been demonstrated to heal some of the most challenging tissue injuries — central nervous system injury [227], critical-sized bone defect [269], ischemic tissue damage [195, 214], and volumetric muscle loss [270, 271]. Such implantable biomaterial scaffolds can facilitate tissue healing and regeneration after sterile injuries [227, 272] or pathogenic infections [225, 273]. One of the issues preventing large scale adoption of such scaffolds is the lack of host-implant integration, deposition of native extracellular matrix (ECM) within scaffolds, and a lack of implant vascularization [274-277]. Here, we report a strategy to tackle these challenges in a polymeric scaffold, based on functionalized self-assembling peptide hydrogels.

After biomaterial scaffolds are implanted *in vivo*, they can either be walled off from the host by fibrous encapsulation [278-280], or integrate dynamically with the host tissue via tunable biodegradation, cellular infiltration, scaffold-based signaling, vascularization/innervation, and optionally, release of sequestered factors [194, 214, 281]. The integration of such implants with the surrounding host tissue can be hampered by low cellular infiltration and a lack of vascularization inside the implant.

Metabolic function of the cells inside the implant requires an adequate supply of oxygen and nutrients such as glucose and glutamine, which cannot be transported efficiently by diffusion in >1 mm sized implants. There are a variety of strategies to

[3]Adapted from **Z. Siddiqui**, B. Sarkar, K. Kim, A. Kumar, R. Paul, A. Mahajan, J. Grasman, J. Yang, V. Kumar. Self-assembling Peptide Hydrogels Facilitate Vascularization in Two-component Scaffolds. **Chemical Engineering Journal**. 422 (2021) 130145.

encourage microvascular perfusion of implants, such as pro-angiogenic scaffolds [214, 235], bioactive factors [249, 282], transplanted cells [283], monocyte-recruiting thin films [284], and TH2 cell recruiting antigens [285]. A platform system that can tune biological response to scaffolds, resulting in angiogenesis, would increase the regenerative efficacy of acellular biomaterials.

3.2 Model System:

Here, we develop a two-component scaffold that combines poly (octamethylene citrate) (POC) scaffolds and nanofibrous self-assembling peptide hydrogels to achieve tunable implant vascularization *in vivo*. POC scaffolds [286] are solid microporous materials that have been used for repair and regeneration of cartilage [287] and urinary bladder smooth muscle [288]. The biodegradation of citrate-based scaffolds releases citric acid, which can enter nearby cells and act as a metabolic fuel. In contrast, supramolecular peptide hydrogels are soft viscoelastic matrices self-assembled from short biofunctional peptides that mimic the ultrastructure of the extracellular matrix [19, 194, 195, 211, 214, 225, 227, 266, 289, 290].

In this work, we aimed to improve the bio-integration of polymeric implants without built-in vasculature [291, 292], by generating composite matrices that non-covalently functionalize POC scaffolds with supra-molecular peptide hydrogels with differing angiogenic properties (Table 3.1, Figure 3.1). We hypothesized that such hybridized matrices would lead to enhanced cellular infiltration after implantation *in vivo* in comparison to pristine POC scaffolds.

Both peptides selected (SLan and SLKr5, Table 3.1) possess identical amphipathic self-assembling domain ($K(SL)_6K$) attached via glycine linkers to angiogenic [19, 195, 214] or anti-angiogenic [211] domains (Figure 3.1). The angiogenic peptide SLan has a terminal VEGF-mimic domain which stimulates angiogenesis of proliferating endothelial cells [19], while the Kringle-5 mimic within the SLKr5 peptide inhibits endothelial cell proliferation [211]. We show that both hydrogels facilitate cellular infiltration within the polymeric scaffold, whereas SLan was dramatically better at promoting angiogenic sprouting within the scaffold pores. Our results demonstrate the initial steps in developing vascularizing hydrogels [293] that may find utility in engineering vascularized tissues [274], and in improving clinical success rates for biomaterial implants and artificial organs [276, 277, 294].

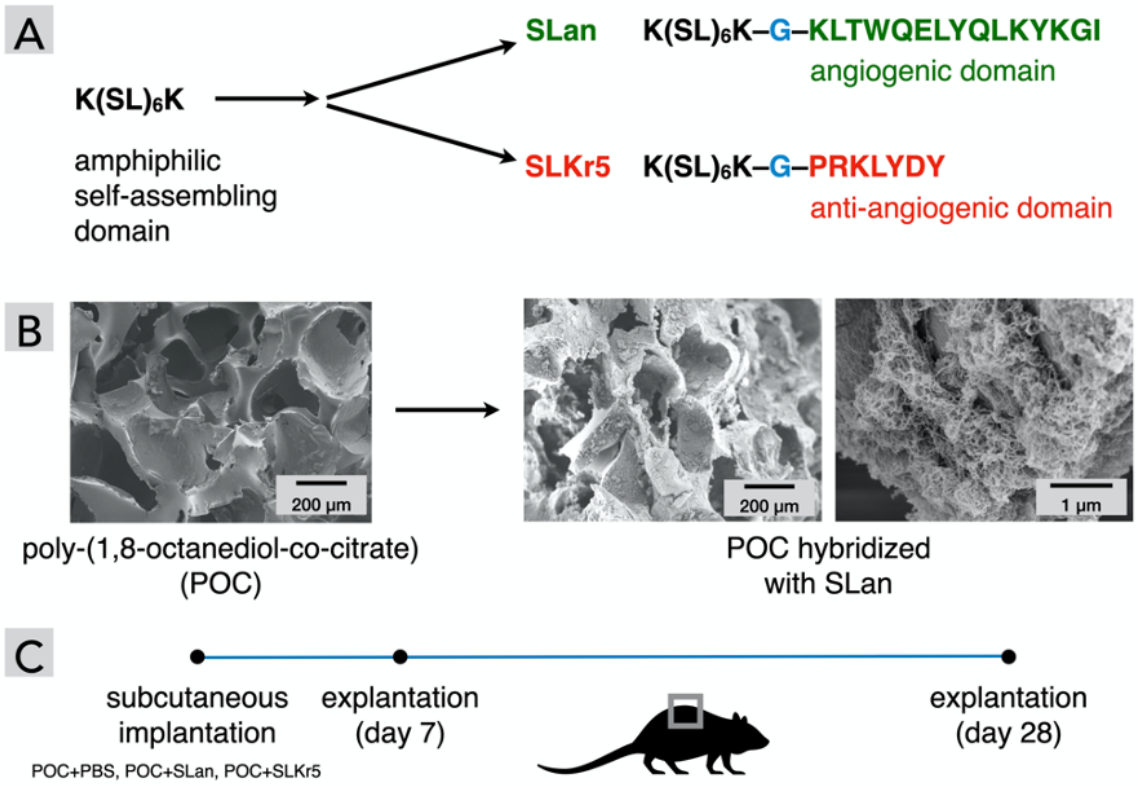

Figure 3.1 Experimental design. (A) SLan and SLKr5 share sequence similarities, differing in their biofunctional moieties. (B) Microporous POC scaffolds before and after loading

with the self-assembling peptide SLan, as observed in scanning electron microscopy (critical-point dried samples). The pores of the polymeric implant are ~100–250 μm. The hydrogels effectively fill these pores and form a nano-porous matrix inside these micro-pores (shown at two magnifications to highlight microscale and nanoscale features). (C) The scheme for testing biological response to POC scaffolds with and without self-assembling peptide hydrogels. Three types of scaffolds ([POC + PBS buffer], [POC + SLan], [POC + SLKr5]) were implanted in dorsal subcutaneous pockets of rats. A set of animals were sacrificed on day 7 to test short-term biological response. Rest of the implants were retrieved on day 28, to characterize long-term cellular infiltration and vascularization into the scaffolds by immunohistochemistry.

Table 3.1 Angiogenic and Anti-angiogenic Peptide Sequences

Peptide	Sequence	Charge	Format	Conformation
SLan *(angiogenic)*	$K(SL)_6K$–G–KLTWQELYQLKYKGI	+4	hydrogel	β-sheet
SLKr5 *(anti-angiogenic)*	$K(SL)_6K$–G–PRKLYDY	+3	hydrogel	β-sheet

3.3 Methods and Materials

3.3.1 Preparation of Microporous Polymeric Scaffolds

Poly(octamethylene citrate) (POC) pre-polymer was prepared by dissolving 1,8-octanediol and adding citric acid at 160°C and maintained at 140°C for 1 hour of polymerization [295]. Pre-polymer was dissolved at a concentration of 25% (w/v) in dioxane. Once dissolved, it was mixed with 90–120 μm (at different ratios ranging from 40 to 90%) sieved NaCl salt until thoroughly combined. The resulting homogeneous slurry was set into molds and placed in a vacuum oven for 3 days at 120°C for complete polymerization [295]. After the scaffold polymerized, no>6 mL volume of porous scaffolds were salt-leached in a 60L DI water tub for 3 days with daily water exchanges. The scaffold was air dried and vacuum dried for 24 hours each. Scaffolds were sterilized by autoclaving and stored in a desiccator until used.

3.3.2 Peptide Synthesis and Characterization

SLan and SLKr5 (Table 3.1) were synthesized with a CEM LibertyBlue solid phase peptide synthesizer with standard Fmoc chemistry (N-terminal acetylated and C-terminal amidated) [19, 211]. Refer to section 2.2.1 for solid phase peptide synthesis method.

3.3.3 Hydrogel Preparation

The SLan and SLKr5 hydrogels were prepared by dissolving lyophilized peptide in 298 mM sucrose at a concentration of 20 mg/mL, mixed with equivalent volumes of HBSS buffer (containing the multivalent counterion phosphate).

3.3.4 Scanning Electron Microscopy

200 μL of SLKr5 or SLan hydrogels were fixed overnight with 2% glutaraldehyde (Sigma). Refer to section 2.2.5 for sample preparation, critical point drying, sputter coating, and scanning electron microscopy methods.

3.3.5 Incorporation of Peptide Hydrogels into Porous Scaffolds

The peptide hydrogels were incorporated into the POC scaffold by adjusting the centrifugation rate. At 1000 RCF, the scaffold collapsed at the bottom of the microcentrifuge tube. At lower speeds of 25–50 RCF, we observed the POC scaffold did not re-immerse with hydrogel. We optimized the incorporation of the hydrogel with the POC by centrifuging at 200 RCF for 5 minutes at 25°C and left the two-component scaffolds submerged in the microcentrifuge tube overnight before implantation.

3.3.6 Subcutaneous Implantation

We followed NJIT-Rutgers Newark Institutional Animal Care and Use Committee (IACUC) and AALAC guidelines. Female Wistar rats (250–275 g) were used for dorsal subcutaneous implantation. POC samples were cut into 1 cm × 1 cm sponges that were embedded with phosphate buffered saline (PBS), SLKr5 [211], or SLan [19]. The rats were anesthetized using 2.5% isoflurane for induction and 1.5% isoflurane for maintenance, followed by shaving of dorsal regions and isopropanol and betadine sterile-prep of the surgical site. Small incisions were made 1 cm from each side of the thoracic or lumbar vertebrae (n=4 sites per animal); the connective tissue (fascia) was cleared to create small 2 cm × 2 cm subcutaneous pockets. Composite scaffolds were placed under sterile conditions in subcutaneous pockets and the incisions were closed with Vetbond (3M, Saint Paul, MN). At 7 and 28 days rats were sacrificed, and implant regions were excised. Harvested tissue sections were immediately fixed with 10% formalin. Samples were then processed by the histology core at the Rutgers Cancer Institute of New Jersey.

3.3.7 Immunohistochemical Staining

The formalin fixed sections were ethanol series dehydrated, solvent exchanged for xylene, and then paraffin embedded using a tissue processor. Samples were blocked in paraffin, sectioned to 6–8 μm sections using a microtome, and stained using hematoxylin and eosin (H&E) or Masson's trichrome (MT) (SigmaAldrich, St. Louis, MO). For immunostaining, Rabbit anti-von Willebrand factor (vWF, Abcam, Cambridge, UK), Rabbit anti-rat α-smooth muscle actin (α-SMA, Gene-Tex, Irvine, CA) and 4′,6-diamidino-2-phenylindole (DAPI, Invitrogen, Carlsbad, CA, USA) were used to stain endothelial cells, vascular

smooth muscle cells, and nuclei, respectively. Donkey anti-rabbit was used as a secondary antibody for vWF staining and goat anti-rabbit as a secondary for α-SMA staining.

3.3.8 Characterization of Histology/Immunostaining

The cell density, infiltration, collagen deposition, blood vessel density and degree of regeneration for subcutaneous and pulp revascularization samples were calculated using QuPath. The polygon tool was used to draw along the border of the entire implant. The cell detection tool was selected to adjust threshold and minimum area parameters to get the most accurate count of cells (threshold usually set between 10 and 15 and area set between 5 and 10). Cell detection was executed with the region area and number of cells were recorded. The area was converted from pixels to mm based on image scale bar size conversion factors. The cell density was extrapolated by dividing the number of cells by outlined area in mm^2. The blood vessel density was calculated within each region and determined by dividing the number of blood vessels by outlined area in mm^2. Analyses were performed across all the regions within each slide (n=4 regions per slide), and then all slides (n=4 different implants per group) for 7 day and 28 day samples were averaged (Table 3.1, Table 3.2).

3.4 Results

SLan and SLKr5 have similar biophysical properties, as reported recently. Both self-assemble into β-sheet nanofibers in aqueous solution at physiological conditions [19, 211]. The underlying nanofibrous architectures correspond to thixotropic hydrogels at the bulk scale [19, 211]. Both hydrogels are reversibly shear-responsive, as demonstrated by oscillatory rheology (particularly with a shear recovery test) [19, 211]. At high shear strain

the viscoelastic hydrogels undergo liquefaction and promptly recover their elastic properties when the strain is lowered, resulting in reassembled hydrogels [19, 211]. The thixotropic nature was observed with repeated strain cycles, demonstrating resilience of the self-assembled materials to retain this strain-dependent response. Thus, these biomaterials can be easily injected *in vivo*, where it can reconstitute into a stiff bolus. The rheological features of the hydrogels the consequences of the underlying non-covalent interactions (ionic bonds, hydrophobic interactions, etc.) that govern fibrillation and supramolecular crosslinking of the nanofibers into 3D meshes.

Integration of POC scaffolds with self-assembled peptide hydrogels (via simple centrifugation) yields hybrid micro-porous scaffolds suffused with nano-porous ECM-mimic peptide matrices (Figure 3.1B). Our previous work has shown that nanofibrous architecture of SLan and SLKr5 hydrogels [19, 211]. Hybridization of self-assembled hydrogels with POC scaffolds yields a two-component system with distinct material and chemical niches, which could be useful for segregation of infiltrating cells and may facilitate attachment and support of cells favoring different surface properties [296, 297]. This system could act as a template for further application of such hydrogels for tuning the property of various porous implants.

To test the biological response to these two-component matrices, we selected an established subcutaneous implantation model in rats (Figure 3.1C) [211, 224]. We implanted three sets of scaffolds in rodent subcutaneous pockets: microporous POC filled with (a) PBS buffer ([POC + PBS]), (b) SLan hydrogel ([POC + SLan]), and (c) SLKr5 hydrogel ([POC + SLKr5]), to determine differing tissue infiltration into pores of the polymeric scaffolds. We explanted the implants at day 7 and day 28, and characterized

cellular infiltration and blood vessel sprouting within the scaffolds by immunohistochemistry (Table 3.1, Table 3.2, Figure 3.2, Figure 3.3).

A typical feature of scaffold-induced foreign body response is the deposition of collagenous extracellular matrices around an implant creating a thick vascularized coating, with minimal tissue ingrowth into a scaffold. While we observed some collagen deposition around all the implants at day 7 and day 28, there was enhanced tissue/collagen growth within hydrogel-filled scaffolds (both [POC + SLan] and [POC + SLKr5]) (Figure 3.2, Figure 3.3), pointing to increased bio-integration of the composite scaffolds. No foreign body giant cells, which are often indicative of adverse immune reaction to a scaffold, were observed in our samples – further demonstrating a lack of foreign body response at day 28 (see Figure 3.3E for a magnified image of hydrogel filled pores).

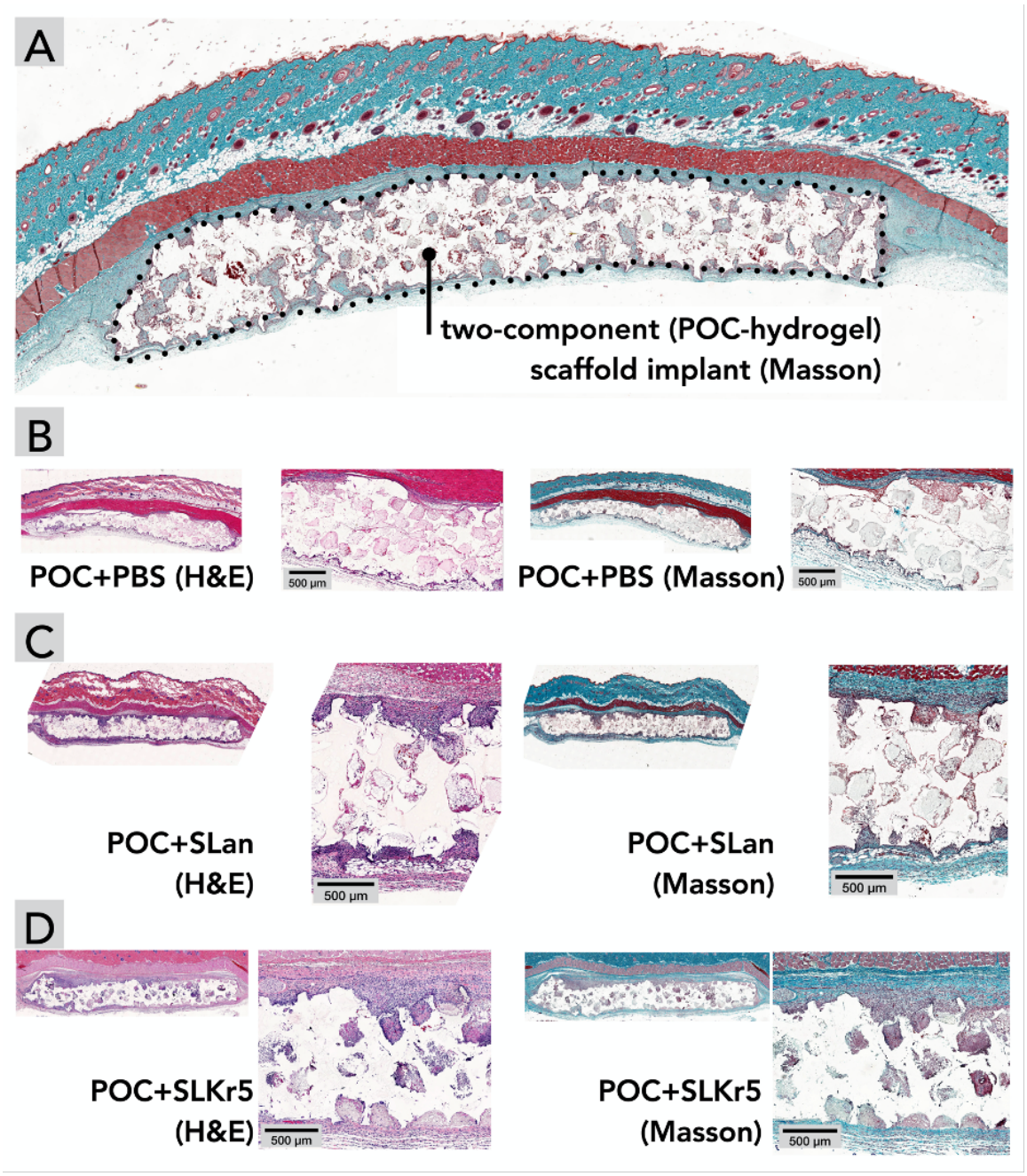

Figure 3.2 Subcutaneous implantations of scaffolds leading to cellular ingress at day 7. (A) Orientation of subcutaneous interconnected porous (100–250 µm) implants. Compared to (B) POC scaffolds with PBS, both (C) POC + SLan and (D) POC + SLKr5 scaffolds show higher cell infiltration in H&E and Masson's Trichome staining.

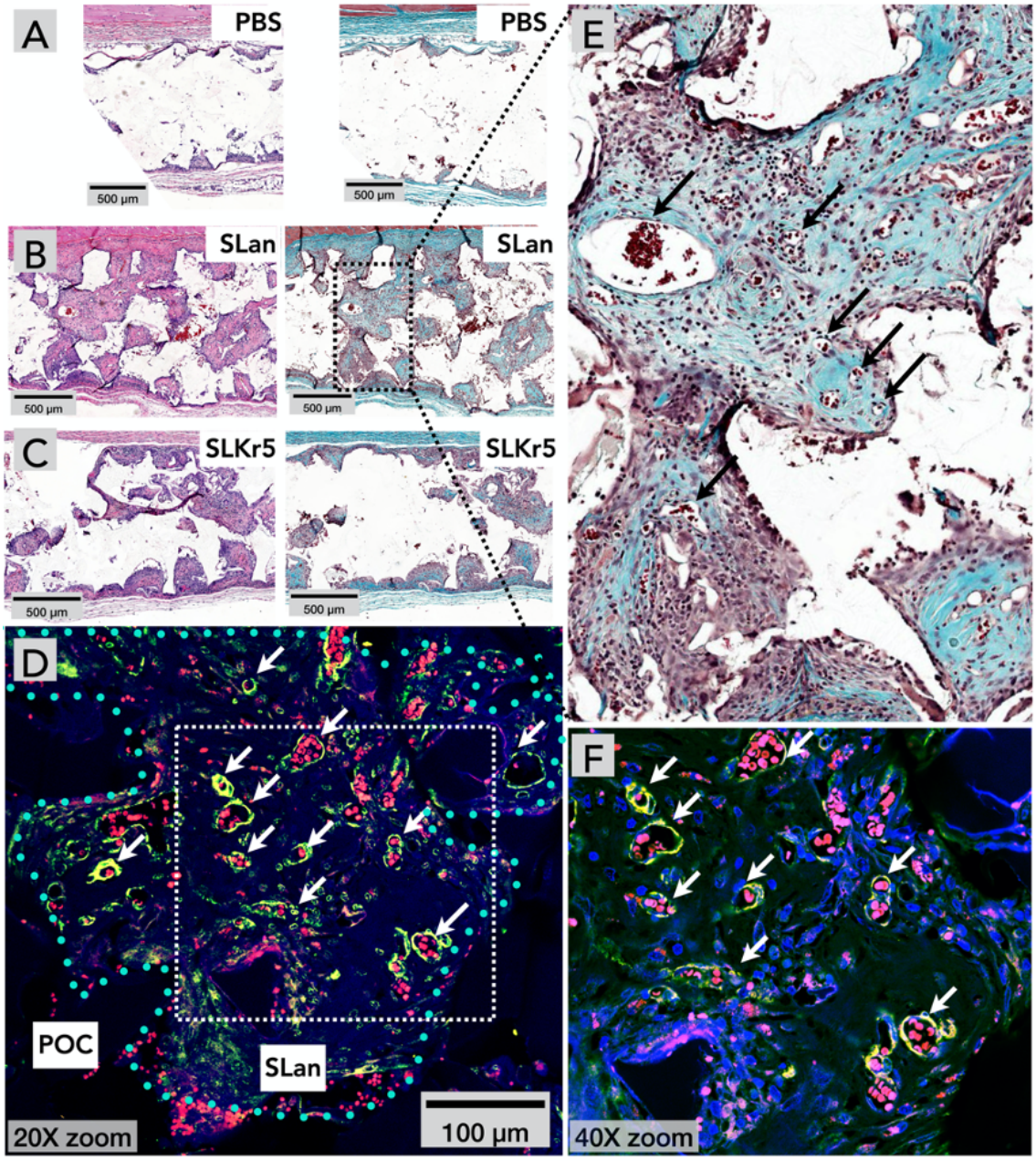

Figure 3.3 Long-term (28 days) integration of two-component scaffolds with host tissue. H&E and Masson's Trichrome staining at 28 days for (A) [POC+PBS] show continued minimal infiltration compared to (B) [POC + SLan], which had significantly more vascularization than (C) [POC + SLKr5]. (D) SLan hydrogel incorporated into the POC scaffold pores mediated angiogenesis, as characterized by 3-panel immunostaining: vWF+ (endothelial cells, red), α-SMA+ (vascular smooth muscle cells, green), and DAPI (nuclei, blue) — the dotted line demarcates the soft hydrogel from the surrounding POC polymer matrix. Composites show ingress of cells and formation of new blood vessels inside the pores of the two-component [POC + SLan]. (E) Magnified section of panel B ([POC + SLan], Masson) shows large number of blood vessels in implant pores (pointed out by black arrows), (F) Confocal microscopy of the pores of panel D at higher zoom shows α-SMA+ mature blood vessels (white arrows).

Table 3.1 Characterization of Biological Response After *in vivo* Subcutaneous Implantation

Formulation	Timepoints (days)	Cellular Infiltration	Blood Vessel Formation
POC + PBS *neutral*	7 28	H&E	H&E, M.T., vWF, α-SMA
POC + SLan *angiogenic*	7 28	H&E	H&E, M.T., vWF, α-SMA
POC + SLKr5 *anti-angiogenic*	7 28	H&E	H&E, M.T., vWF, α-SMA

Table 3.2 Qualitative Histomorphometric Differences Seen in POC Scaffold Implants

	Hematoxylin & Eosin		Masson's Trichrome		
	Cellular infiltration	Central pores infiltrated	Collagen deposition	Revascularization within pores	Fibrous encapsulation
7 Day					
POC + PBS	|	N/A	|	|	||
POC + SLKr5	|||	|||	|||	||	|
POC + SLan	||||	||||	||||	||||	|
28 Day					
POC + PBS	|	|	|	|	||
POC + SLKr5	||||	||||	||||	|||	|
POC + SLan	|||||	|||||	|||||	|||||	|

*Qualitative measures graded on a scale of | - |||||

[POC + PBS] scaffolds showed low cellular infiltration into ~100–250 μm interconnected pores at both day 7 (Figure 3.2B) and day 28 (Figure 3.3A), with no tissue deposition within scaffolds over 28 days (Figure 3.2, Figure 3.3, Table 3). [POC + SLan] scaffolds showed rapid cellular infiltration (Figure 3.2) with robust collagenous tissue deposition within scaffolds by day 28. [POC + SLKr5] also showed significant cellular infiltration similar to [POC + SLan], and similar ECM deposition within scaffolds. There are clear differences in the tissue influx within specific pores between groups. By day 28, the full thickness of [POC + SLan] samples have tissue infiltrates. To further illustrate the

degree of infiltration and comparative differences between scaffolds, we also conducted qualitative blinded analysis of histologic sections.

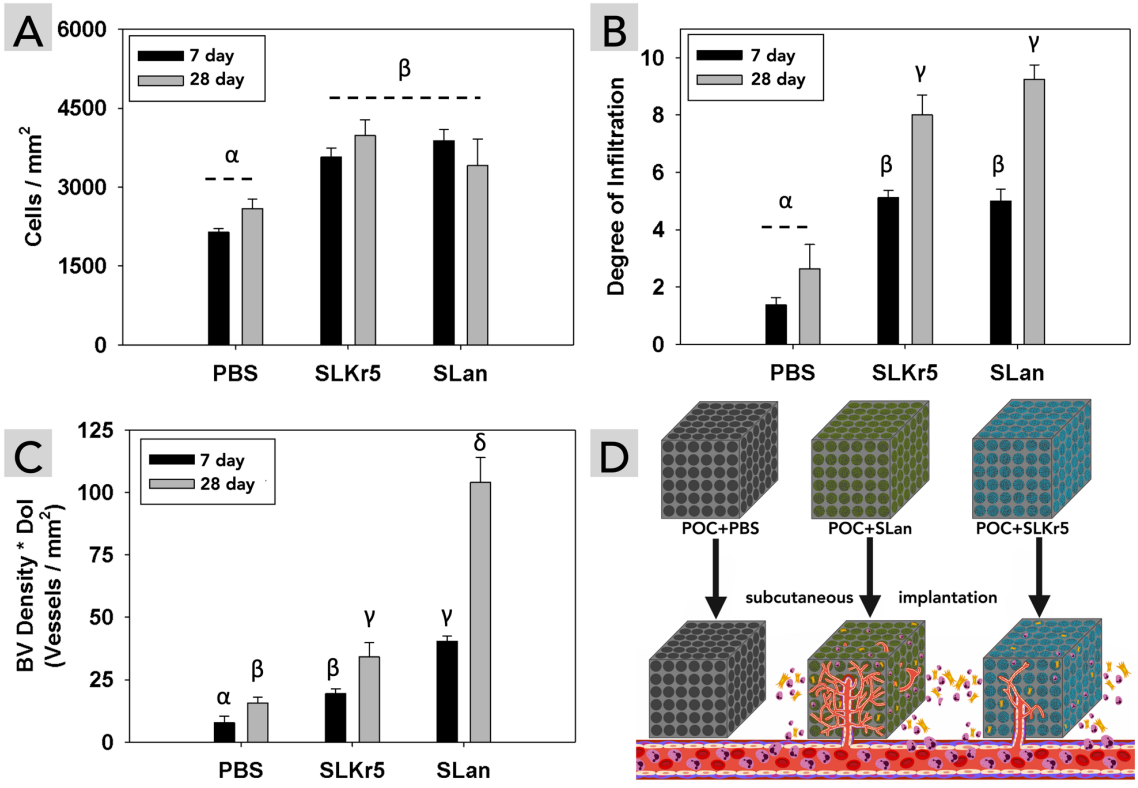

Figure 3.4 Comparison of cellular infiltration and vascularization into scaffolds. (A–C) Self-assembling peptide hydrogels modulate cellular infiltration into two-component scaffolds and affect implant vascularization. Pristine POC scaffolds had low cellular infiltration and low density of blood vessels (degree of infiltration: scale of 0 refers to no cellular infiltration within the scaffold whereas a scale of 10 refers to complete cellular infiltration throughout the bulk of the scaffold). [POC + SLKr5] scaffolds had high levels of cell infiltration but low vascularization. [POC + SLan] scaffolds had similar cell infiltration as [POC + SLKr5], but had statistically higher vascular ingress, especially at day 28 timepoint (n=4; different Greek letters indicate statistical significance between groups $p<0.05$). (D) A scheme depicting cellular infiltration and vascularization into microporous scaffolds.

We observed a striking difference in scaffold vascularization among the three implants, especially at the day 28 timepoint (Figure 3.3). The tissue infiltrates with [POC + SLan] scaffolds show numerous blood vessels (Figure 3.3E) – the number of blood

vessels was significantly higher than those in [POC + PBS] and [POC + SLKr5] implants. We decided to investigate whether the vessels formed were nascent leaky blood vessels without supporting mural cells, which are unstable and prone to resorption. We used a 3-panel imaging in immunohistochemistry that points out both endothelial cells (von Willebrand Factor vWF, red) and mural cells such as smooth muscle cells and pericytes (alpha-smooth muscle actin, α-SMA, green). Within scaffold pores, we observed large (15–50 μm) blood vessels lined by mural cells (as shown by colocalization of vWF and α-SMA (yellow). Lower vascularization in SLKr5-loaded scaffolds is congruent with our previous finding that the Kringle-5 like domain in SLKr5 imparts partial anti-angiogenic efficacy [211, 290] but serves as a scaffold for tissue deposition [211].

3.5 Discussion

3.5.1 Advantages of Two-Component Scaffolds

Self-assembling peptide hydrogels formed via non-covalent interaction-driven liquid-liquid phase separation [181], can facilitate tissue regeneration [222, 223, 229, 298]. Here we demonstrate that acellular nanofibrous peptide hydrogels can potentiate vascularization within microscopic polymeric pores *in vivo*.

Tissue-engineered scaffolds could be either solid scaffolds that need to be surgically implanted (e.g., covalently crosslinked polymeric materials) [299] or injectable scaffolds that can assemble *in vivo* (e.g., noncovalently crosslinked supramolecular hydrogels) [194]. The former is more suitable for repairing hard tissues, whereas the latter can more easily integrate with soft tissues, as their material properties mimic corresponding tissue characteristics [19, 211, 227]. Tuning of material and biochemical properties of POC

scaffolds [300, 301] have yielded a class of citrate-based polymers with diverse applications in tissue engineering [299, 300, 302, 303]. Our findings extend the use cases for such polymeric biomaterials and may lead to strategies for tunable promotion of peri-/intra-implant vascularization using such soft matrices within/on porous scaffold materials [304].

3.5.2 Controllable Angiogenesis *in vivo*

Tissue engineering involves balancing trade-offs [234, 275]. An inflammatory response is initiated by invasion of neutrophils and monocytes to an implant; a part of this ensuing cascade leads to the production of pro-angiogenic factors [222, 278, 305]. The resultant blood vessels then create channels for further infiltration of probing myeloid cells. This positive feedback loop, if not controlled, may lead to chronic inflammation. Thus, it may be desirable to develop tools to de-couple cellular infiltration from angiogenesis. The anti-angiogenic peptide hydrogel SLKr5 is compatible with stromal cells but prevents formation of blood vessels by endothelial cells [211]. Such anti-angiogenic hydrogels coupled with microporous scaffolds such as POC, may thus invite cell infiltration with minimal vascularization in the implant, adding an important regulatory tool in our design toolbox.

Two-component matrices such as the one developed here can bring together ECM-mimicking material/structural features of self-assembling peptide hydrogels and facile synthesis of polymeric scaffolds such as POC, providing a platform that retains synthetic simplicity and low batch-to-batch variability, while enabling *in vivo* implant integration [278-281].

Migration and formation of blood vessels into a two-component scaffold may depend on not only the chemical functionality embedded by design, but also on the material

features, surface charge, and the immune response triggered by the matrices [222]. Recruitment of myeloid cells to implanted peptide hydrogels may produce angiogenic cytokines, contributing to vascularization of the implant [222]. Similar mechanisms may be partly responsible for vascularizing the two-component scaffolds [POC + SLan] and [POC + SLKr5]. Despite similar formal charges on the building blocks (Table 3.1) and similar rheological properties [19, 211], [POC + SLan] has dramatically higher extent of implant vascularization than [POC + SLKr5], by day 28 (Figure 3.3, Figure 3.4). We attribute the difference in the vascularization to the distinct bioactive moieties in the peptide sequences (Table 3.1, Figure 3.1).

The anti-angiogenic peptide SLKr5 shares the central self-assembling domain with SLan and has the opposite biofunctional property (of blocking angiogenesis) — providing us an interesting pair of promoter/inhibitor dopants to influence biofunctional performance of POC scaffolds in opposing fashion (Figure 3.3, Figure 3.4). Such patterning of implanted scaffolds may offer an alternative way to provide pre-programmed signals to endogenous cells, in contrast to environmental stimuli [306]. A patterned acellular scaffold that is infiltrated by different populations of cells into segregated compartments or layers may be useful for functional tissue replacement.

The blood vessels formed inside [POC + SLan] scaffolds can be observed in both H&E and Masson's trichrome staining (Figure 3.3). We confirmed that these blood vessels have a mature medial layer via staining for vascular smooth muscle cells (Figure 3.3D), suggesting that they are mature non-transient structures. Such 25–50 μm blood vessels form within 28 days, preferentially within the angiogenic hydrogel containing pockets of

the POC implant (Figure 3.3E). We demonstrate that *in vivo* properties of hard polymeric scaffolds can be tuned by non-covalently doping with self-assembling peptide hydrogels.

3.5.3 Features of the Acellular Regenerative Biomaterials

Polymeric implants can be ideal, from the standpoint of material properties, for repair and regeneration of tissues experiencing high shear rate — such as muscle, cartilage, and bone. Vascularizing these implants *in vivo* can improve their functional integration with the surrounding tissue. Such scaffolds can be great tools for tackling large volumetric tissue defects. In particular, the ability to rapidly generate robust vasculature in a wound bed would be advantageous for tissues with high metabolic rate, such as skeletal muscle [307, 308]. Here we show that hybridization with an angiogenic peptide hydrogel can lead to rapid (in less than a month) formation of large, mature (25–50 μm, α-SMA^{+}) blood vessels inside the central region of implants (over 2 mm in thickness), without exogenous cells or growth factors (Figure 3.3D–F). Such scaffold-based signaling may lead to off-the-shelf acellular regenerative options [194, 223, 233, 234], with low batch-to-batch variability and without pronounced foreign body response associated with synthetic scaffolds [222, 278-281, 309].

3.5.4 Limitations and Future Directions

We next aim to characterize the cellular infiltrates into these two-component scaffolds as a function of infiltrating vasculature and how they change temporally. We expect that the combination of cellular infiltration and vascularization will enhance the efficacy of local/hematopoietic progenitor cells to stimulate tissue regeneration. Such studies would

improve our understanding of the cell biology of vascularization in the implants and help us optimize the regenerative sequence post-injury.

The potential of our strategy can be extended even further by bioprinting scaffold/hydrogel pairs that allow a certain tissue formation (say, blood vessels), while blocking another (say, nerve fibers). In embryogenesis, such discrete structures form elegantly, but they are relatively difficult to recapitulate in laboratory conditions, especially as similar molecules guide both nerves and blood vessels (e.g., Netrins, VEGF-A, FGF-2, etc.) [244].

We have not yet studied the long-term (>6 months) biodegradability of these peptide hydrogels *in vivo*. It's possible that higher extents of vascularization may correlate with faster degradation rates. If such degradation coincides with concomitant deposition of extracellular matrix by the infiltrating cells, the integration of the hydrogel with the surrounding tissue may be favored, thus enhancing functional regeneration. Hydrogels that are degraded quickly can even be candidates as sacrificial components in multi-component regenerative scaffolds [194].

3.6 Conclusion

We have demonstrated a simple strategy of implanting two-component scaffolds *in vivo* for functional angiogenesis, where the components vary by chemical structure, material properties, porosity, and biological response. Self-assembling peptide nanofibers form ECM-mimetic matrices inside polymeric implants, instruct cellular infiltration, and guide angiogenic sprouting. Our study will be helpful for researchers interested in designing

patterned biomimetic scaffolds that can engender component-specific biological response *in vivo*, resulting in segregated biomimetic tissue substitutes.

CHAPTER 4

PRECLINICAL EFFICACY OF PRO- AND ANTI-ANGIOGENIC PEPTIDE HYDROGELS TO TREAT AGE RELATED MACULAR DEGENERATION[4]

4.1 Introduction

Age-related macular degeneration (AMD) affects 11 million patients in the United States and is the leading cause of visual disability in industrialized countries [310]. A subtype of AMD, wet AMD (neovascular AMD), is characterized by abnormal growth of vessels in choroidal and retinal circulations promoted by vascular endothelial growth factors (VEGF) [311]. Neovascularization coupled with high vascular permeability leads to macular edema or hemorrhage and eventual visual impairment [312].

Anti-VEGF is the most common treatment paradigm for wet AMD and many other retinal diseases, including proliferative diabetic retinopathy and retinal vein occlusions [313]. Current anti-VEGF therapies require regular intravitreal injections that are associated with sight-threatening complications including endophthalmitis [314]. Administration routes alternative to intravitreal injections such as topical administrations have been unsuccessful to date due to the difficulty in reaching choroidal blood vessels [315]. Recently, a new promising strategy has emerged capitalizing on the sustained release of anti-VEGF agents to the posterior segment of the eye, employing implants, nano-formulations, and hydrogels [315]. While the results of research in the area are encouraging [315], wet AMD therapies are still faced with significant challenges in their inherent bioactivity, payload quantity, targeted delivery, sustained release, biocompatibility, and optical clarity; therapeutics which successfully address these shortcomings will have

[4]Adapted from A. Acevedo-Jake, Siyu Shi, **Z. Siddiqui**, S. Sanyal, R. Schur, S. Kaja, A. Yuan, V. Kumar. Preclinical Efficacy of Pro- and Anti-angiogenic Peptide Hydrogels to Treat Age-related Macular Degeneration. **Bioengineering**. 8 (2021) 190.

improved performance and will result in better long-term patient outcomes

Peptide-based hydrogels successfully address many of the challenges above, and additionally are readily synthesized at low-cost and high purity, can be conjugated to other polymers, fluorophores or chemical moieties in a straightforward manner to alter or improve their physical properties, can be modified to be persistent, biodegradable or responsive to stimuli, and can serve as excellent biomimetic scaffolds—all characteristics which prime their use as biomaterials for medical applications [298, 316-322]. While many strategies developing covalently crosslinked hydrogels have shown great potential in the biomedical field [206, 323-326], non-covalently crosslinked hydrogels, whose assembly and structure are solely guided by weak supramolecular interactions, confer additional advantages such as self-healing, high elasticity, and shear thinning [318, 326, 327]. Rational design of the base peptide sequence governs both the final structure and the inherent functionality of the final material, while the ability to easily tune peptide sequences facilitates modularity in these platforms [208, 222, 318, 328, 329]. Multi-domain peptide MDP hydrogels exemplify many of the characteristics above and are composed of an alternating A-B-A sequence motif, where the terminal A blocks contain either positively or negatively charged amino acids (ex. K/R or E/D), and the B midblock domain contains a repetitive β-sheet domain of alternating hydrophobic and hydrophilic amino acids (ex. $(SL)_6$) [208, 222-224, 330]. Upon aqueous dissolution, β-sheet monomers spontaneously associate into dimers to exclude solvent and form a hydrophobic core (Figure 4.1) while hydrophilic residues associate with solvent. Further assembly of dimers produces short fibers, though significant anisotropic fiber extension is prevented by the proximity of many charged A domains [205, 331, 332]. Subsequent addition of charged

ions, drugs or other polymers facilitates terminal charge shielding in these domains and allows for unidirectional fiber extension as well as three-dimensional intertangling of multiple fibers, ultimately giving rise to stiff, optically clear, thixotropic hydrogels [197, 198, 208, 223, 266, 333, 334]. While this base sequence has shown excellent promise as a scaffold for wound healing, drug delivery and tissue regeneration [197, 198, 222-224, 266, 330, 333, 334], additional functionality can be incorporated by appending short epitopes at one of the termini, generating new A-B-A-C-type hydrogels which can be used to promote neurogenesis or dentinogenesis, modulate inflammation, reduce bacterial load or regulate lipoprotein homeostasis [18, 19, 225-227, 335]. Of these designer hydrogels, versions which are either pro- or anti-angiogenic have recently shown great potential for tissue regeneration in several disparate biomedical applications [19, 194, 195, 211, 214, 226, 336, 337].

In this study, we investigated the preclinical efficacy of two novel peptide hydrogels, one containing a pro-angiogenic [19, 315] motif and the other an anti-angiogenic motif in a rat wet AMD model (Figure 4.1). Both novel peptide hydrogels demonstrate biocompatibility, targeted delivery, sustained release, and optical clarity — important design criteria for biomaterials for wet AMD treatment. Surprisingly, the overall efficacy of the pro-angiogenic peptide hydrogel was significantly improved compared to the anti-angiogenic peptide hydrogel, and its performance was found comparable to Aflibercept (Eylea®), an approved treatment for wet AMD. Our results suggest a possible new protective role of VEGF in stabilizing neovascularization and reducing vascular permeability in wet AMD.

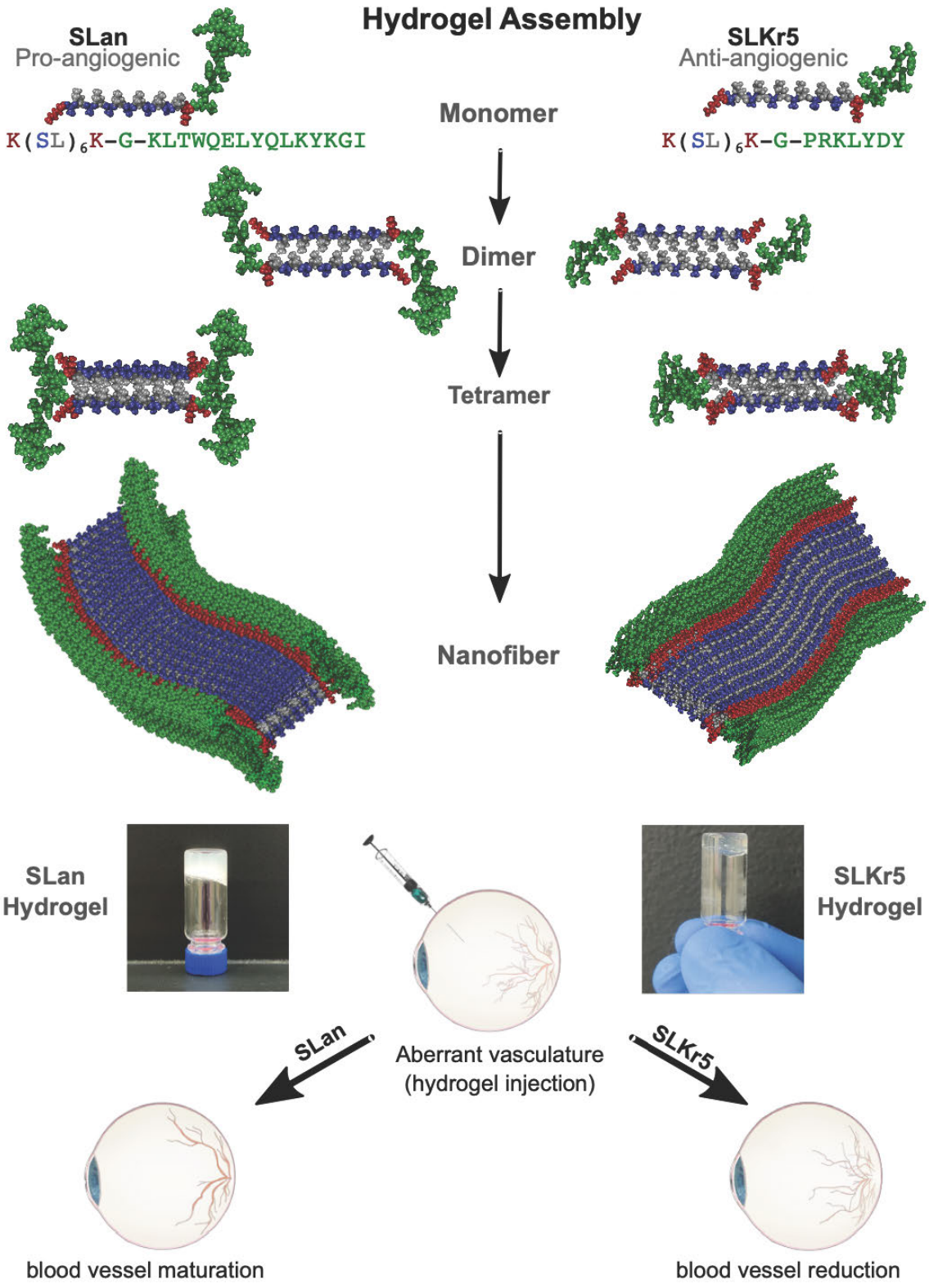

Figure 4.1 Schematic of the proposed assembly mechanism of the hydrogels.

4.2 Methods and Materials

4.2.1 Peptide Preparation and Characterization

Pro-angiogenic peptide SLan (peptide sequence K(SL)6K–G–KLTWQELYQLKYKGI) and anti-angiogenic peptide SLKr5 (peptide sequence K(SL)6K–G–PRKLYDY) were synthesized with a CEM LibertyBlue solid phase peptide synthesizer using standard Fmoc chemistry (Table 3.1), refer to section 2.2.1 for solid phase peptide synthesis methods. Peptide purity was verified >85% by an Agilent 1100 series HPLC instrument with an Agilent (Santa Clara, CA, USA) C3 reverse phase column, and products were monitored by UV at 280 nm. The identity of the peptides was verified with an Orbitrap Q Exactive LC/MS (Thermo Scientific, Waltham, MA, USA) instrument. Lyophilized pro-angiogenic and anti-angiogenic peptides were formulated as gels with the addition of 298 mM sucrose and passed through a 0.22 μm filter for sterilization, and multivalent counterions (PO_4^{3-}) in 1X PBS (autoclaved), to maintain osmolarity, shield charges, and form salt-bridges between the terminal lysines of the peptides. Sterile filtering should not affect the overall structure of the peptides or hydrogels, as the gel is formed through non-covalent interactions as it self-assembles. Chemical characterization of the pro-angiogenic peptide has been previously reported [19]. Optical transparency of gels was observed during optical imaging in the eye; optimization of imaging with trial eyes led to the choice of concentrations used, which were noted to be optically transparent both *in vivo* and *in vitro*. Two concentrations of anti-angiogenic peptide hydrogel (low concentration — 0.02 w% and high concentration — 0.2 w%) and one concentration of pro-angiogenic peptide hydrogel (1.0 w%) were thereby selected to proceed with *in vivo* studies because these hydrogels remain optically clear at these concentrations.

4.2.2 Rat Laser-induced Choroidal Neovascularization Model

A rat laser-induced CNV model is a well-established animal model for wet AMD. All animal studies were in accordance with State and Federal Guidelines and approved by the IACUC committee of Experimentica Ltd. (Forest Park, IL, USA). Briefly, animals were anesthetized, given a subcutaneous injection of ketamine and medetomidine, and a 0.5% solution of tropicamide (Alcon, Fort Worth, TX, USA) was applied to the cornea to dilate the pupil. Laser photocoagulation (power 150 mW, 100 μM spot size, 100 ms duration) was performed once using a 532 nm diode laser (Novus Spectra, Lumenis, Israel) attached to a slit lamp. A coverslip and Viscotears® gel (Novartis, Cambridge, MA, USA) were used to applanate the cornea, four laser lesions were performed in each eye, and anesthesia immediately reversed. Immediately after lasering, unilateral intravitreal (IVT) administrations of 5 μL peptide hydrogels each were performed via a glass microsyringe (33 gauge needle, Hamilton Bonaduz AG, Bonaduz, Switzerland). Eight male rats were treated with low concentration anti-angiogenic peptide hydrogel (0.02 w%), six with high concentration anti-angiogenic peptide hydrogel (0.2 w%), seven with pro-angiogenic peptide hydrogel (1 w%), six with Aflibercept (200 μg), and six with 298 mM sucrose solution (vehicle). The contralateral eye served as control. Rats were followed using *in vivo* imaging for 14 days via fluorescein angiography (FA) and spectral-domain optical coherence tomography (SD-OCT).

4.2.3 Analysis of Choroidal Neovascularization Lesions with *in vivo* Imaging

To determine the preclinical efficacy of pro-angiogenic and anti-angiogenic hydrogels, the CNV lesions were monitored using spectral-domain optical coherence tomography (SD-OCT) and fluorescein angiography (FA) at baseline on day 0 (after lasering), and at follow-

up days 3, day 7, and day 14 (end of the study period). Rats received subcutaneous injections of 1 mL of 5% fluorescein sodium salt (Sigma-Aldrich Finland Oy, cat. No. F6377), as is typical for rodents [338-340]. Vascular leakage was examined using a Heidelberg Spectralis HRA2 system (Heidelberg Engineering, Germany). CNV lesions and retinal thickness were monitored using an Envisu R2210 SD-OCT system (Bioptigen Inc./Leica Microsystems, Morrisville, NC, USA). For imaging, the rat was placed into the holder and the imaging systems aligned with the first infrared reflectance image taken from the system, then sodium fluorescein was administered and consecutive FA images taken every 60 seconds from the retinal and choroidal focus level for a period of 5 minutes from the sodium fluorescein injection. Qualitatively, lasered spots were evaluated based on the presence or absence of a retinal vascular leak. The presence of CNV was identified from lasered spots that have a leakage as observed by comparing the dynamics of the fluorescein signal in a series of fundus FA images. SD-OCT imaging was used as a secondary confirmation of CNV or in questionable FA, where the presence of intraretinal fluid in SD-OCT images would suggest the presence of CNV. Quantitatively, vascular leakage was measured using FIJI (v. 2.0) software by outlining the area of vascular leak manually from the last FA image of each imaging session. All researchers were blinded on the treatment each animal received during measurement.

4.2.4 Data Analysis

Quantitative data were plotted, analyzed, and presented as mean standard deviation (SD) or standard error of mean (SEM). Lesion size as well as leakiness was compared within each group and between each group, and accordingly, parametric data was analyzed using one-way ANOVA test, while non-parametric data was analyzed using Kruskal–

Wallis ANOVA. Multiple comparison tests were performed as appropriate, and data with common Greek symbols showed no statistical significance at $p<0.05$ level.

4.3 Results

4.3.1 Tolerability of Peptide Hydrogels

Therapeutic utility and tolerability were evaluated in the rat laser-induced choroidal neovascularization model, a commonly used animal model for wet AMD [341]. No adverse reactions due to the study compounds were observed. Animals were monitored for any notable changes in body weight and animal behavior, as well as signs of inflammation in the eye for the duration of the study period. Rat weight was not affected by the treatments ($p=0.542$), and no redness, swelling or loss of function was noted in any of the eyes, nor were any gross morphology changes noted. At the time of explant, gross observation of animal and organs revealed no untoward observation. We observed optical transparency of gels during optical imaging in the eye; optimization of imaging with trial eyes led to the choice of concentrations used, which were noted to be optically transparent both *in vivo* and *in vitro*.

4.3.2 Qualitative Analysis of CNV Lesions

The presence of leaky CNV lesions was determined from FA (Figure 4.2) and SD-OCT (Figure 4.3) images acquired immediately after CNV induction (day 0 in Figure 4.3), on day 3, day 7, and day 14 post-CNV.

We first analyzed CNV lesions qualitatively. Lesions were graded as “leaky” or not “leaky” by a researcher experienced in the CNV model (Figure 4.4). On day 7, only 4.2% of lesions treated with Aflibercept and 7.1% of lesions treated with pro-angiogenic peptide

hydrogel had the presence of leaky lesions, significantly less than lesions treated with vehicle solution (41.7%, p=0.002 and p=0.003, respectively). The treatment effects of pro-angiogenic peptide hydrogel were comparable to that of Aflibercept (p=0.65). Lesions treated with either low concentration or high concentration of anti-angiogenic peptide hydrogel showed statistically non-significant benefit compared to vehicle solution (low concentration 28.1% non-leaky p=0.29 and high concentration 29.2% non-leaky p=0.33, respectively). On day 14, all treatment groups showed a higher percentage of leaky CNV lesions, with a statistically significant difference compared to the vehicle group. Lesions treated with pro-angiogenic peptide hydrogel had the lowest percentage of leaky lesions (57.1%), followed by high concentration of anti-angiogenic hydrogel (62.5%), and low concentration of anti-angiogenic hydrogel (71.9%). Aflibercept treated lesions had a similar percentage of leaky lesions compared to the vehicle control group (75%).

4.3.3 Quantitative Analysis of CNV Lesions

CNV lesions were analyzed quantitatively by evaluating the average areas of vascular leak per lesion based on FA images (Figure 4.5). On day 0, average lesion areas were similar among all groups ($p>0.05$). On day 7, the lesions treated with pro-angiogenic peptide hydrogel and Aflibercept had a significantly smaller area of vascular leak compared to lesions treated with vehicle solution (p=0.007). The average area of vascular leak was similar in pro-angiogenic peptide hydrogel group and Aflibercept group (714.3 μm^2 vs. 666.7 μm^2, respectively, p=0.96). The average area of vascular leak in the high and low concentrations of anti-angiogenic peptide hydrogel groups were 4208.3 μm^2 and 2781.3 μm^2, non-statistically significantly smaller than that in the vehicle group (5833.3 μm^2, p=0.50 and 0.11, respectively).

On day 14, all treatment groups showed higher average area of vascular leak, with no statistically significant difference compared to the vehicle group. The area of vascular leak was the lowest in the pro-angiogenic peptide hydrogel group (3642.9 μm^2), and the highest in the vehicle group (9025.0 μm^2).

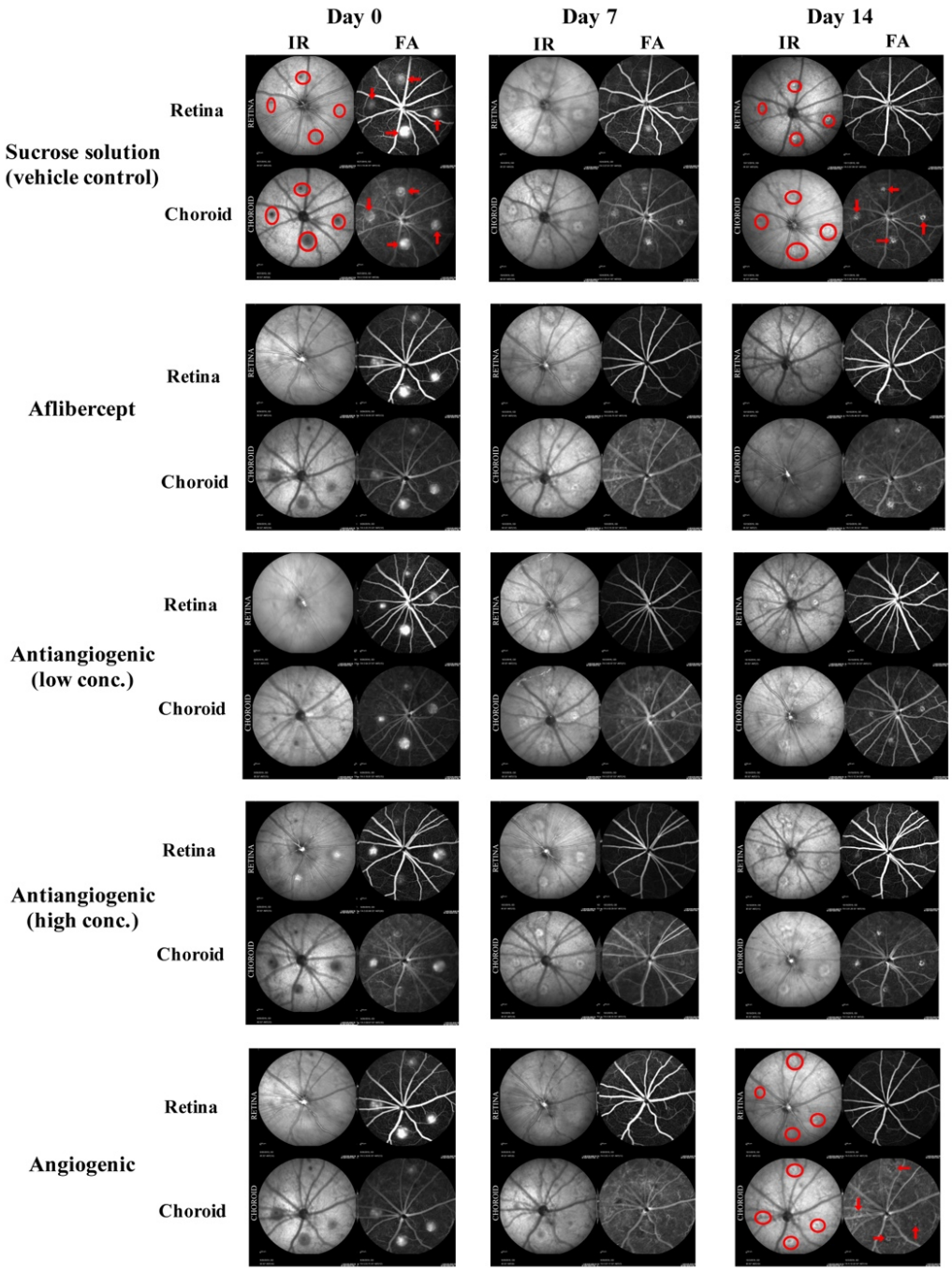

Figure 4.2 Representative infrared reflectance (IR) and fluorescein angiography (FA) images taken 5 minutes post sodium fluorescein injection for both the retinal and the choroidal focus planes in CNV induced eyes. Lasered spots in the choroidal and retinal focus planes are indicated by red circles at day 0 for reference and appear as a shadowed area by IR. Bright spots in these focus planes during FA imaging show areas of vascular leakage, which are indicated by red arrows in day 0. Day 0 images are representative of leaky lesions, while a representative non-leaky lesion is shown in the day 14 angiogenic group.

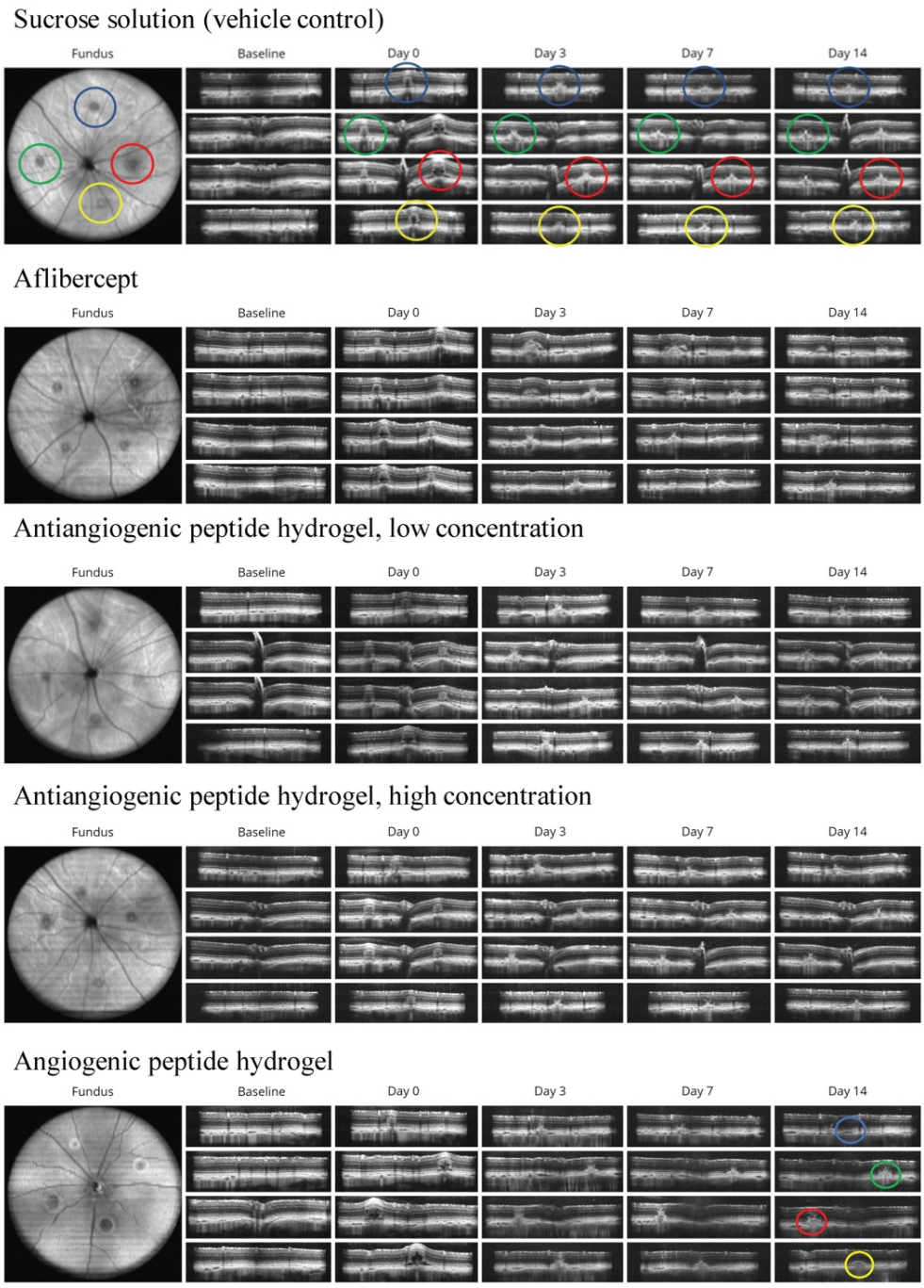

Figure 4.3 Representative SC-ODT images from experimental groups at baseline, immediately after photocoagulation on day 0, and follow ups on days 3, 7, and 14. The presence of intraretinal fluid in SD-OCT images suggests the presence of CNV; circles in the fundus image outline the location of each laser photocoagulation spot (approximately at 12 o'clock (blue), 3 o'clock (red), 6 o'clock (yellow) and 9 o'clock (green)) over different timepoints showing the development of CNV for each group. The four fundus images were taken through the retina containing one of the four lesions. Day 0 images are representative of leaky lesions, while a representative non-leaky lesion is shown in the day 14 angiogenic group.

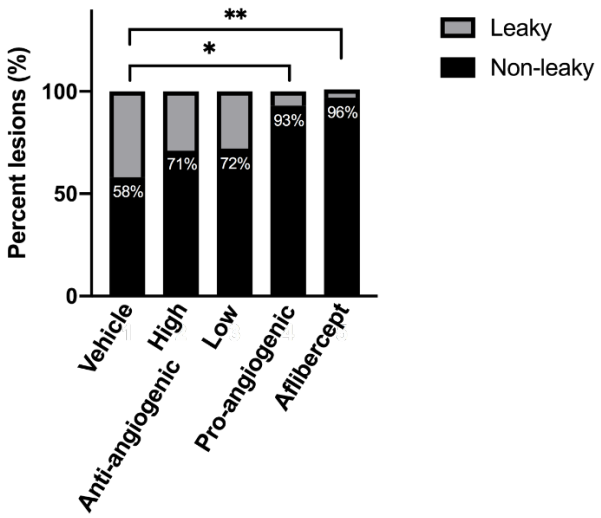

Figure 4.4 Number of lesions without leaky vessels at day 14 based on *in vivo* FA and SD-OCT imaging of experimental groups: sucrose vehicle, anti-angiogenic peptide hydrogel (high), anti- angiogenic peptide hydrogel (low), pro-angiogenic peptide hydrogel, and Aflibercept, respectively. The pro-angiogenic peptide hydrogel and Aflibercept showed protective effects compared to the vehicle group (* $p<0.05$, ** $p<0.01$).

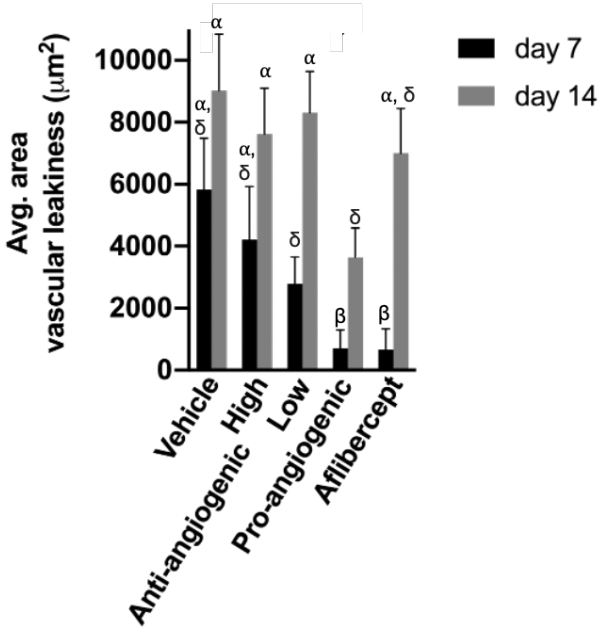

Figure 4.5 Average area of vascular leak at day 7 and day 14 based on fluorescein angiography imaging of experimental groups: vehicle, anti-angiogenic peptide hydrogel (high), anti-angiogenic peptide hydrogel (low), pro-angiogenic peptide hydrogel, and Aflibercept. At day 7, the pro-angiogenic peptide hydrogel and Aflibercept groups had smaller area of vascular leakiness compared to the vehicle group ($p<0.05$). Similar Greek letter show no significant difference between groups.

4.4 Discussion

In this study, we demonstrated the tolerability and therapeutic efficacy of pro-angiogenic and anti-angiogenic peptide hydrogels in a choroidal neovascularization (CNV) rat model and demonstrated the potential for pro-angiogenic peptide hydrogels performing comparably to Aflibercept. In addition, pro-angiogenic and anti-angiogenic peptide hydrogels suggest potentially quicker effects than Aflibercept.

Treatment strategies for wet AMD have evolved in the last decade, drastically changing patient outcomes. Before the advent of anti-VEGF therapy for wet AMD, patients would progressively lose vision and become permanently blind. With the approval of Ranibizumab and Aflibercept for wet AMD and the off-label use of Bevacizumab, visual acuity after treatment initially improves or stabilizes. However, more than 70% of patients do not maintain driving vision in the long term [342]. These therapeutics also have other limitations, including the need to indefinitely receive intravitreal injections due to non-lasting effects and relatively short half-lives at 4–8 days. Some patients require injections as frequently as monthly. Each intravitreal injection carries the risk of endophthalmitis, retinal tear, ocular hypertension, retinal hemorrhage, and iatrogenic cataract, in addition to subjective risks such as anxiety and pain [343].

Our study yielded the surprising results that both the pro-angiogenic and anti-angiogenic peptide hydrogel showed significant improvement in CNV lesions comparable to Aflibercept. We hypothesized that the pro-angiogenic peptide hydrogel may stabilize vasculature and prevent the vascular permeability that results in leaky lesions. It has been observed that hypoxia contributes to the pathogenesis of vascular permeability and fragility in wet AMD. Pro-angiogenic peptide hydrogel may protect vascular integrity by improving

oxygen delivery in neovasculature [344]. Additionally, it has been observed that different isoforms of VEGF have different effects on vascular permeability [345]. Therefore, it is possible that the pro-angiogenic peptide was structurally more like the VEGF isoforms that do not induce vascular permeability. Previous publications have shown that pro-angiogenic peptide hydrogel can promote maturation of new vessels [19, 337], thereby preventing vascular permeability in immature vessels [346].

4.5 Conclusion

There are several limitations to our study. We used a small number of animals and follow up time was limited to 14 days, a short time frame for a chronic disease. The effect of pro-angiogenic and anti-angiogenic peptide hydrogels showed trends of improvement compared to vehicle control and Aflibercept, but the differences were not statistically significant due to the small number of animals studied.

The pro-angiogenic hydrogel showed significant treatment effects comparable to the standard of care Aflibercept in both the number of leaky lesions and the area of vascular leak. In addition, both pro-angiogenic and anti-angiogenic peptide hydrogels showed moderate improvement of CNV lesions at day 14. The pro-angiogenic peptide hydrogel showed more favorable treatment responses at day 14, suggesting the possibility of longer lasting effects than Aflibercept. Pro-angiogenic and anti-angiogenic self-assembling peptide hydrogels could potentially provide several advantages compared to existing anti-VEGF intravitreal injections.

In conclusion, the preclinical study suggests that pro-angiogenic peptide hydrogels are comparable to Aflibercept at treating CNV in rats. Follow up studies in larger animal

pre-clinical studies will be needed to elucidate the total length of activity with pro-angiogenic and anti-angiogenic peptide hydrogels.

CHAPTER 5

CONCLUSIONS AND FUTURE DIRECTIONS

Through a solid phase peptide synthesis (SPPS) we synthesized SLan, an angiogenic self-assembling peptide hydrogel (SAPH). SLan contains a functional mimic of vascular endothelial growth factor (VEGF), termed QK, that uses scaffold based signaling to potentially promote vascularization (for example conformally within the tooth root). SAPH form antiparallel β-sheets, which can be observed by various analytical tests such as Fourier transform infrared spectroscopy (FTIR) and circular dichroism (CD). These β-sheet based fibers entangle and hydrate into hydrogels. These peptide hydrogels consist of a sequence of amino acids, and they can be divided into two portions; the self-assembling domain or "backbone" which self-assembles into these nanofibrous structures and the "mimic" (QK), which attaches covalently to the backbone. Hydrogels offer the ability to design a 3D scaffold that can aid in particular biological functions, such as cell adhesion and proliferation (for example in two-component scaffold to enhance their bio-integration) and can be delivered to an injury site effectively due to being syringe injected and aspirated (for example into the eye).

Recent revascularization treatments to promote angiogenesis have revolved around growth factor and stem cell therapies. Currently, growth factors such as Fibroblast growth factor (FGF) and Vascular endothelial growth factor (VEGF) can be delivered *in vivo* to stimulate angiogenesis. There are several strategies for therapeutic vascularization such as angiogenic therapies utilizing VEGF isoforms VEGF-A121 and VEGF-A165 which are currently being used in clinical trials [347]. In addition, there are a number of RNA based

techniques such as Bonauer et al's use of microRNA (miR) and they have shown efficacy in their own drug, termed antagomir-92a, which saw a significant decrease in toe necrosis in mice [190]. While other avenues have been explored, we believe that mimicking nature's angiogenic scaffolds may prove to be the most successful, particularly with the use of self-assembling peptide hydrogels with high density epitopes mimicking SLan. We have shown the design of a peptide hydrogel with this VEGF mimicking motif to promote controlled angiogenesis through chemical immobilized functional mimic of this growth factor.

Angiogenesis is critical for tissue healing and regeneration. Promoting angiogenesis in materials implanted within dental pulp after pulpectomy is a major clinical challenge in endodontics. We demonstrate the ability of acellular self-assembling peptide hydrogels to create extracellular matrix mimetic architectures that guide *in vivo* development of neovasculature and tissue deposition. The hydrogels possess facile injectability, as well as sequence-level functionalizability. We explore the therapeutic utility of an angiogenic hydrogel, SLan, to regenerate vascularized pulp-like soft tissue in a large animal (canine) orthotopic model. In addition to evaluating the angiogenic potential of SLan in this large animal model, we also assessed a previously published dentinogenic SAPH which consists of a β-sheet forming peptide backbone conjugated to matrix extracellular phosphoglycoprotein mimic (dentonin) sequence at the C-terminus (eighteen). The material properties and biophysical characterization for this dentinogenic peptide hydrogel was performed in a similar manner as SLan (Chapter 2), confirming the hierarchical self-assembly through biophysical techniques, including scanning electron microscopy and atomic force microscopy (determine overall ultrastructure and consistent individual nanofiber formation), rheology (demonstrate thixotropy and injectability), and

ESI-MS, FTIR and CD (verify spectroscopic characterization). We also assessed *in vitro* cytocompatibility and proliferation with 3T3 fibroblasts and dental pulp stem cells (DPSCs). Live/Dead viability assay was performed to confirm that the dentinogenic peptide displayed no toxicity. Further, this peptide was evaluated against DPSCs to demonstrate its ability to induce DPSC proliferation and facilitate calcium deposition, essential for robust dentin production. *In vivo* biocompatibility was also evaluated by subcutaneous implantation in Wistar rats which displayed cellular infiltration into the hydrogel bolus and the lack of fibrous encapsulation. Interestingly, the dentinogenic SAPH and carrier controls showed poor disorganized tissue ingrowth at the terminal (1 month) timepoint in the canine pulpectomy study. However, the SLan SAPH regenerated soft tissue, recapitulating key features of native pulp, such as blood vessels, neural filaments, and an odontoblast-like layer next to dentinal tubules. Our study establishes angiogenic peptide hydrogels as potent scaffolds for promoting soft tissue regeneration *in vivo*.

One of the major constraints against using polymeric scaffolds as tissue-regenerative matrices is a lack of adequate implant vascularization. Self-assembling peptide hydrogels can sequester small molecules and biological macromolecules, and they can support infiltrating cells *in vivo*. Here we demonstrate the ability of self-assembling peptide hydrogels to facilitate angiogenic sprouting into polymeric scaffolds after subcutaneous implantation. We constructed two-component scaffolds that incorporated microporous polymeric scaffolds and viscoelastic nanoporous peptide hydrogels. Nanofibrous hydrogels modified the biocompatibility and vascular integration of polymeric scaffolds with microscopic pores (pore diameters: 100–250 μm). In spite of similar amphiphilic sequences, charges, secondary structures, and

supramolecular nanostructures, two soft hydrogels studied herein had different abilities to aid implant vascularization, but had similar levels of cellular infiltration. The functional difference of the peptide hydrogels was predicted by the difference in the bioactive moieties inserted into the primary sequences of the peptide monomers. Our study highlights the utility of soft supra-molecular hydrogels to facilitate host-implant integration and control implant vascularization in biodegradable polyester scaffolds *in vivo*. Our study provides useful tools in designing multi-component regenerative scaffolds that recapitulate vascularized architectures of native tissues.

Pro-angiogenic (SLan) and anti-angiogenic (SLKr5, derived from the extracellular plasminogen Kringle, domain 5 [211]) peptide hydrogels were evaluated against the standard of care wet age-related macular degeneration (AMD) therapy, Aflibercept (Eylea®). AMD was modeled in rats (laser-induced choroidal neovascularization (CNV) model), where the contralateral eye served as the control. After administration of therapeutics, vasculature was monitored for 14 days to evaluate leakiness. Rats were treated with either a low or high concentration of SLKr5, SLan, the current standard of care Aflibercept and sucrose (vehicle control). Post lasering, efficacy was determined over 14 days via fluorescein angiography (FA) and spectral-domain optical coherence tomography (SD-OCT). Before and after treatment, the average areas of vascular leak per lesion were evaluated as well as the overall vessel leakiness. Unexpectedly, treatment with the SLan hydrogel showed significant, immediate improvement in reducing vascular leak; in the short term, SLan performed better than SLKr5 and was comparable to Aflibercept. On day 7, only 4.2% of lesions treated with Aflibercept and 7.1% of lesions treated with SLan had the presence of leaky lesions, significantly less than lesions treated with vehicle solution

(41.7%) and both low and high concentrations of SLKr5 (28.1% and 29.2%, respectively). After 14 days, both the pro-angiogenic and anti-angiogenic hydrogels show a trend of improvement, comparable to Aflibercept. Based on our results, SLan may prove to be an alternative therapeutic approach to treat wet AMD over a longer-term treatment period.

Ongoing work with SLan include evaluating the binding kinetics to its cognate receptor, VEGFR1 and VEGFR2, and evaluating the angiogenic ability of SLan to revascularize and translation in small and large animal models. We are currently assessing both the immobilized kinetics with surface plasmon resonance, SPR (based on a previous published study on another SAPH [335]), as well as solution-state kinetics with microscale thermophoresis (MST).

Future work with SLan includes identifying types of cells infiltrating the revascularized dental pulp and determining long term efficacy in rodent and canine pulpectomy studies, respectively. Rodent pulpectomy is an ideal small animal model due to the plethora of available antibodies to identify cellular infiltrate and to elucidate a potential mechanism of action of SLan. Further, SLan conditions will be evaluated at 3 and 6 months in canine pulpectomy to understand long term efficacy of the proangiogenic hydrogel. Pulp sensitivity and cone beam CT, along with histology, at these additional timepoints will help us understand the angiogenic effect of SLan. Finally, evaluating anti-microbial peptides with SLan at various ratios in these pulpectomy studies may help more accurately treat dental pulp disease.

REFERENCES

[1] V. Mastrullo, W. Cathery, E. Velliou, P. Madeddu, P. Campagnolo, Angiogenesis in tissue engineering: as nature intended?, Frontiers in Bioengineering and Biotechnology 8 (2020) 188.

[2] X. Meng, Y. Xing, J. Li, C. Deng, Y. Li, X. Ren, D. Zhang, Rebuilding the vascular network: in vivo and in vitro approaches, Frontiers in Cell and Developmental Biology 9 (2021) 639299.

[3] L. Hou, J.J. Kim, Y.J. Woo, N.F. Huang, Stem cell-based therapies to promote angiogenesis in ischemic cardiovascular disease, American Journal of Physiology Heart and Circulatory Physiology 310(4) (2016) H455-65.

[4] S. Mohsin, J.C. Wu, M.A. Sussman, Predicting the future with stem cells, Circulation 129(2) (2014) 136-8.

[5] Q. Sun, E.A. Silva, A. Wang, J.C. Fritton, D.J. Mooney, M.B. Schaffler, P.M. Grossman, S. Rajagopalan, Sustained release of multiple growth factors from injectable polymeric system as a novel therapeutic approach towards angiogenesis, Pharmaceutical Research 27(2) (2010) 264-71.

[6] Q. Sun, R.R. Chen, Y. Shen, D.J. Mooney, S. Rajagopalan, P.M. Grossman, Sustained vascular endothelial growth factor delivery enhances angiogenesis and perfusion in ischemic hind limb, Pharmaceutical Research 22(7) (2005) 1110-6.

[7] M. Giacca, S. Zacchigna, VEGF gene therapy: therapeutic angiogenesis in the clinic and beyond, Gene Therapy 19(6) (2012) 622-9.

[8] J. Lu, V.J. Pompili, H. Das, Neovascularization and hematopoietic stem cells, Cell Biochemistry and Biophysics 67(2) (2013) 235-45.

[9] R.R. Chen, J.K. Snow, J.P. Palmer, A.S. Lin, C.L. Duvall, R.E. Guldberg, D.J. Mooney, Host immune competence and local ischemia affects the functionality of engineered vasculature, Microcirculation 14(2) (2007) 77-88.

[10] R.C. Goncalves, A. Banfi, M.B. Oliveira, J.F. Mano, Strategies for re-vascularization and promotion of angiogenesis in trauma and disease, Biomaterials 269 (2021) 120628.

[11] T. Anada, C.C. Pan, A.M. Stahl, S. Mori, J. Fukuda, O. Suzuki, Y. Yang, Vascularized bone-mimetic hydrogel constructs by 3D bioprinting to promote osteogenesis and angiogenesis, International Journal of Molecular Sciences 20(5) (2019) 1096.

[12] S. Khorshidi, A. Solouk, H. Mirzadeh, S. Mazinani, J.M. Lagaron, S. Sharifi, S. Ramakrishna, A review of key challenges of electrospun scaffolds for tissue-engineering applications, Journal of Tissue Engineering and Regenerative Medicine 10(9) (2016) 715-38.

[13] Z. Siddiqui, A.M. Acevedo-Jake, A. Griffith, N. Kadincesme, K. Dabek, D. Hindi, K.K. Kim, Y. Kobayashi, E. Shimizu, V. Kumar, Cells and material-based strategies for regenerative endodontics, Bioactive Materials 14 (2022) 234-249.

[14] S. Saberianpour, M. Heidarzadeh, M.H. Geranmayeh, H. Hosseinkhani, R. Rahbarghazi, M. Nouri, Tissue engineering strategies for the induction of angiogenesis using biomaterials, Journal of Biological Engineering 12 (2018) 36.

[15] V.L. Tsang, S.N. Bhatia, Three-dimensional tissue fabrication, Advanced Drug Delivery Reviews 56(11) (2004) 1635-47.

[16] A.W. Peterson, D.J. Caldwell, A.Y. Rioja, R.R. Rao, A.J. Putnam, J.P. Stegemann, Vasculogenesis and angiogenesis in modular collagen-fibrin microtissues, Biomaterials Science 2(10) (2014) 1497-1508.

[17] T. Bezgin, A.D. Yilmaz, B.N. Celik, M.E. Kolsuz, H. Sonmez, Efficacy of platelet-rich plasma as a scaffold in regenerative endodontic treatment, Journal of Endodontics 41(1) (2015) 36-44.

[18] P.K. Nguyen, W. Gao, S.D. Patel, Z. Siddiqui, S. Weiner, E. Shimizu, B. Sarkar, V.A. Kumar, Self-assembly of a dentinogenic peptide hydrogel, ACS Omega 3(6) (2018) 5980-5987.

[19] Z. Siddiqui, B. Sarkar, K.K. Kim, N. Kadincesme, R. Paul, A. Kumar, Y. Kobayashi, A. Roy, M. Choudhury, J. Yang, E. Shimizu, V.A. Kumar, Angiogenic hydrogels for dental pulp revascularization, Acta Biomaterialia 126 (2021) 109-118.

[20] A. Hand, M. Frank, Fundamentals of oral histology and physiology, First Edition, John Wiley & Sons (2015).

[21] E.V. Shchetinin, Pathogenetic aspects of dental pulp pathology, Медицинский вестник Северного Кавказа 10(2) (2015) 187.

[22] V. Zaleckiene, V. Peciuliene, V. Brukiene, S. Drukteinis, Traumatic dental injuries: etiology, prevalence and possible outcomes, Stomatologija 16(1) (2014) 7-14.

[23] I.J. Marton, The influence of chronic apical periodontitis on oral and general health, Fogorvosi Szemle 100(5) (2007), 193-199.

[24] S. Bouillaguet, D. Manoil, M. Girard, J. Louis, N. Gaia, S. Leo, J. Schrenzel, V. Lazarevic, Root microbiota in primary and secondary apical periodontitis, Frontiers in Microbiology 9 (2018) 2374.

[25] H. Prinz, Diseases of the soft structure of the teeth and their treatment; a text-book for students and practitioners, Lea & Febiger (1922).

[26] A. Schuurs, Pathology of the hard dental tissues, John Eiley & Sons (2012).

[27] L. Bjorndal, I.A. Mjor, Pulp-dentin biology in restorative dentistry. Part 4: Dental caries --characteristics of lesions and pulpal reactions, Quintessence International 32(9) (2001) 717-36.

[28] Mitsiadis, T. A., e. al., Dental pulp stem cells, niches, and notch signaling in tooth injury, Advances in Dental Research 23(3) 2011.

[29] K.M. Hargreaves, L.H. Berman, Cohen's pathways of the pulp expert consult, Elsevier Health Sciences (2015).

[30] J.H. Jang, H.W. Shin, J.M. Lee, H.W. Lee, E.C. Kim, S.H. Park, An overview of pathogen recognition receptors for innate immunity in dental pulp, Mediators of Inflammation 2015 (2015) 794143.

[31] L. Hu, Y. Liu, S. Wang, Stem cell-based tooth and periodontal regeneration, Oral Diseases 24(5) (2018) 696-705.

[32] M. Rafter, Apexification: a review, Dental Traumatology 21(1) (2005) 1-8.

[33] T. Morotomi, A. Washio, C. Kitamura, Current and future options for dental pulp therapy, The Japanese Dental Science Review 55(1) (2019) 5-11.

[34] F. Garcia-Godoy, P.E. Murray, Recommendations for using regenerative endodontic procedures in permanent immature traumatized teeth, Dental Traumatology 28(1) (2012) 33-41.

[35] S. Kim, SJ. Shin, Y. Song, E. Kim, In vivo experiments with dental pulp stem cells for pulp-dentin complex regeneration, Mediators of Inflammation 2015 (2015) 409347.

[36] C. Smith, D. Setchell, F. Harty, Factors influencing the success of conventional root canal therapy- a five-year retrospective study, International Endodontic Journal 26 (1993) 321-333.

[37] R. Weiger, D. Axmann-Krcmar, C. Loest, Prognosis of conventional root canal treatment reconsidered, Endodontics & Dental Traumatology 14 (1998) 1-9.

[38] L.S.S. Antunes, C. R.; Salles, A. G.; Gomes, C. C.; Antunes, L. A., Does conventional endodontic treatment impact oral health-related quality of life? A systematic review, European Endodontic Journal 3 (2018) 2-8.

[39] P. Carrotte, Endodontics: part 5. Basic instruments and materials for root canal treatment, British Dental Journal 197(8) (2004) 455-64.

[40] J.O. Andreasen, B. Farik, E.C. Munksgaard, Long-term calcium hydroxide as a root canal dressing may increase risk of root fracture, Dental Traumatology 18(3) (2002) 134-7.

[41] T. Dammaschke, D. Steven, M. Kaup, K.H. Ott, Long-term survival of root-canal-treated teeth: a retrospective study over 10 years, Journal of Endodontics 29(10) (2003) 638-43.

[42] B. Patel, Endodontic treatment, retreatment, and surgery mastering clinical practice, First Edition, Springer International Publishing (2016).

[43] D.G. Moussa, C. Aparicio, Present and future of tissue engineering scaffolds for dentin-pulp complex regeneration, Journal of Tissue Engineering and Regenerative Medicine 13(1) (2019) 58-75.

[44] F. Goldberg, C. Cantarini, D. Alfie, R.L. Macchi, A. Arias, Relationship between unintentional canal overfilling and the long-term outcome of primary root canal treatments and nonsurgical retreatments: a retrospective radiographic assessment, International Endodontic Journal 53(1) (2020) 19-26.

[45] E. Wigsten, T. Kvist, P. Jonasson, EndoReCo, T. Davidson, Comparing quality of life of patients undergoing root canal treatment or tooth extraction, Journal of Endodontics 46(1) (2020) 19-28.

[46] M. Jafarian, A. Etebarian, Reasons for extraction of permanent teeth in general dental practices in Tehran, Iran, Medical Principles and Practice 22(3) (2013) 239-44.

[47] P. Cullingham, A. Saksena, M.N. Pemberton, Patient safety: reducing the risk of wrong tooth extraction, British Dental Journal 222(10) (2017) 759-763.

[48] C. Jung, S. Kim, T. Sun, Y.B. Cho, M. Song, Pulp-dentin regeneration: current approaches and challenges, Journal of Tissue Engineering 10 (2019).

[49] A.R. Diogenes, N.B. Ruparel, F.B. Teixeira, K.M. Hargreaves, Translational science in disinfection for regenerative endodontics, Journal of Endodontics 40(4) (2014) S52-57.

[50] I. Fagogeni, J. Metlerska, M. Lipski, T. Falgowski, G. Maciej, A. Nowicka, Materials used in regenerative endodontic procedures and their impact on tooth discoloration, Journal of Oral Science 61(3) (2019) 379-385.

[51] T. Jeeruphan, J. Jantarat, K. Yanpiset, L. Suwannapan, P. Khewsawai, K.M. Hargreaves, Mahidol study 1: comparison of radiographic and survival outcomes of immature teeth treated with either regenerative endodontic or apexification methods: a retrospective study, Journal of Endodontics 38(10) (2012) 1330-6.

[52] L.M. Lin, D. Ricucci, T.M. Saoud, A. Sigurdsson, B. Kahler, Vital pulp therapy of mature permanent teeth with irreversible pulpitis from the perspective of pulp biology, Australian Endodontic Journal 46(1) (2020) 154-166.

[53] S.N. Hanna, R. Perez Alfayate, J. Prichard, Vital pulp therapy an insight over the available literature and future expectations, European Endodontic Journal J 5(1) (2020) 46-53.

[54] M. Torabinejad, Mineral trioxide affrefate: properties and clinical applications, Wiley Blackwell (2014).

[55] V. Orti, P.Y. Collart-Dutilleul, S. Piglionico, O. Pall, F. Cuisinier, I. Panayotov, Pulp regeneration concepts for nonvital teeth: from tissue engineering to clinical approaches, Tissue engineering Part B Reviews 24(6) (2018) 419-442.

[56] D.E. Witherspoon, Vital pulp therapy with new materials: new directions and treatment perspectives -- permanent teeth, Journal of Endodontics 34(7) (2008) S25-28.

[57] N. Akhlaghi, A. Khademi, Outcomes of vital pulp therapy in permanent teeth with different medicaments based on review of the literature, Dental Research Journal 12(5) (2015) 406-17.

[58] Y. Cao, M. Song, E. Kim, W. Shon, N. Chugal, G. Bogen, L. Lin, R.H. Kim, N.H. Park, M.K. Kang, Pulp-dentin regeneration: current state and future prospects, Journal of Dental Research 94(11) (2015) 1544-1551.

[59] F. Chmilewsky, C. Jeanneau, J. Dejou, I. About, Sources of dentin-pulp regeneration signals and their modulation by the local microenvironment, Journal of Endodontics 40(4) (2014) S19-25.

[60] P.L. Tomson, P.J. Lumley, A.J. Smith, P.R. Cooper, Growth factor release from dentine matrix by pulp-capping agents promotes pulp tissue repair-associated events, International Endodontics Journal 50(3) (2017) 281-292.

[61] J. Yang, G. Yuan, Z. Chen, Pulp regeneration: current approaches and future challenges, Frontiers in Physiology 7 (2016) 58.

[62] L. He, S.G. Kim, Q. Gong, J. Zhong, S. Wang, X. Zhou, L. Ye, J. Ling, J.J. Mao, Regenerative endodontics for adult patients, Journal of Endodontics 43(9S) (2017) S57-S64.

[63] G. Jadhav, N. Shah, A. Logani, Revascularization with and without platelet-rich plasma in nonvital, immature, anterior teeth: a pilot clinical study, Journal of Endodontics 38(12) (2012) 1581-1587.

[64] M. Nakashima, K. Iohara, M.C. Bottino, A.F. Fouad, J.E. Nor, G.T. Huang, Animal models for stem cell-based pulp regeneration: foundation for human clinical applications, Tissue Engineering Part B Reviews 25(2) (2019) 100-113.

[65] Y. Yin, X. Li, X.T. He, R.X. Wu, H.H. Sun, F.M. Chen, Leveraging stem cell homing for therapeutic regeneration, Journal of Dental Research 96(6) (2017) 601-609.

[66] Y. Itoh, J.I. Sasaki, M. Hashimoto, C. Katata, M. Hayashi, S. Imazato, Pulp regeneration by 3-dimensional dental pulp stem cell constructs, Journal of Dental Research 97(10) (2018) 1137-1143.

[67] B. Sui, C. Chen, X. Kou, B. Li, K. Xuan, S. Shi, Y. Jin, Pulp stem cell-mediated functional pulp regeneration, Journal of Dental Research 98(1) (2019) 27-35.

[68] J. Han, D. Menicanin, S. Gronthos, P.M. Bartold, Stem cells, tissue engineering and periodontal regeneration, Australian Dental Journal 59(1) (2014) 117-130.

[69] F. Tatsuhiro, T. Seiko, T. Yusuke, T.T. Reiko, S. Kazuhito, Dental pulp stem cell-derived, scaffold-free constructs for bone regeneration, International Journal of Molecular Sciences 19(7) (2018) 1846.

[70] X. Zhu, J. Liu, Z. Yu, C.A. Chen, H. Aksel, A.A. Azim, G.T. Huang, A miniature swine model for stem cell-based de novo regeneration of dental pulp and dentin-like tissue, Tissue Engineering Part C Methods 24(2) (2018) 108-120.

[71] T. Suzuki, C.H. Lee, M. Chen, W. Zhao, S.Y. Fu, J.J. Qi, G. Chotkowski, S.B. Eisig, A. Wong, J.J. Mao, Induced migration of dental pulp stem cells for in vivo pulp regeneration, Journal of Dental Research 90(8) (2011) 1013-1018.

[72] Y.J. Chen, Y.H. Zhao, Y.J. Zhao, N.X. Liu, X. Lv, Q. Li, F.M. Chen, M. Zhang, Potential dental pulp revascularization and odonto-/osteogenic capacity of a novel transplant combined with dental pulp stem cells and platelet-rich fibrin, Cell & Tissue Research 361(2) (2015) 439-455.

[73] R.A. Gangolli, S.M. Devlin, J.A. Gerstenhaber, P.I. Lelkes, M. Yang, A bilayered poly (lactic-co-glycolic acid) scaffold provides differential cues for the differentiation of dental pulp stem cells, Tissue Engineering Part A 25(3-4) (2019) 224-233.

[74] T. Yamamoto, Y. Osako, M. Ito, M. Murakami, Y. Hayashi, H. Horibe, K. Iohara, N. Takeuchi, N. Okui, H. Hirata, H. Nakayama, K. Kurita, M. Nakashima, Trophic effects of dental pulp stem cells on schwann cells in peripheral nerve regeneration, Cell Transplantation 25(1) (2016) 183-193.

[75] D. Tziafas, K. Kodonas, Differentiation potential of dental papilla, dental pulp, and apical papilla progenitor cells, Journal of Endodontics 36(5) (2010) 781-789.

[76] P.T. Sharpe, Dental mesenchymal stem cells, Development 143(13) (2016) 2273-2280.

[77] S. Gronthos, M. Mankani, J. Brahim, P.G. Robey, S. Shi, Postnatal human dental pulp stem cells (DPSCs) in vitro and in vivo, Proceedings of the National Academy of Sciences of the United States of America 97(25) (2000) 13625-13630.

[78] W. Sonoyama, Y. Liu, T. Yamaza, R.S. Tuan, S. Wang, S. Shi, G.T. Huang, Characterization of the apical papilla and its residing stem cells from human immature permanent teeth: a pilot study, Journal of Endodontics 34(2) (2008) 166-171.

[79] A. Louvrier, L. Terranova, C. Meyer, F. Meyer, E. Euvrard, M. Kroemer, G. Rolin, Which experimental models and explorations to use in regenerative endodontics? A comprehensive review on standard practices, Molecular Biology Reports 48(4) (2021) 3799-3812.

[80] H. Bakhtiar, S.A. Mazidi, S. Mohammadi Asl, M.R. Ellini, A. Moshiri, M.H. Nekoofar, P.M.H. Dummer, The role of stem cell therapy in regeneration of dentine-pulp complex: a systematic review, Progress in Biomaterials 7(4) (2018) 249-268.

[81] I. Lambrichts, R.B. Driesen, Y. Dillen, P. Gervois, J. Ratajczak, T. Vangansewinkel, E. Wolfs, A. Bronckaers, P. Hilkens, Dental pulp stem cells: their potential in reinnervation and angiogenesis by using scaffolds, Journal of Endodontics 43(9S) (2017) S12-S16.

[82] M.M. Cordeiro, Z. Dong, T. Kaneko, Z. Zhang, M. Miyazawa, S. Shi, A.J. Smith, J.E. Nor, Dental pulp tissue engineering with stem cells from exfoliated deciduous teeth, Journal of Endodontics 34(8) (2008) 962-969.

[83] W. Zhang, Y. Zheng, H. Liu, X. Zhu, Y. Gu, Y. Lan, J. Tan, H. Xu, R. Guo, A non-invasive monitoring of USPIO labeled silk fibroin/hydroxyapatite scaffold loaded DPSCs for dental pulp regeneration, Materials Science & Engineering. C, Materials for Biological Applications 103 (2019) 109736.

[84] K. Xuan, B. Li, H. Guo, W. Sun, X. Kou, X. He, Y. Zhang, J. Sun, A. Liu, L. Liao, S. Liu, W. Liu, C. Hu, S. Shi, Y. Jin, Deciduous autologous tooth stem cells regenerate dental pulp after implantation into injured teeth, Science Translational Medicine 10(455) (2018).

[85] G.T. Huang, T. Yamaza, L.D. Shea, F. Djouad, N.Z. Kuhn, R.S. Tuan, S. Shi, Stem/progenitor cell-mediated de novo regeneration of dental pulp with newly deposited continuous layer of dentin in an in vivo model, Tissue Engineering Part A 16(2) (2010) 605-615.

[86] Y. Zheng, X.Y. Wang, Y.M. Wang, X.Y. Liu, C.M. Zhang, B.X. Hou, S.L. Wang, Dentin regeneration using deciduous pulp stem/progenitor cells, Journal of Dental Research 91(7) (2012) 676-682.

[87] N. El Shazley, A. Hamdy, H.A. El-Eneen, R.M. El Backly, M.M. Saad, W. Essam, H. Moussa, M. El Tantawi, H. Jain, M.K. Marei, Bioglass in alveolar bone regeneration in orthodontic patients: randomized controlled clinical trial, Journal of Dental Research Clinical and Translational Research 1(3) (2016) 244-255.

[88] K. Iohara, K. Imabayashi, R. Ishizaka, A. Watanabe, J. Nabekura, M. Ito, K. Matsushita, H. Nakamura, M. Nakashima, Complete pulp regeneration after pulpectomy by transplantation of CD105+ stem cells with stromal cell-derived factor-1, Tissue Engineering Part A 17(15-16) (2011) 1911-1920.

[89] H. Duncan, P. Cooper, Clinical approaches in endodontic regeneration, First Edition, Springer (2019).

[90] G.T. Huang, M. Al-Habib, P. Gauthier, Challenges of stem cell-based pulp and dentin regeneration: a clinical perspective, Endodontic Topics 28(1) (2013) 51-60.

[91] L. Hu, B. Zhao, Z. Gao, J. Xu, Z. Fan, C. Zhang, J. Wang, S. Wang, Regeneration characteristics of different dental derived stem cell sheets, Journal of Oral Rehabilitation 47 (2019) 66-72.

[92] J.Y. Kim, X. Xin, E.K. Moioli, J. Chung, C.H. Lee, M. Chen, S.Y. Fu, P.D. Koch, J.J. Mao, Regeneration of dental-pulp-like tissue by chemotaxis-induced cell homing, Tissue Engineering Part A 16(10) (2010) 3023-3031.

[93] G.T. Huang, S. Gronthos, S. Shi, Mesenchymal stem cells derived from dental tissues vs. those from other sources: their biology and role in regenerative medicine, Journal of Dental Research 88(9) (2009) 792-806.

[94] H.F. Duncan, Y. Kobayashi, E. Shimizu, Growth factors and cell homing in dental tissue regeneration, Current Oral Health Reports 5(4) (2018) 276-285.

[95] J.-W. Wang, C.-Y. Chen, Y.-M. Kuo, Preparation and characterization of chitosan-coated hydroxyapatite nanoparticles as a promising non-viral vector for gene delivery, Journal of Applied Polymer Science 121(6) (2011) 3531-3540.

[96] A.A.o. Endodontists, Regenertive Endodontists. https://www.aae.org/specialty/clinical-resources/regenerative-endodontics/# Retrieved on November 30th, 2021.

[97] H. Lv, Y. Chen, Z. Cai, L. Lei, M. Zhang, R. Zhou, X. Huang, The efficacy of platelet-rich fibrin as a scaffold in regenerative endodontic treatment: a retrospective controlled cohort study, BioMed Central Oral Health 18(1) (2018) 139.

[98] E. Shimizu, G. Jong, N. Partridge, P.A. Rosenberg, L.M. Lin, Histologic observation of a human immature permanent tooth with irreversible pulpitis after revascularization/regeneration procedure, Journal of Endodontics 38(9) (2012) 1293-1297.

[99] M. Nakashima, K. Iohara, M. Murakami, H. Nakamura, Y. Sato, Y. Ariji, K. Matsushita, Pulp regeneration by transplantation of dental pulp stem cells in pulpitis: a pilot clinical study, Stem Cell Research & Therapy 8(1) (2017) 61.

[100] S. Vaseenon, N. Chattipakorn, S.C. Chattipakorn, The possible role of basic fibroblast growth factor in dental pulp, Archives of Oral Biology 109 (2020) 104574.

[101] M. Zhang, F. Jiang, X. Zhang, S. Wang, Y. Jin, W. Zhang, X. Jiang, The effects of platelet-derived growth factor-BB on human dental pulp stem cells mediated dentin-pulp complex regeneration, Stem Cells Translational Medicine 6(12) (2017) 2126-2134.

[102] S. Seang, P. Pavasant, C.N. Limjeerajarus, Iloprost induces dental pulp angiogenesis in a growth factor-free 3-dimensional organ culture system, Journal of Endodontics 44(5) (2018) 759-764 e2.

[103] S. Tian, J. Wang, F. Dong, N. Du, W. Li, P. Song, Y. Liu, Concentrated growth factor promotes dental pulp cells proliferation and mineralization and facilitates recovery of dental pulp tissue, Medical Science Monitor 25 (2019) 10016-10028.

[104] S. Davaie, T. Hooshmand, S. Ansarifard, Different types of bioceramics as dental pulp capping materials: A systematic review, Ceramics International 47(15) (2021) 20781-20792.

[105] J. Mente, S. Hufnagel, M. Leo, A. Michel, H. Gehrig, D. Panagidis, D. Saure, T. Pfefferle, Treatment outcome of mineral trioxide aggregate or calcium hydroxide direct pulp capping: long-term results, Journal of Endodontics 40(11) (2014) 1746-1751.

[106] M. Lipski, A. Nowicka, K. Kot, L. Postek-Stefanska, I. Wysoczanska-Jankowicz, L. Borkowski, P. Andersz, A. Jarzabek, K. Grocholewicz, E. Sobolewska, K. Wozniak, A. Drozdzik, Factors affecting the outcomes of direct pulp capping using Biodentine, Clinical Oral Investigations 22(5) (2018) 2021-2029.

[107] A.L. Jalan, M.M. Warhadpande, D.M. Dakshindas, A comparison of human dental pulp response to calcium hydroxide and Biodentine as direct pulp-capping agents, Journal of Conservative Dentistry 20(2) (2017) 129-133.

[108] S. Wang, M.M. Falk, A. Rashad, M.M. Saad, A.C. Marques, R.M. Almeida, M.K. Marei, H. Jain, Evaluation of 3D nano-macro porous bioactive glass scaffold for hard tissue engineering, Journal of Materials Science Materials in Medicine 22(5) (2011) 1195-203.

[109] S. Wang, T.J. Kowal, M.K. Marei, M.M. Falk, H. Jain, Nanoporosity significantly enhances the biological performance of engineered glass tissue scaffolds, Tissue Engineering Part A 19(13-14) (2013) 1632-1640.

[110] T.J. Kowal, N.C. Hahn, S. Eider, J.Y. Marzillier, D.M. Fodera, U. Thamma, H. Jain, M.M. Falk, New bioactive glass scaffolds with exceptional qualities for bone tissue regeneration: response of osteoblasts and osteoclasts, Biomedical Materials 13(2) (2018) 025005.

[111] J. Liu, C.A. Chen, X. Zhu, B.R. Morrow, U. Thamma, T.J. Kowal, H.M. Moawad, M.M. Falk, H. Jain, G.T. Huang, Potential of tailored amorphous multiporous calcium silicate glass for pulp capping regenerative endodontics-A preliminary assessment, Journal of Dentistry 109 (2021) 103655.

[112] J.W. Lim, K.J. Jang, H. Son, S. Park, J.E. Kim, H.B. Kim, H. Seonwoo, Y.H. Choung, M.C. Lee, J.H. Chung, Aligned nanofiber-guided bone regeneration barrier incorporated with equine bone-derived hydroxyapatite for alveolar bone regeneration, Polymers 13(1) (2020) 60.

[113] F. Cristofaro, M. Gigli, N. Bloise, H. Chen, G. Bruni, A. Munari, L. Moroni, N. Lotti, L. Visai, Influence of the nanofiber chemistry and orientation of biodegradable poly(butylene succinate)-based scaffolds on osteoblast differentiation for bone tissue regeneration, Nanoscale 10(18) (2018) 8689-8703.

[114] S.Y. Chew, Aligned protein-polymer composite fibers enhance nerve regeneration: A potential tissue-engineering platform, Advanced Functional Materials 17 (2007) 1288-1296.

[115] V. Kishore, W. Bullock, X. Sun, W.S. Van Dyke, O. Akkus, Tenogenic differentiation of human MSCs induced by the topography of electrochemically aligned collagen threads, Biomaterials 33(7) (2012) 2137-2144.

[116] D. Kai, M.P. Prabhakaran, G. Jin, S. Ramakrishna, Guided orientation of cardiomyocytes on electrospun aligned nanofibers for cardiac tissue engineering, Journal of Biomedical Materials Research Part B, Applied Biomaterials 98(2) (2011) 379-386.

[117] M.C. Lee, H. Seonwoo, K.J. Jang, S. Pandey, J. Lim, S. Park, J.E. Kim, Y.H. Choung, P. Garg, J.H. Chung, Development of novel gene carrier using modified nano hydroxyapatite derived from equine bone for osteogenic differentiation of dental pulp stem cells, Bioactive Materials 6(9) (2021) 2742-2751.

[118] M.A. Khan, V.M. Wu, S. Ghosh, V. Uskokovic, Gene delivery using calcium phosphate nanoparticles: Optimization of the transfection process and the effects of citrate and poly(l-lysine) as additives, Journal of Colloid and Interface Science 471 (2016) 48-58.

[119] L. Zhao, W. Zhao, Y. Liu, X. Chen, Y. Wang, Nano-hydroxyapatite-derived drug and gene co-delivery system for anti-angiogenesis therapy of breast cancer, Medical Science Monitor 23 (2017) 4723-4732.

[120] R. Khalifehzadeh, H. Arami, DNA-templated strontium-doped calcium phosphate nanoparticles for gene delivery in bone cells, American Chemical Society Biomaterials Science & Engineering 5(7) (2019) 3201-3211.

[121] S. Horsophonphong, A. Sercia, C.M. Franca, A. Tahayeri, A.P. Reddy, P.A. Wilmarth, R. Surarit, A.J. Smith, J.L. Ferracane, L.E. Bertassoni, Equivalence of human and bovine dentin matrix molecules for dental pulp regeneration: proteomic analysis and biological function, Archives of Oral Biology 119 (2020) 104888.

[122] C.L. Corless, C.M. Barnett, M.C. Heinrich, Gastrointestinal stromal tumours: origin and molecular oncology, Nature Reviews Cancer 11(12) (2011) 865-878.

[123] N. Kamaly, B. Yameen, J. Wu, O.C. Farokhzad, Degradable controlled-release polymers and polymeric nanoparticles: mechanisms of controlling drug release, Chemical Reviews 116(4) (2016) 2602-2663.

[124] S.S. Kelkar, T.M. Reineke, Theranostics: combining imaging and therapy, Bioconjugate Chemistry 22(10) (2011) 1879-903.

[125] A. Olar, K.D. Aldape, Using the molecular classification of glioblastoma to inform personalized treatment, Journal of Pathology 232(2) (2014) 165-177.

[126] G.G.S. Powathil, M.; Chaplain, M. A. J., Systems oncology: towards patient-specific treatment regimes informed by multiscale mathematical modelling, Seminars in Cancer Biology 30 (2015) 13-20.

[127] C.C. Quinn, A.L. Gruber-Baldini, M. Shardell, K. Weed, S.S. Clough, M. Peeples, M. Terrin, L. Bronich-Hall, E. Barr, D. Lender, Mobile diabetes intervention study: testing a personalized treatment/behavioral communication intervention for blood glucose control, Contemporary Clinical Trials 30(4) (2009) 334-346.

[128] E. Rietzel, A.K. Liu, K.P. Doppke, J.A. Wolfgang, A.B. Chen, G.T. Chen, N.C. Choi, Design of 4D treatment planning target volumes, International Journal of Radiation Oncology, Biology, Physics 66(1) (2006) 287-95.

[129] F. Rosch, H. Herzog, S.M. Qaim, The beginning and development of the theranostic approach in nuclear medicine, as exemplified by the radionuclide pair (86)Y and (90)Y, Pharmaceuticals 10(2) (2017) 56.

[130] U.T. Shain, O., Personalized vaccines for cancer immunotherapy, Science 359 (2018) 1355-1360.

[131] E.Z. Wang, N.; McGee, S.; Milanese, J.-S.; Masoudi-Nejad, A.; O'Connor-McCourt, M., Predictive genomics: A cancer hallmark network framework for predicting tumor clinical phenotypes using genome sequencing data, Seminars in Cancer Biology 30 (2015) 4-12.

[132] B. Werner, J.G. Scott, A. Sottoriva, A.R. Anderson, A. Traulsen, P.M. Altrock, The cancer stem cell fraction in hierarchically organized tumors can be estimated using mathematical modeling and patient-specific treatment trajectories, Cancer Research 76(7) (2016) 1705-13.

[133] J. Xie, S. Lee, X. Chen, Nanoparticle-based theranostic agents, Advanced Drug Delivery Reviews 62(11) (2010) 1064-1079.

[134] M. Ghilezan, D. Yan, A. Martinez, Adaptive radiation therapy for prostate cancer, Seminars in Radiation Oncology 20(2) (2010) 130-137.

[135] S.M. Janib, A.S. Moses, J.A. MacKay, Imaging and drug delivery using theranostic nanoparticles, Advanced Drug Delivery Reviews 62(11) (2010) 1052-1063.

[136] G. Ghosh, X. Yan, A.G. Lee, S.J. Kron, S.P. Palecek, Quantifying the sensitivities of EGF receptor (EGFR) tyrosine kinase inhibitors in drug resistant non-small cell lung cancer (NSCLC) cells using hydrogel-based peptide array, Biosensors & Bioelectronics 26(2) (2010) 424-431.

[137] M.S. Mozaffari, G. Emami, H. Khodadadi, B. Baban, Stem cells and tooth regeneration: prospects for personalized dentistry, EPMA Journal 10(1) (2019) 31-42.

[138] N. Mandakhbayar, A. El-Fiqi, K. Dashnyam, H.W. Kim, Feasibility of defect tunable bone engineering using electroblown bioactive fibrous scaffolds with dental stem cells, American Chemical Society Biomaterials Science & Engineering 4(3) (2018) 1019-1028.

[139] J. Han, W. Jeong, M.K. Kim, S.H. Nam, E.K. Park, H.W. Kang, Demineralized dentin matrix particle-based bio-ink for patient-specific shaped 3D dental tissue regeneration, Polymers 13(8) (2021) 1294.

[140] B.R. Coyac, F. Chicatun, B. Hoac, V. Nelea, C. Chaussain, S.N. Nazhat, M.D. McKee, Mineralization of dense collagen hydrogel scaffolds by human pulp cells, Journal of Dental Research 92(7) (2013) 648-654.

[141] Q. Alqahtani, S.H. Zaky, A. Patil, E. Beniash, H. Ray, C. Sfeir, Decellularized swine dental pulp tissue for regenerative root canal therapy, Journal of Dental Research 97(13) (2018) 1460-1467.

[142] M. Ducret, A. Montembault, J. Josse, M. Pasdeloup, A. Celle, R. Benchrih, F. Mallein-Gerin, B. Alliot-Licht, L. David, J.C. Farges, Design and characterization of a chitosan-enriched fibrin hydrogel for human dental pulp regeneration, Dental Materials 35(4) (2019) 523-533.

[143] M.J. Osmond, M.D. Krebs, Tunable chitosan-calcium phosphate composites as cell-instructive dental pulp capping agents, Journal of Biomaterials Science 32(11) (2021) 1450-1465.

[144] A. Bakopoulou, A. Georgopoulou, I. Grivas, C. Bekiari, O. Prymak, K. Loza, M. Epple, G.C. Papadopoulos, P. Koidis, M. Chatzinikolaidou, Dental pulp stem cells in chitosan/gelatin scaffolds for enhanced orofacial bone regeneration, Dental Materials 35(2) (2019) 310-327.

[145] M. Cicciu, L. Fiorillo, G. Cervino, Chitosan use in dentistry: A systematic review of recent clinical studies, Marine Drugs 17(7) (2019) 417.

[146] E. Ahmadian, A. Eftekhari, S.M. Dizaj, S. Sharifi, M. Mokhtarpour, A.N. Nasibova, R. Khalilov, M. Samiei, The effect of hyaluronic acid hydrogels on dental pulp stem cells behavior, International Journal of Biological Macromolecules 140 (2019) 245-254.

[147] M. Casale, A. Moffa, P. Vella, L. Sabatino, F. Capuano, B. Salvinelli, M.A. Lopez, F. Carinci, F. Salvinelli, Hyaluronic acid: perspectives in dentistry. A systematic review, International Journal of Immunopathology and Pharmacology. 29(4) (2016) 572-582.

[148] P. Zhai, X. Peng, B. Li, Y. Liu, H. Sun, X. Li, The application of hyaluronic acid in bone regeneration, International Journal of Biological Macromolecules 151 (2020) 1224-1239.

[149] J. Ni, R. Shu, C. Li, Efficacy evaluation of hyaluronic acid gel for the restoration of gingival interdental papilla defects, Journal of Oral and Maxillofacial Surgery 77(12) (2019) 2467-2474.

[150] E. Sanchez-Fernandez, A. Magan-Fernandez, F. O'Valle, M. Bravo, F. Mesa, Hyaluronic acid reduces inflammation and crevicular fluid IL-1β concentrations in peri-implantitis: a randomized controlled clinical trial, Journal of Periodontal & Implant Science 51(1) (2021) 63-74.

[151] V. Chrepa, O. Austah, A. Diogenes, Evaluation of a commercially available hyaluronic acid hydrogel (Restylane) as injectable scaffold for dental pulp regeneration: an in vitro evaluation, Journal of Endodontics 43(2) (2017) 257-262.

[152] G.S. Jensen, V.L. Attridge, M.R. Lenninger, K.F. Benson, Oral intake of a liquid high-molecular-weight hyaluronan associated with relief of chronic pain and reduced use of pain medication: results of a randomized, placebo-controlled double-blind pilot study, Journal of Medicinal Food 18(1) (2015) 95-101.

[153] K.K. Niloy, M. Gulfam, K.B. Compton, D. Li, G.T.J. Huang, T.L. Lowe, Methacrylated hyaluronic acid–based hydrogels maintain stemness in human dental pulp stem cells, Regenerative Engineering and Translational Medicine 6(3) (2019) 262-272.

[154] C.R. Silva, P.S. Babo, M. Gulino, L. Costa, J.M. Oliveira, J. Silva-Correia, R.M.A. Domingues, R.L. Reis, M.E. Gomes, Injectable and tunable hyaluronic acid hydrogels releasing chemotactic and angiogenic growth factors for endodontic regeneration, Acta Biomaterialia 77 (2018) 155-171.

[155] P. Snetkov, K. Zakharova, S. Morozkina, R. Olekhnovich, M. Uspenskaya, Hyaluronic acid: the influence of molecular weight on structural, physical, physico-chemical, and degradable properties of biopolymer, Polymers 12(8) (2020) 1800.

[156] C.D. Hummer, F. Angst, W. Ngai, C. Whittington, S.S. Yoon, L. Duarte, C. Manitt, E. Schemitsch, High molecular weight intraarticular hyaluronic acid for the treatment of knee osteoarthritis: a network meta-analysis, BioMed Central Musculoskeletal Disorders 21(1) (2020) 702.

[157] R. Al-Khateeb, I. Olszewska-Czyz, Biological molecules in dental applications: hyaluronic acid as a companion biomaterial for diverse dental applications, Heliyon 6(4) (2020) e03722.

[158] K. Areevijit, N. Dhanesuan, J.A. Luckanagul, S. Rungsiyanont, Biocompatibility study of modified injectable hyaluronic acid hydrogel with mannitol/BSA to alveolar bone cells, Journal of Biomaterials Applications 35(10) (2021) 1294-1303.

[159] J. Schmidt, N. Pilbauerova, T. Soukup, T. Suchankova-Kleplova, J. Suchanek, Low Molecular Weight Hyaluronic Acid Effect on Dental Pulp Stem Cells In Vitro, Biomolecules 11(1) (2020) 22.

[160] X. Ling, Y. Shen, R. Sun, M. Zhang, C. Li, J. Mao, J. Xing, C. Sun, J. Tu, Tumor-targeting delivery of hyaluronic acid–platinum(iv) nanoconjugate to reduce toxicity and improve survival, Polymer Chemistry 6(9) (2015) 1541-1552.

[161] S. Ekici, P. Ilgin, S. Butun, N. Sahiner, Hyaluronic acid hydrogel particles with tunable charges as potential drug delivery devices, Carbohydrate Polymers 84(4) (2011) 1306-1313.

[162] I.S. Bayer, Hyaluronic acid and controlled release: a review, Molecules 25(11) (2020) 2649.

[163] D. Orlenko, V. Yakovenko, L. Vyshnevska, Research on the development of dental gel technology with metronidazole benzoate and hyaluronic acid, ScienceRise: Pharmaceutical Science 6(22) (2019) 24-29.

[164] N. Mandras, M. Alovisi, J. Roana, P. Crosasso, A. Luganini, D. Pasqualini, E. Genta, S. Arpicco, G. Banche, A. Cuffini, E. Berutti, Evaluation of the bactericidal activity of a hyaluronic acid-vehicled clarithromycin antibiotic mixture by confocal laser scanning microscopy, Applied Sciences 10(8) (2020) 761.

[165] J. Jitpibull, N. Tangjit, S. Dechkunakorn, N. Anuwongnukroh, T. Srikhirin, T. Vongsetskul, H. Sritanaudomchai, Effect of surface chemistry-modified polycaprolactone scaffolds on osteogenic differentiation of stem cells from human exfoliated deciduous teeth, European Journal of Oral Sciences 129(2) (2021) e12766.

[166] H.-J. Kang, S.-S. Park, T. Saleh, K.-M. Ahn, B.-T. Lee, In vitro and in vivo evaluation of Ca/P-hyaluronic acid/gelatin based novel dental plugs for one-step socket preservation, Materials & Design 194 (2020) 108891.

[167] A.F. Fouad, The microbial challenge to pulp regeneration, Advances in Dental Research 23(3) (2011) 285-289.

[168] S.H. Park, J.Y. Park, Y.B. Ji, H.J. Ju, B.H. Min, M.S. Kim, An injectable click-crosslinked hyaluronic acid hydrogel modified with a BMP-2 mimetic peptide as a bone tissue engineering scaffold, Acta Biomaterialia 117 (2020) 108-120.

[169] L. Luo, Y. Zhang, H. Chen, F. Hu, X. Wang, Z. Xing, A.A. Albashari, J. Xiao, Y. He, Q. Ye, Effects and mechanisms of basic fibroblast growth factor on the proliferation and regenerative profiles of cryopreserved dental pulp stem cells, Cell Proliferation 54(2) (2021) e12969.

[170] A. Jaukovic, T. Kukolj, D. Trivanovic, I. Okic-Dordevic, H. Obradovic, M. Miletic, V. Petrovic, S. Mojsilovic, D. Bugarski, Modulating stemness of mesenchymal stem cells from exfoliated deciduous and permanent teeth by IL-17 and bFGF, Journal of Cellular Physiology 236(11) (2021) 7322-7341.

[171] J. Kim, J.C. Park, S.H. Kim, G.I. Im, B.S. Kim, J.B. Lee, E.Y. Choi, J.S. Song, K.S. Cho, C.S. Kim, Treatment of FGF-2 on stem cells from inflamed dental pulp tissue from human deciduous teeth, Oral Diseases 20(2) (2014) 191-204.

[172] A.K. Morito, Y.; Suzuki, K.; Inoue, K.; Kuroda, N.; Gomi, K.; Arai, T.; Sato, T., Effects of basic fibroblast growth factor on the development of the stem cell properties of human dental pulp cells, Archives of Histology and Cytology 72(1) (2009) 51-64.

[173] H. Honda, N. Tamai, N. Naka, H. Yoshikawa, A. Myoui, Bone tissue engineering with bone marrow-derived stromal cells integrated with concentrated growth factor in Rattus norvegicus calvaria defect model, Journal of Artificial Organs 16(3) (2013) 305-315.

[174] B. Yu, Z. Wang, Effect of concentrated growth factors on beagle periodontal ligament stem cells in vitro, Molecular Medicine Reports 9(1) (2014) 235-242.

[175] R.S. Jin, G.; Chai, J.; Gou, X.; Yuan, G.; Chen, Z., Effects of concentrated growth factor on proliferation, migration, and differentiation of human dental pulp stem cells in vitro, Journal of Tissue Engineering 9 (2018) 1-10.

[176] Z. Li, L. Liu, L. Wang, D. Song, The effects and potential applications of concentrated growth factor in dentin-pulp complex regeneration, Stem Cell Research & Therapy 12(1) (2021) 357.

[177] L.F. Rodella, G. Favero, R. Boninsegna, B. Buffoli, M. Labanca, G. Scari, L. Sacco, T. Batani, R. Rezzani, Growth factors, CD34 positive cells, and fibrin network analysis in concentrated growth factors fraction, Microscopy Research and Technique 74(8) (2011) 772-777.

[178] S.R. Motamedian, F.S. Tabatabaei, F. Akhlaghi, M. Torshabi, P. Gholamin, A. Khojasteh, Response of dental pulp stem cells to synthetic, allograft, and xenograft bone scaffolds, The International Journal of Periodontics & Restorative Dentistry 37(1) (2017) 49-59.

[179] L.A. Chisini, M.C.M. Conde, G. Grazioli, A.S.S. Martin, R.V. Carvalho, L.R.M. Sartori, F.F. Demarco, Bone, periodontal and dental pulp regeneration in dentistry: A systematic scoping review, Brazilian Dental Journal 30(2) (2019) 77-95.

[180] K.M. Galler, R.N. D'Souza, J.D. Hartgerink, G. Schmalz, Scaffolds for dental pulp tissue engineering, Advances in Dental Research 23(3) (2011) 333-339.

[181] Z. Yuan, H. Nie, S. Wang, C.H. Lee, A. Li, S.Y. Fu, H. Zhou, L. Chen, J.J. Mao, Biomaterial selection for tooth regeneration, Tissue Engineering Part B Reviews 17(5) (2011) 373-388.

[182] S.H. Jiang, H.R. Zou, Various scaffolds for dentine-pulp complex regeneration, Chinese Journal of Stomatology 53(11) (2018) 784-788.

[183] V.T. Sakai, Z. Zhang, Z. Dong, K.G. Neiva, M.A. Machado, S. Shi, C.F. Santos, J.E. Nor, SHED differentiate into functional odontoblasts and endothelium, Journal of Dental Research 89(8) (2010) 791-796.

[184] K. Lee, E.A. Silva, D.J. Mooney, Growth factor delivery-based tissue engineering: general approaches and a review of recent developments, Journal of the Royal Society Interface 8(55) (2011) 153-170.

[185] M.C. Bottino, D. Pankajakshan, J.E. Nor, Advanced scaffolds for dental pulp and periodontal regeneration, Dental Clinics of North America 61(4) (2017) 689-711.

[186] S. Goenka, V. Sant, S. Sant, Graphene-based nanomaterials for drug delivery and tissue engineering, Journal of Controlled Release 173 (2014) 75-88.

[187] H. Zhao, R. Ding, X. Zhao, Y. Li, L. Qu, H. Pei, L. Yildirimer, Z. Wu, W. Zhang, Graphene-based nanomaterials for drug and/or gene delivery, bioimaging, and tissue engineering, Drug Discovery Today 22(9) (2017) 1302-1317.

[188] W. Li, M. Mao, N. Hu, J. Wang, J. Huang, W. Zhang, S. Gu, A graphene oxide-copper nanocomposite for the regeneration of the dentin-pulp complex: An odontogenic and neurovascularization-inducing material, Chemical Engineering Journal 417(1) (2021) 129299.

[189] K. Petrak, R. Vissapragada, S. Shi, Z. Siddiqui, K.K. Kim, B. Sarkar, V.A. Kumar, Challenges in translating from bench to bed-side: pro-angiogenic peptides for ischemia treatment, Molecules 24(7) (2019) 1219.

[190] A. Bonauer, G. Carmona, M. Iwasaki, M. Mione, M. Koyanagi, A. Fischer, J. Burchfield, H. Fox, C. Doebele, K. Ohtani, E. Chavakis, M. Potente, M. Tjwa, C. Urbich, A.M. Zeiher, S. Dimmeler, MicroRNA-92a controls angiogenesis and functional recovery of ischemic tissues in mice, Science 324(5935) (2009) 1710-1713.

[191] C.Y. Moon, O.H. Nam, M. Kim, H.S. Lee, S.N. Kaushik, D.A. Cruz Walma, H.W. Jun, K. Cheon, S.C. Choi, Effects of the nitric oxide releasing biomimetic nanomatrix gel on pulp-dentin regeneration: Pilot study, PLoS One 13(10) (2018) e0205534.

[192] A.S. Muller, M. Artner, K. Janjic, M. Edelmayer, C. Kurzmann, A. Moritz, H. Agis, Synthetic clay-based hypoxia mimetic hydrogel for pulp regeneration: the impact on cell activity and release kinetics based on dental pulp-derived cells in vitro, Journal of Endodontics 44(8) (2018) 1263-1269.

[193] L. Luo, A.A. Albashari, X. Wang, L. Jin, Y. Zhang, L. Zheng, J. Xia, H. Xu, Y. Zhao, J. Xiao, Y. He, Q. Ye, Effects of transplanted heparin-poloxamer hydrogel combining dental pulp stem cells and bFGF on spinal cord injury repair, Stem Cells International 2018 (2018) 2398521.

[194] B. Sarkar, P.K. Nguyen, W. Gao, A. Dondapati, Z. Siddiqui, V.A. Kumar, Angiogenic self-assembling peptide scaffolds for functional tissue regeneration, Biomacromolecules 19(9) (2018) 3597-3611.

[195] V.A. Kumar, N.L. Taylor, S. Shi, B.K. Wang, A.A. Jalan, M.K. Kang, N.C. Wickremasinghe, J.D. Hartgerink, Highly angiogenic peptide nanofibers, American Chemical Society Nano 9(1) (2015) 860-8.

[196] P. Hitscherich, P.K. Nguyen, A. Kannan, A. Chirayath, S. Anur, B. Sarkar, E.J. Lee, V.A. Kumar, Injectable self-assembling peptide hydrogels for tissue writing and embryonic stem cell culture, Journal of Biomedical Nanotechnology 14(4) (2018) 802-807.

[197] N.C. Wickremasinghe, V.A. Kumar, J.D. Hartgerink, Two-step self-assembly of liposome-multidomain peptide nanofiber hydrogel for time-controlled release, Biomacromolecules 15(10) (2014) 3587-95.

[198] K.K. Kim, Z. Siddiqui, M. Patel, B. Sarkar, V.A. Kumar, A self-assembled peptide hydrogel for cytokine sequestration, Journal of Materials Chemistry B 8(5) (2020) 945-950.

[199] E. Beniash, J.D. Hartgerink, H. Storrie, J.C. Stendahl, S.I. Stupp, Self-assembling peptide amphiphile nanofiber matrices for cell entrapment, Acta biomaterialia 1(4) (2005) 387-97.

[200] C.L. Pizzey, W.C. Pomerantz, B.J. Sung, V.M. Yuwono, S.H. Gellman, J.D. Hartgerink, A. Yethiraj, N.L. Abbott, Characterization of nanofibers formed by self-assembly of β-peptide oligomers using small angle x-ray scattering, Journal of Chemical Physics 129(9) (2008) 095103.

[201] W.C. Pomerantz, V.M. Yuwono, C.L. Pizzey, J.D. Hartgerink, N.L. Abbott, S.H. Gellman, Nanofibers and lyotropic liquid crystals from a class of self-assembling beta-peptides, Angewandte Chemie 47(7) (2008) 1241-4.

[202] J.D. Hartgerink, E. Beniash, S.I. Stupp, Peptide-amphiphile nanofibers: a versatile scaffold for the preparation of self-assembling materials, Proceedings of the National Academy of Sciences of the United States of America 99(8) (2002) 5133-8.

[203] S.E. Paramonov, H.W. Jun, J.D. Hartgerink, Modulation of peptide-amphiphile nanofibers via phospholipid inclusions, Biomacromolecules 7(1) (2006) 24-6.

[204] S.E. Paramonov, H.W. Jun, J.D. Hartgerink, Self-assembly of peptide-amphiphile nanofibers: the roles of hydrogen bonding and amphiphilic packing, Journal of the American Chemical Society 128(22) (2006) 7291-8.

[205] H. Dong, S.E. Paramonov, L. Aulisa, E.L. Bakota, J.D. Hartgerink, Self-assembly of multidomain peptides: balancing molecular frustration controls conformation and nanostructure, Journal of the American Chemical Society 129(41) (2007) 12468-72.

[206] I.C. Li, J.D. Hartgerink, Covalent capture of aligned self-assembling nanofibers, Journal of the American Chemical Society 139(23) (2017) 8044-8050.

[207] V. Gauba, J.D. Hartgerink, Self-assembled heterotrimeric collagen triple helices directed through electrostatic interactions, Journal of the American Chemical Society 129(9) (2007) 2683-90.

[208] E.L. Bakota, O. Sensoy, B. Ozgur, M. Sayar, J.D. Hartgerink, Self-assembling multidomain peptide fibers with aromatic cores, Biomacromolecules 14(5) (2013) 1370-8.

[209] K.L. Niece, J.D. Hartgerink, J.J. Donners, S.I. Stupp, Self-assembly combining two bioactive peptide-amphiphile molecules into nanofibers by electrostatic attraction, Journal of the American Chemical Society 125(24) (2003) 7146-7.

[210] M.B. Murphy, J.D. Hartgerink, A. Goepferich, A.G. Mikos, Synthesis and in vitro hydroxyapatite binding of peptides conjugated to calcium-binding moieties, Biomacromolecules 8(7) (2007) 2237-43.

[211] P.K. Nguyen, B. Sarkar, Z. Siddiqui, M. McGowan, P. Iglesias-Montoro, S. Rachapudi, S. Kim, W. Gao, E. Lee, V.A. Kumar, Self-assembly of an anti-angiogenic nanofibrous peptide hydrogel, American Chemical Society Applied Bio Materials 1(3) (2018) 865-870.

[212] H.G. Augustin, G.Y. Koh, Organotypic vasculature: from descriptive heterogeneity to functional pathophysiology, Science 357(6353) (2017) eaal2379

[213] P. Carmeliet, R.K. Jain, Molecular mechanisms and clinical applications of angiogenesis, Nature 473(7347) (2011) 298-307.

[214] V.A. Kumar, Q. Liu, N.C. Wickremasinghe, S. Shi, T.T. Cornwright, Y. Deng, A. Azares, A.N. Moore, A.M. Acevedo-Jake, N.R. Agudo, S. Pan, D.G. Woodside, P. Vanderslice, J.T. Willerson, R.A. Dixon, J.D. Hartgerink, Treatment of hind limb ischemia using angiogenic peptide nanofibers, Biomaterials 98 (2016) 113-119.

[215] R. Khurana, M. Simons, J.F. Martin, I.C. Zachary, Role of angiogenesis in cardiovascular disease: a critical appraisal, Circulation 112(12) (2005) 1813-1824.

[216] B.H. Annex, Therapeutic angiogenesis for critical limb ischaemia, Nature Reviews Cardiology 10(7) (2013) 387-96.

[217] J.D. Weaver, D.M. Headen, J. Aquart, C.T. Johnson, L.D. Shea, H. Shirwan, A.J. Garcia, Vasculogenic hydrogel enhances islet survival, engraftment, and function in leading extrahepatic sites, Science Advances 3(6) (2017) e1700184.

[218] A.R. Amini, C.T. Laurencin, S.P. Nukavarapu, Bone tissue engineering: recent advances and challenges, Critical Reviews in Biomedical Engineering 40(5) (2012) 363-408.

[219] P.S. Briquez, L.E. Clegg, M.M. Martino, F.M. Gabhann, J.A. Hubbell, Design principles for therapeutic angiogenic materials, Nature Reviews Materials 1(1) (2016) 15006.

[220] B. Grigoryan, S.J. Paulsen, D.C. Corbett, D.W. Sazer, C.L. Fortin, A.J. Zaita, P.T. Greenfield, N.J. Calafat, J.P. Gounley, A.H. Ta, F. Johansson, A. Randles, J.E. Rosenkrantz, J.D. Louis-Rosenberg, P.A. Galie, K.R. Stevens, J.S. Miller, Multivascular networks and functional intravascular topologies within biocompatible hydrogels, Science 364(6439) (2019) 458-464.

[221] R. Gianni-Barrera, N. Di Maggio, L. Melly, M.G. Burger, E. Mujagic, L. Gurke, D.J. Schaefer, A. Banfi, Therapeutic vascularization in regenerative medicine, Stem Cells Transl Med 9(4) (2020) 433-444.

[222] T.L. Lopez-Silva, D.G. Leach, A. Azares, I.C. Li, D.G. Woodside, J.D. Hartgerink, Chemical functionality of multidomain peptide hydrogels governs early host immune response, Biomaterials 231 (2020) 119667.

[223] A.N. Moore, J.D. Hartgerink, Self-Assembling Multidomain Peptide Nanofibers for Delivery of Bioactive Molecules and Tissue Regeneration, Accounts of Chemical Research 50(4) (2017) 714-722.

[224] A.N. Moore, T.L. Lopez Silva, N.C. Carrejo, C.A. Origel Marmolejo, I.C. Li, J.D. Hartgerink, Nanofibrous peptide hydrogel elicits angiogenesis and neurogenesis without drugs, proteins, or cells, Biomaterials 161 (2018) 154-163.

[225] B. Sarkar, Z. Siddiqui, P.K. Nguyen, N. Dube, W. Fu, S. Park, S. Jaisinghani, R. Paul, S.D. Kozuch, D. Deng, P. Iglesias-Montoro, M. Li, D. Sabatino, D.S. Perlin, W. Zhang, J. Mondal, V.A. Kumar, Membrane-disrupting nanofibrous peptide hydrogels, American Chemical Society Biomaterials Science & Engineering 5(9) (2019) 4657-4670.

[226] X. Ma, A. Agas, Z. Siddiqui, K. Kim, P. Iglesias-Montoro, J. Kalluru, V. Kumar, J. Haorah, Angiogenic peptide hydrogels for treatment of traumatic brain injury, Bioactive Materials 5(1) (2020) 124-132.

[227] B. Sarkar, X. Ma, A. Agas, Z. Siddiqui, P. Iglesias-Montoro, P.K. Nguyen, K.K. Kim, J. Haorah, V.A. Kumar, In vivo neuroprotective effect of a self-assembled peptide hydrogel, Chemical Engineering Journal 408 (2021) 127295.

[228] E. Shimizu, D. Ricucci, J. Albert, A.S. Alobaid, J.L. Gibbs, G.T. Huang, L.M. Lin, Clinical, radiographic, and histological observation of a human immature permanent tooth with chronic apical abscess after revitalization treatment, Journal of Endodontics 39(8) (2013) 1078-83.

[229] K.M. Galler, J.D. Hartgerink, A.C. Cavender, G. Schmalz, R.N. D'Souza, A customized self-assembling peptide hydrogel for dental pulp tissue engineering, Tissue Engineering Part A 18(1-2) (2012) 176-84.

[230] F. Mangione, M. EzEldeen, C. Bardet, J. Lesieur, M. Bonneau, F. Decup, B. Salmon, R. Jacobs, C. Chaussain, S. Opsahl-Vital, Implanted dental pulp cells fail to induce regeneration in partial pulpotomies, Journal of Dental Research 96(12) (2017) 1406-1413.

[231] P. Bankhead, M.B. Loughrey, J.A. Fernandez, Y. Dombrowski, D.G. McArt, P.D. Dunne, S. McQuaid, R.T. Gray, L.J. Murray, H.G. Coleman, J.A. James, M. Salto-Tellez, P.W. Hamilton, QuPath: Open source software for digital pathology image analysis, Scientific Reports 7(1) (2017) 16878.

[232] L.D. D'Andrea, G. Iaccarino, R. Fattorusso, D. Sorriento, C. Carannante, D. Capasso, B. Trimarco, C. Pedone, Targeting angiogenesis: structural characterization and biological properties of a de novo engineered VEGF mimicking peptide, Proceedings of the National Academy of Sciences of the United States of America 102(40) (2005) 14215-20.

[233] J.A. Burdick, R.L. Mauck, J.H. Gorman, 3rd, R.C. Gorman, Acellular biomaterials: an evolving alternative to cell-based therapies, Science Translational Medicine 5(176) (2013) 176ps4.

[234] M.J. Webber, E.A. Appel, E.W. Meijer, R. Langer, Supramolecular biomaterials, Nature Materials 15(1) (2016) 13-26.

[235] M.J. Webber, J. Tongers, C.J. Newcomb, K.T. Marquardt, J. Bauersachs, D.W. Losordo, S.I. Stupp, Supramolecular nanostructures that mimic VEGF as a strategy for ischemic tissue repair, Proceedings of the National Academy of Sciences of the United States of America 108(33) (2011) 13438-13443.

[236] E.W. Fish, The reaction of the dental pulp to peripheral injury of the dentine, Proceedings of the Royal Society of London B 108(756) (1931) 196-208.

[237] Y. Zhao, X. Yuan, B. Liu, U.S. Tulu, J.A. Helms, Wnt-responsive odontoblasts secrete new dentin after superficial tooth injury, Journal of Dental Research 97(9) (2018) 1047-1054.

[238] O.A. Nada, R.M. El Backly, Stem cells from the apical papilla (SCAP) as a tool for endogenous tissue regeneration, Frontiers in Bioengineering and Biotechnology 6 (2018) 103.

[239] R. Wigler, A.Y. Kaufman, S. Lin, N. Steinbock, H. Hazan-Molina, C.D. Torneck, Revascularization: a treatment for permanent teeth with necrotic pulp and incomplete root development, Journal of Endodontics 39(3) (2013) 319-326.

[240] L. He, J. Zhong, Q. Gong, S.G. Kim, S.J. Zeichner, L. Xiang, L. Ye, X. Zhou, J. Zheng, Y. Liu, C. Guan, B. Cheng, J. Ling, J.J. Mao, Treatment of necrotic teeth by apical revascularization: meta-analysis, Scientific Reports 7(1) (2017) 13941.

[241] G. Chen, J. Chen, B. Yang, L. Li, X. Luo, X. Zhang, L. Feng, Z. Jiang, M. Yu, W. Guo, W. Tian, Combination of aligned PLGA/Gelatin electrospun sheets, native dental pulp extracellular matrix and treated dentin matrix as substrates for tooth root regeneration, Biomaterials 52 (2015) 56-70.

[242] B. Chang, K.K.H. Svoboda, X. Liu, Cell polarization: from epithelial cells to odontoblasts, European Journal of Cell Biology 98(1) (2019) 1-11.

[243] T. Gonzalez-Martinez, P. Perez-Pinera, B. Diaz-Esnal, J.A. Vega, S-100 proteins in the human peripheral nervous system, Microscopy Research and Technique 60(6) (2003) 633-638.

[244] T. Walchli, A. Wacker, K. Frei, L. Regli, M.E. Schwab, S.P. Hoerstrup, H. Gerhardt, B. Engelhardt, Wiring the vascular network with neural cues: A CNS perspective, Neuron 87(2) (2015) 271-296.

[245] C. Zhan, M. Huang, X. Yang, J. Hou, Dental nerves: a neglected mediator of pulpitis, International Endodontic Journal 54(1) (2021) 85-99.

[246] H. Zhao, J. Feng, K. Seidel, S. Shi, O. Klein, P. Sharpe, Y. Chai, Secretion of shh by a neurovascular bundle niche supports mesenchymal stem cell homeostasis in the adult mouse incisor, Cell Stem Cell 14(2) (2014) 160-173.

[247] N. Kaukua, M.K. Shahidi, C. Konstantinidou, V. Dyachuk, M. Kaucka, A. Furlan, Z. An, L. Wang, I. Hultman, L. Ahrlund-Richter, H. Blom, H. Brismar, N.A. Lopes, V. Pachnis, U. Suter, H. Clevers, I. Thesleff, P. Sharpe, P. Ernfors, K. Fried, I. Adameyko, Glial origin of mesenchymal stem cells in a tooth model system, Nature 513(7519) (2014) 551-554.

[248] J. Pizzicannella, S.D. Pierdomenico, A. Piattelli, G. Varvara, L. Fonticoli, O. Trubiani, F. Diomede, 3D human periodontal stem cells and endothelial cells promote bone development in bovine pericardium-based tissue biomaterial, Materials 12(13) (2019) 2157.

[249] L. He, J. Zhou, M. Chen, C.S. Lin, S.G. Kim, Y. Zhou, L. Xiang, M. Xie, H. Bai, H. Yao, C. Shi, P.G. Coelho, T.G. Bromage, B. Hu, N. Tovar, L. Witek, J. Wu, K. Chen, W. Gu, J. Zheng, T.J. Sheu, J. Zhong, J. Wen, Y. Niu, B. Cheng, Q. Gong, D.M. Owens, M. Stanislauskas, J. Pei, G. Chotkowski, S. Wang, G. Yang, D.J. Zegarelli, X. Shi, M. Finkel, W. Zhang, J. Li, J. Cheng, D.P. Tarnow, X. Zhou, Z. Wang, X. Jiang, A. Romanov, D.W. Rowe, S. Wang, L. Ye, J. Ling, J. Mao, Parenchymal and stromal tissue regeneration of tooth organ by pivotal signals reinstated in decellularized matrix, Nature Materials 18(6) (2019) 627-637.

[250] V. Rosa, Z. Zhang, R.H. Grande, J.E. Nor, Dental pulp tissue engineering in full-length human root canals, J Dent Res 92(11) (2013) 970-975.

[251] C.C. Huang, R. Narayanan, S. Alapati, S. Ravindran, Exosomes as biomimetic tools for stem cell differentiation: Applications in dental pulp tissue regeneration, Biomaterials 111 (2016) 103-115.

[252] X. Li, C. Ma, X. Xie, H. Sun, X. Liu, Pulp regeneration in a full-length human tooth root using a hierarchical nanofibrous microsphere system, Acta Biomaterialia 35 (2016) 57-67.

[253] C.C. Huang, R. Narayanan, N. Warshawsky, S. Ravindran, Dual ECM biomimetic scaffolds for dental pulp regenerative applications, Frontiers in Physiology 9 (2018) 495.

[254] H. Chen, H. Fu, X. Wu, Y. Duan, S. Zhang, H. Hu, Y. Liao, T. Wang, Y. Yang, G. Chen, Z. Li, W. Tian, Regeneration of pulpo-dentinal-like complex by a group of unique multipotent CD24a(+) stem cells, Science Advances 6(15) (2020) eaay1514.

[255] S.E. Millar, A pulpy story, Nature Materials 18(6) (2019) 530-531.

[256] R. Ishizaka, K. Iohara, M. Murakami, O. Fukuta, M. Nakashima, Regeneration of dental pulp following pulpectomy by fractionated stem/progenitor cells from bone marrow and adipose tissue, Biomaterials 33(7) (2012) 2109-2118.

[257] K. Iohara, M. Murakami, N. Takeuchi, Y. Osako, M. Ito, R. Ishizaka, S. Utunomiya, H. Nakamura, K. Matsushita, M. Nakashima, A novel combinatorial therapy with pulp stem cells and granulocyte colony-stimulating factor for total pulp regeneration, Stem Cells Translational Medicine 2(7) (2013) 521-533.

[258] Y. Wang, Y. Zhao, W. Jia, J. Yang, L. Ge, Preliminary study on dental pulp stem cell-mediated pulp regeneration in canine immature permanent teeth, Journal of Endodontics 39(2) (2013) 195-201.

[259] J.W. Yang, Y.F. Zhang, C.Y. Wan, Z.Y. Sun, S. Nie, S.J. Jian, L. Zhang, G.T. Song, Z. Chen, Autophagy in SDF-1alpha-mediated DPSC migration and pulp regeneration, Biomaterials 44 (2015) 11-23.

[260] P.R. Arany, A. Cho, T.D. Hunt, G. Sidhu, K. Shin, E. Hahm, G.X. Huang, J. Weaver, A.C. Chen, B.L. Padwa, M.R. Hamblin, M.H. Barcellos-Hoff, A.B. Kulkarni, J.M. D, Photoactivation of endogenous latent transforming growth factor-beta1 directs dental stem cell differentiation for regeneration, Science Translational Medicine 6(238) (2014) 238ra69.

[261] K.H. Vining, J.C. Scherba, A.M. Bever, M.R. Alexander, A.D. Celiz, D.J. Mooney, Synthetic light-curable polymeric materials provide a supportive niche for dental pulp stem cells, Advanced Materials 30(4) (2018).

[262] X. Luo, B. Yang, L. Sheng, J. Chen, H. Li, L. Xie, G. Chen, M. Yu, W. Guo, W. Tian, CAD based design sensitivity analysis and shape optimization of scaffolds for bio-root regeneration in swine, Biomaterials 57 (2015) 59-72.

[263] M. Yadlapati, C. Biguetti, F. Cavalla, F. Nieves, C. Bessey, P. Bohluli, G.P. Garlet, A. Letra, W.D. Fakhouri, R.M. Silva, Characterization of a vascular endothelial growth factor-loaded bioresorbable delivery system for pulp regeneration, Journal of Endodontics 43(1) (2017) 77-83.

[264] R. Langer, J.P. Vacanti, Tissue engineering, Science 260(5110) (1993) 920-926.

[265] D.P. Kavanagh, N. Kalia, Hematopoietic stem cell homing to injured tissues, Stem Cell Reviews and Reports 7(3) (2011) 672-682.

[266] V.A. Kumar, N.L. Taylor, S. Shi, N.C. Wickremasinghe, R.N. D'Souza, J.D. Hartgerink, Self-assembling multidomain peptides tailor biological responses through biphasic release, Biomaterials 52 (2015) 71-78.

[267] J. Zhang, H. Chen, M. Zhao, G. Liu, J. Wu, 2D nanomaterials for tissue engineering application, Nano Research 13(8) (2020) 2019-2034.

[268] X. Gao, Z. Xu, G. Liu, J. Wu, Polyphenols as a versatile component in tissue engineering, Acta Biomaterialia 119 (2021) 57-74.

[269] C.T. Johnson, M.C.P. Sok, K.E. Martin, P.P. Kalelkar, J.D. Caplin, E.A. Botchwey, A.J. Garcia, Lysostaphin and BMP-2 co-delivery reduces S. aureus infection and regenerates critical-sized segmental bone defects, Science Advances 5(5) (2019) eaaw1228.

[270] B.M. Sicari, J.P. Rubin, C.L. Dearth, M.T. Wolf, F. Ambrosio, M. Boninger, N.J. Turner, D.J. Weber, T.W. Simpson, A. Wyse, E.H. Brown, J.L. Dziki, L.E. Fisher, S. Brown, S.F. Badylak, An acellular biologic scaffold promotes skeletal muscle formation in mice and humans with volumetric muscle loss, Science Translational Medicine 6(234) (2014) 234ra58.

[271] J.M. Grasman, D.M. Do, R.L. Page, G.D. Pins, Rapid release of growth factors regenerates force output in volumetric muscle loss injuries, Biomaterials 72 (2015) 49-60.

[272] G.Y. Chen, G. Nunez, Sterile inflammation: sensing and reacting to damage, Nature Reviews Immunology 10(12) (2010) 826-837.

[273] M. Cicuendez, J.C. Doadrio, A. Hernandez, M.T. Portoles, I. Izquierdo-Barba, M. Vallet-Regi, Multifunctional pH sensitive 3D scaffolds for treatment and prevention of bone infection, Acta Biomaterialia 65 (2018) 450-461.

[274] R.K. Jain, P. Au, J. Tam, D.G. Duda, D. Fukumura, Engineering vascularized tissue, Nature Biotechnology 23(7) (2005) 821-3.

[275] A. Atala, F.K. Kasper, A.G. Mikos, Engineering complex tissues, Science Translational Medicine 4(160) (2012) 160rv12.

[276] H. Bae, A.S. Puranik, R. Gauvin, F. Edalat, B. Carrillo-Conde, N.A. Peppas, A. Khademhosseini, Building vascular networks, Science Translational Medicine 4(160) (2012) 160ps23.

[277] F.A. Auger, L. Gibot, D. Lacroix, The pivotal role of vascularization in tissue engineering, Annual Review of Biomedical Engineering 15 (2013) 177-200.

[278] K. Sadtler, M.T. Wolf, S. Ganguly, C.A. Moad, L. Chung, S. Majumdar, F. Housseau, D.M. Pardoll, J.H. Elisseeff, Divergent immune responses to synthetic and biological scaffolds, Biomaterials 192 (2019) 405-415.

[279] S.D. Sommerfeld, C. Cherry, R.M. Schwab, L. Chung, D.R. Maestas, Jr., P. Laffont, J.E. Stein, A. Tam, S. Ganguly, F. Housseau, J.M. Taube, D.M. Pardoll, P. Cahan, J.H. Elisseeff, Interleukin-36gamma-producing macrophages drive IL-17-mediated fibrosis, Science Immunology 4(40) (2019).

[280] L. Chung, D.R. Maestas, Jr., A. Lebid, A. Mageau, G.D. Rosson, X. Wu, M.T. Wolf, A.J. Tam, I. Vanderzee, X. Wang, J.I. Andorko, H. Zhang, R. Narain, K. Sadtler, H. Fan, D. Cihakova, C.J. Le Saux, F. Housseau, D.M. Pardoll, J.H. Elisseeff, Interleukin 17 and senescent cells regulate the foreign body response to synthetic material implants in mice and humans, Science Translational Medicine 12(539) (2020).

[281] K. Sadtler, K. Estrellas, B.W. Allen, M.T. Wolf, H. Fan, A.J. Tam, C.H. Patel, B.S. Luber, H. Wang, K.R. Wagner, J.D. Powell, F. Housseau, D.M. Pardoll, J.H. Elisseeff, Developing a pro-regenerative biomaterial scaffold microenvironment requires T helper 2 cells, Science 352(6283) (2016) 366-370.

[282] Y.D. Lin, C.Y. Luo, Y.N. Hu, M.L. Yeh, Y.C. Hsueh, M.Y. Chang, D.C. Tsai, J.N. Wang, M.J. Tang, E.I. Wei, M.L. Springer, P.C. Hsieh, Instructive nanofiber scaffolds with VEGF create a microenvironment for arteriogenesis and cardiac repair, Science Translational Medicine 4(146) (2012) 146ra109.

[283] J.D. Roh, R. Sawh-Martinez, M.P. Brennan, S.M. Jay, L. Devine, D.A. Rao, T. Yi, T.L. Mirensky, A. Nalbandian, B. Udelsman, N. Hibino, T. Shinoka, W.M. Saltzman, E. Snyder, T.R. Kyriakides, J.S. Pober, C.K. Breuer, Tissue-engineered vascular grafts transform into mature blood vessels via an inflammation-mediated process of vascular remodeling, Proceedings of the National Academy of Sciences of the United States of America 107(10) (2010) 4669-4674.

[284] A.O. Awojoodu, M.E. Ogle, L.S. Sefcik, D.T. Bowers, K. Martin, K.L. Brayman, K.R. Lynch, S.M. Peirce-Cottler, E. Botchwey, Sphingosine 1-phosphate receptor 3 regulates recruitment of anti-inflammatory monocytes to microvessels during implant arteriogenesis, Proceedings of the National Academy of Sciences of the United States of America 110(34) (2013) 13785-13790.

[285] B.J. Kwee, B.R. Seo, A.J. Najibi, A.W. Li, T.-Y. Shih, D. White, D.J. Mooney, Treating ischemia via recruitment of antigen-specific T cells, Science Advances 5(7) (2019) eaav6313.

[286] J. Yang, A.R. Webb, G.A. Ameer, Novel citric acid-based biodegradable elastomers for tissue engineering, Advanced Materials 16(6) (2004) 511-516.

[287] C.G. Jeong, H. Zhang, S.J. Hollister, Three-dimensional poly(1,8-octanediol-co-citrate) scaffold pore shape and permeability effects on sub-cutaneous in vivo chondrogenesis using primary chondrocytes, Acta Biomaterialia 7(2) (2011) 505-514.

[288] A.K. Sharma, P.V. Hota, D.J. Matoka, N.J. Fuller, D. Jandali, H. Thaker, G.A. Ameer, E.Y. Cheng, Urinary bladder smooth muscle regeneration utilizing bone marrow derived mesenchymal stem cell seeded elastomeric poly(1,8-octanediol-co-citrate) based thin films, Biomaterials 31(24) (2010) 6207-6217.

[289] V.A. Kumar, S. Shi, B.K. Wang, I.C. Li, A.A. Jalan, B. Sarkar, N.C. Wickremasinghe, J.D. Hartgerink, Drug-triggered and cross-linked self-assembling nanofibrous hydrogels, Journal of the American Chemical Society. 137(14) (2015) 4823-4830.

[290] B. Sarkar, Z. Siddiqui, K.K. Kim, P.K. Nguyen, X. Reyes, T.J. McGill, V.A. Kumar, Implantable anti-angiogenic scaffolds for treatment of neovascular ocular pathologies, Drug delivery and Translational Research 10(5) (2020) 1191-1202.

[291] Y. Zheng, M.A. Roberts, Tissue engineering: Scalable vascularized implants, Nature Materials 15(6) (2016) 597-599.

[292] B. Zhang, M. Montgomery, M.D. Chamberlain, S. Ogawa, A. Korolj, A. Pahnke, L.A. Wells, S. Masse, J. Kim, L. Reis, A. Momen, S.S. Nunes, A.R. Wheeler, K. Nanthakumar, G. Keller, M.V. Sefton, M. Radisic, Biodegradable scaffold with built-in vasculature for organ-on-a-chip engineering and direct surgical anastomosis, Nature Materials 15(6) (2016) 669-678.

[293] X. Li, B. Cho, R. Martin, M. Seu, C. Zhang, Z. Zhou, J.S. Choi, X. Jiang, L. Chen, G. Walia, J. Yan, M. Callanan, H. Liu, K. Colbert, J. Morrissette-McAlmon, W. Grayson, S. Reddy, J.M. Sacks, H.Q. Mao, Nanofiber-hydrogel composite-mediated angiogenesis for soft tissue reconstruction, Science Translational Medicine 11(490) (2019).

[294] H. Sekine, T. Shimizu, K. Sakaguchi, I. Dobashi, M. Wada, M. Yamato, E. Kobayashi, M. Umezu, T. Okano, In vitro fabrication of functional three-dimensional tissues with perfusable blood vessels, Nature Communications 4 (2013) 1399.

[295] H. Qiu, J. Yang, P. Kodali, J. Koh, G.A. Ameer, A citric acid-based hydroxyapatite composite for orthopedic implants, Biomaterials 27(34) (2006) 5845-5854.

[296] A.J. Engler, S. Sen, H.L. Sweeney, D.E. Discher, Matrix elasticity directs stem cell lineage specification, Cell 126(4) (2006) 677-689.

[297] M.P. Lutolf, J.A. Hubbell, Synthetic biomaterials as instructive extracellular microenvironments for morphogenesis in tissue engineering, Nature Biotechnology 23(1) (2005) 47-55.

[298] J. Li, R. Xing, S. Bai, X. Yan, Recent advances of self-assembling peptide-based hydrogels for biomedical applications, Soft Matter 15(8) (2019) 1704-1715.

[299] C. Ma, X. Tian, J.P. Kim, D. Xie, X. Ao, D. Shan, Q. Lin, M.R. Hudock, X. Bai, J. Yang, Citrate-based materials fuel human stem cells by metabonegenic regulation, Proceedings of the National Academy of Sciences of the United States of America 115(50) (2018) E11741-E11750.

[300] C. Ma, M.L. Kuzma, X. Bai, J. Yang, Biomaterial-based metabolic regulation in regenerative engineering, Advanced Sciences 6(19) (2019) 1900819.

[301] J. Yang, D. Motlagh, A.R. Webb, G.A. Ameer, Novel biphasic elastomeric scaffold for small-diameter blood vessel tissue engineering, Tissue Engineering 11(11-12) (2005) 1876-1886.

[302] C. Ma, E. Gerhard, Q. Lin, S. Xia, A.D. Armstrong, J. Yang, In vitro cytocompatibility evaluation of poly(octamethylene citrate) monomers toward their use in orthopedic regenerative engineering, Bioactive Materials 3(1) (2018) 19-27.

[303] C. Ma, E. Gerhard, D. Lu, J. Yang, Citrate chemistry and biology for biomaterials design, Biomaterials 178 (2018) 383-400.

[304] E.A. Phelps, N. Landazuri, P.M. Thule, W.R. Taylor, A.J. Garcia, Bioartificial matrices for therapeutic vascularization, Proceedings of the National Academy of Sciences of the United States of America 107(8) (2010) 3323-3328.

[305] A. Li, S. Dubey, M.L. Varney, B.J. Dave, R.K. Singh, IL-8 directly enhanced endothelial cell survival, proliferation, and matrix metalloproteinases production and regulated angiogenesis, Journal of Immunology 170(6) (2003) 3369-3376.

[306] B.A. Badeau, M.P. Comerford, C.K. Arakawa, J.A. Shadish, C.A. DeForest, Engineered modular biomaterial logic gates for environmentally triggered therapeutic delivery, Nature Chemistry 10(3) (2018) 251-258.

[307] K.H. Nakayama, C. Alcazar, G. Yang, M. Quarta, P. Paine, L. Doan, A. Davies, T.A. Rando, N.F. Huang, Rehabilitative exercise and spatially patterned nanofibrillar scaffolds enhance vascularization and innervation following volumetric muscle loss, Nature Partner Journals Regenerative Medicine 3 (2018) 16.

[308] D. Gholobova, L. Terrie, M. Gerard, H. Declercq, L. Thorrez, Vascularization of tissue-engineered skeletal muscle constructs, Biomaterials 235 (2020) 119708.

[309] J.M. Anderson, A. Rodriguez, D.T. Chang, Foreign body reaction to biomaterials, Seminars in Immunology 20(2) (2008) 86-100.

[310] K.L. Pennington, M.M. DeAngelis, Epidemiology of age-related macular degeneration (AMD): associations with cardiovascular disease phenotypes and lipid factors, Eye and Vision 3 (2016) 34.

[311] J. Ambati, B.J. Fowler, Mechanisms of age-related macular degeneration, Neuron 75(1) (2012) 26-39.

[312] J.D. Gass, A. Agarwal, A.M. Lavina, K.A. Tawansy, Focal inner retinal hemorrhages in patients with drusen: an early sign of occult choroidal neovascularization and chorioretinal anastomosis, Retina 23(6) (2003) 741-751.

[313] M. Amadio, S. Govoni, A. Pascale, Targeting VEGF in eye neovascularization: What's new?: A comprehensive review on current therapies and oligonucleotide-based interventions under development, Pharmacological Research 103 (2016) 253-269.

[314] V. Daien, V. Nguyen, R.W. Essex, N. Morlet, D. Barthelmes, M.C. Gillies, G. Fight Retinal Blindness! Study, Incidence and outcomes of infectious and noninfectious endophthalmitis after intravitreal injections for age-related macular degeneration, Ophthalmology 125(1) (2018) 66-74.

[315] I. Seah, X. Zhao, Q. Lin, Z. Liu, S.Z.Z. Su, Y.S. Yuen, W. Hunziker, G. Lingam, X.J. Loh, X. Su, Use of biomaterials for sustained delivery of anti-VEGF to treat retinal diseases, Eye 34(8) (2020) 1341-1356.

[316] E. Radvar, H.S. Azevedo, Supramolecular Peptide/Polymer Hybrid Hydrogels for Biomedical Applications, Macromolecular Bioscience 19(1) (2019) e1800221.

[317] C.C. Hu, Y.C. Chiu, J.R. Chaw, C.F. Chen, H.W. Liu, Thermo-responsive hydrogel as an anti-VEGF drug delivery system to inhibit retinal angiogenesis in Rex rabbits, Technology and Health Care 27(S1) (2019) 153-163.

[318] J.D. Tang, C. Mura, K.J. Lampe, Stimuli-Responsive, Pentapeptide, Nanofiber Hydrogel for Tissue Engineering, Journal of the American Chemical Society 141(12) (2019) 4886-4899.

[319] A.H. Van Hove, K. Burke, E. Antonienko, E. Brown, 3rd, D.S. Benoit, Enzymatically-responsive pro-angiogenic peptide-releasing poly(ethylene glycol) hydrogels promote vascularization in vivo, Journal of Controlled Release 217 (2015) 191-201.

[320] J.A. Hammer, A. Ruta, J.L. West, Using Tools from Optogenetics to Create Light-Responsive Biomaterials: LOVTRAP-PEG Hydrogels for Dynamic Peptide Immobilization, Annals of Biomedical Engineering 48(7) (2020) 1885-1894.

[321] K. Wang, R.N. Mitra, M. Zheng, Z. Han, Nanoceria-loaded injectable hydrogels for potential age-related macular degeneration treatment, Journal of Biomedical Materials Research Part A 106(11) (2018) 2795-2804.

[322] Y. Yu, X. Lin, Q. Wang, M. He, Y. Chau, Long-term therapeutic effect in nonhuman primate eye from a single injection of anti-VEGF controlled release hydrogel, Bioengineering & Translational Medicine 4(2) (2019) e10128.

[323] E.L. Bakota, L. Aulisa, K.M. Galler, J.D. Hartgerink, Enzymatic cross-linking of a nanofibrous peptide hydrogel, Biomacromolecules 12(1) (2011) 82-87.

[324] J.L. Drury, T. Boontheekul, D.J. Mooney, Cellular cross-linking of peptide modified hydrogels, Journal of Biomechanical Engineering 127(2) (2005) 220-228.

[325] R. Pugliese, M. Maleki, R.N. Zuckermann, F. Gelain, Self-assembling peptides cross-linked with genipin: resilient hydrogels and self-standing electrospun scaffolds for tissue engineering applications, Biomaterials Science 7(1) (2018) 76-91.

[326] R. Pugliese, F. Gelain, Cross-linked self-assembling peptides and their post-assembly functionalization via one-pot and in situ gelation system, International Journal of Molecular Sciences 21(12) (2020) 4261.

[327] L. Zeng, M. Song, J. Gu, Z. Xu, B. Xue, Y. Li, Y. Cao, A highly stretchable, tough, fast self-healing hydrogel based on peptide(-)metal ion coordination, Biomimetics 4(2) (2019) 36.

[328] V.A. Kumar, B.K. Wang, S.M. Kanahara, Rational design of fiber forming supramolecular structures, Experimental Biology and Medicine 241(9) (2016) 899-908.

[329] S. Roberts, T.S. Harmon, J.L. Schaal, V. Miao, K.J. Li, A. Hunt, Y. Wen, T.G. Oas, J.H. Collier, R.V. Pappu, A. Chilkoti, Injectable tissue integrating networks from recombinant polypeptides with tunable order, Nature Materials 17(12) (2018) 1154-1163.

[330] N.C. Carrejo, A.N. Moore, T.L. Lopez Silva, D.G. Leach, I.C. Li, D.R. Walker, J.D. Hartgerink, Multidomain peptide hydrogel accelerates healing of full-thickness wounds in diabetic mice, American Chemical Society Biomaterials Science & Engineering 4(4) (2018) 1386-1396.

[331] L. Aulisa, H. Dong, J.D. Hartgerink, Self-assembly of multidomain peptides: sequence variation allows control over cross-linking and viscoelasticity, Biomacromolecules 10(9) (2009) 2694-8.

[332] T.L. Lopez-Silva, D.G. Leach, I.C. Li, X. Wang, J.D. Hartgerink, Self-assembling multidomain peptides: design and characterization of neutral peptide-based materials with pH and ionic strength independent self-assembly, American Chemical Society Biomaterials Science & Engineering 5(2) (2019) 977-985.

[333] D.G. Leach, N. Dharmaraj, S.L. Piotrowski, T.L. Lopez-Silva, Y.L. Lei, A.G. Sikora, S. Young, J.D. Hartgerink, STINGel: Controlled release of a cyclic dinucleotide for enhanced cancer immunotherapy, Biomaterials 163 (2018) 67-75.

[334] V.A. Kumar, N.C. Wickremasinghe, S. Shi, J.D. Hartgerink, Nanofibrous snake venom hemostat, American Chemical Society Biomaterials Science & Engineering 1(12) (2015) 1300-1305.

[335] V. Harbour, C. Casillas, Z. Siddiqui, B. Sarkar, S. Sanyal, P. Nguyen, K.K. Kim, A. Roy, P. Iglesias-Montoro, S. Patel, F. Podlaski, P. Tolias, W. Windsor, V. Kumar, Regulation of lipoprotein homeostasis by self-assembling peptides, American Chemical Society Applied Bio Materials 3(12) (2020) 8978-8988.

[336] P. Kumar, S. Kumar, E.P. Udupa, U. Kumar, P. Rao, T. Honnegowda, Role of angiogenesis and angiogenic factors in acute and chronic wound healing, Plastic and Aesthetic Research 2(5) (2015) 243.

[337] N.C. Wickremasinghe, V.A. Kumar, S. Shi, J.D. Hartgerink, Controlled angiogenesis in peptide nanofiber composite hydrogels, American Chemical Society Biomaterials Science & Engineering 1(9) (2015) 845-854.

[338] S. Ragauskas, E. Kielczewski, J. Vance, S. Kaja, G. Kalesnykas, In vivo multimodal imaging and analysis of mouse laser-induced choroidal neovascularization model, Journal of Visualized Experiments (131) (2018).

[339] A. Ebneter, C. Agca, C. Dysli, M.S. Zinkernagel, Investigation of retinal morphology alterations using spectral domain optical coherence tomography in a mouse model of retinal branch and central retinal vein occlusion, PLoS One 10(3) (2015) e0119046.

[340] X. Chen, J.M. Kezic, J.V. Forrester, G.L. Goldberg, I.P. Wicks, C.C. Bernard, P.G. McMenamin, In vivo multi-modal imaging of experimental autoimmune uveoretinitis in transgenic reporter mice reveals the dynamic nature of inflammatory changes during disease progression, Journal of Neuroinflammation 12 (2015) 17.

[341] H.E. Grossniklaus, S.J. Kang, L. Berglin, Animal models of choroidal and retinal neovascularization, Progress in Retinal and Eye Research 29(6) (2010) 500-519.

[342] J.G. Garweg, J.J. Zirpel, C. Gerhardt, I.B. Pfister, The fate of eyes with wet AMD beyond four years of anti-VEGF therapy, Graefe's Archive for Clinical and Experimental Ophthalmology 256(4) (2018) 823-831.

[343] A. Grzybowski, R. Told, S. Sacu, F. Bandello, E. Moisseiev, A. Loewenstein, U. Schmidt-Erfurth, B. Euretina, 2018 Update on intravitreal injections: euretina expert consensus recommendations, Ophthalmologica 239(4) (2018) 181-193.

[344] J. Blasiak, G. Petrovski, Z. Vereb, A. Facsko, K. Kaarniranta, Oxidative stress, hypoxia, and autophagy in the neovascular processes of age-related macular degeneration, Biomed Research International 2014 (2014) 768026.

[345] K. Ourradi, T. Blythe, C. Jarrett, S.L. Barratt, G.I. Welsh, A.B. Millar, VEGF isoforms have differential effects on permeability of human pulmonary microvascular endothelial cells, Respiratory Research 18(1) (2017) 116.

[346] L. Chen, Y. Cui, B. Li, J. Weng, W. Wang, S. Zhang, X. Huang, X. Guo, Q. Huang, Advanced glycation end products induce immature angiogenesis in in vivo and ex vivo mouse models, American Journal of Physiology Heart and Circulatory Physiology 318(3) (2020) H519-H533.

[347] R.J. Lederman, F.O. Mendelsohn, R.D. Anderson, J.F. Saucedo, A.N. Tenaglia, J.B. Hermiller, W.B. Hillegass, K. Rocha-Singh, T.E. Moon, M.J. Whitehouse, B.H. Annex, T. Investigators, Therapeutic angiogenesis with recombinant fibroblast growth factor-2 for intermittent claudication (the TRAFFIC study): a randomised trial, Lancet 359(9323) (2002) 2053-2058.